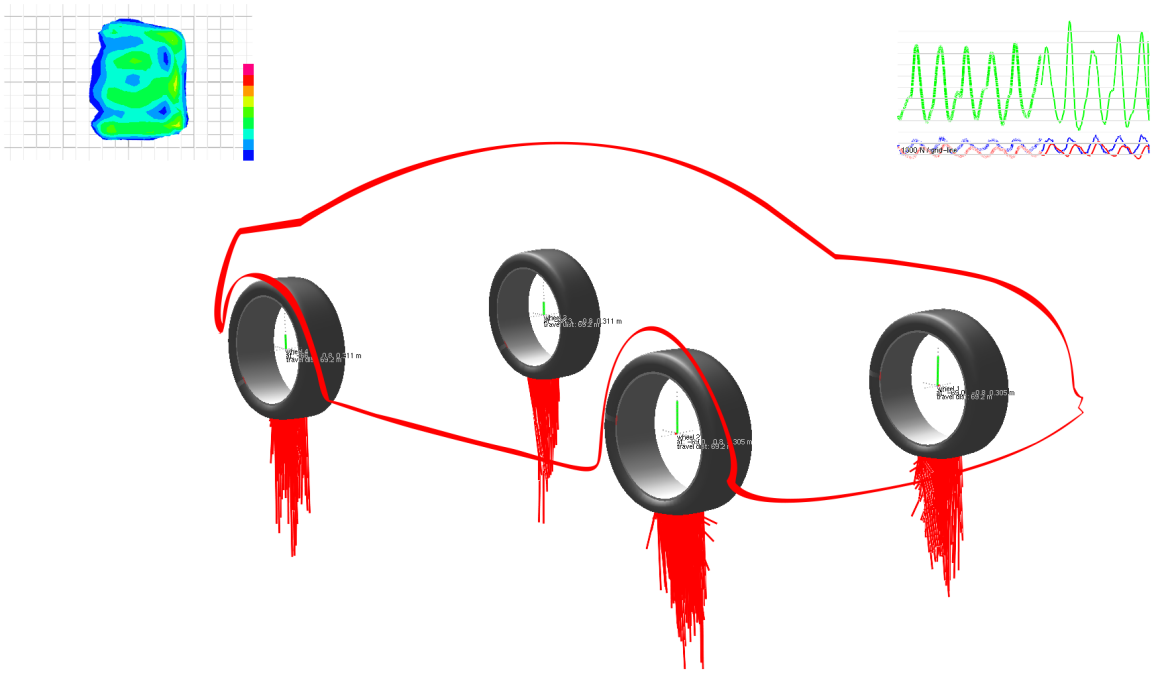
CHALMERS



Accelerated Road Load Simulation

Road Load Data for Fatigue Analysis in Concept Phase

Master's thesis in Applied Mechanics

JIANQIAO LIU
VIJAY RAMNATH

Department of Applied Mechanics
CHALMERS UNIVERSITY OF TECHNOLOGY
Göteborg, Sweden 2016

MASTER'S THESIS IN APPLIED MECHANICS

Accelerated Road Load Simulation

Road Load Data for Fatigue Analysis in Concept Phase

JIANQIAO LIU
VIJAY RAMNATH

Department of Applied Mechanics
Division of Vehicle Engineering and Autonomous Systems
CHALMERS UNIVERSITY OF TECHNOLOGY

Göteborg, Sweden 2016

Accelerated Road Load Simulation
Road Load Data for Fatigue Analysis in Concept Phase
JIANQIAO LIU
VIJAY RAMNATH

© JIANQIAO LIU, VIJAY RAMNATH, 2016

Master's thesis 2016:01
ISSN 1652-8557
Department of Applied Mechanics
Division of Vehicle Engineering and Autonomous Systems
Chalmers University of Technology
SE-412 96 Göteborg
Sweden
Telephone: +46 (0)31-772 1000

Cover:
Sine road contact patch animation from Cosin Scientific Software.

Chalmers Reproservice
Göteborg, Sweden 2016

Accelerated Road Load Simulation
Road Load Data for Fatigue Analysis in Concept Phase
Master's thesis in Applied Mechanics
JIANQIAO LIU
VIJAY RAMNATH
Department of Applied Mechanics
Division of Vehicle Engineering and Autonomous Systems
Chalmers University of Technology

Abstract

This thesis work was carried out at China Euro Vehicle Technology (CEVT) in Gothenburg, Sweden. This thesis work compares 'VI-CarRealTime', which is a real time simulation software with a simplified vehicle model, against the automotive industry standard software for vehicle dynamics - 'ADAMS/Car', at a road load simulation capability. The aim of this thesis work is to evaluate the performance of VI-CarRealTime with regard to load calculation accuracy and simulation time. VI-CarRealTime and ADAMS/Car simulations are run for an existing demo model and the CEVT model with both Pacejka tire model and FTire tire model over various road surfaces of increasing complexity. Matlab is then used for post-processing and comparison of corresponding wheel center normal and longitudinal forces. Road load simulation results for wheel center forces are analysed and presented for flat, cleat, and washboard roads and a trade-off between simulation time saved and load calculation accuracy is established. Rudimentary calculations for tire forces, resonance frequencies are also performed to understand the approximate force range. In conclusion, VI-CarRealTime offers a fast and reasonably accurate alternative to ADAMS/Car in tire force simulations. This opens doors to quick optimization studies and sensitivity analyses at the vehicle development concept phase. However it is recommended to perform a thorough validation of all vehicle dynamic parameters before claiming robustness of VI-CarRealTime.

Keywords: Vehicle dynamics, Road load simulation, ADAMS/Car, VI-CarRealTime, FTire

Acknowledgements

We would like to thank Johnny Engström and CEVT for providing us with this invaluable opportunity and for the continuous support, direction and encouragement. We would also like to thank Lucas Börjesson for helping us through the entirety of the project with software debugging and for generosity with regard to data. We also thank our supervisor from Chalmers University Thomas Abrahamsson for valuable inputs and critical guidance during the thesis work. Speical thanks to our friend Sidharth Malik for tips on software usage. Stefano Badii from VI-Grade Tech support was of immediate help during troubleshooting for VI-CarRealTime related issues.
- Jianqiao Liu & Vijay Ramnath, Gothenburg, July 2016

I would like to thank my family and Eva Lendaro for all their love and support. Working as a simulation engineer is no easy task, hence I would like to thank Vijay for being a great partner, sharing good days but also enduring frustrating days together. - J.L.

I would like to thank my family and friends for their continuous support. Special thanks to Jianqiao for a memorable time working together. - V.R.

Nomenclature

- ACAR: ADAMS/Car
- CEVT: China Euro Vehicle Technology AB
- DAE: Differential Algebraic Equations
- DOF: Degree of Freedom
- FEA: Finite Element Analysis
- MBD: Multibody Dynamics
- MDO: Multi-Disciplinary Optimization
- OEM: Original Equipment Manufacturer
- VI, VI-CRT: VI-CarRealTime

Contents

Abstract i

Acknowledgements i

Nomenclature iii

Contents v

1 Introduction 1
1.1 Purpose . . . 1
1.2 Scope and Limitations . . . 1

2 Background 2
2.1 Road Load Simulation In ADAMS/Car . . . 2
2.1.1 Multibody Simulation . . . 2
2.1.2 ADAMS/Car . . . 2
2.1.3 VI-CarRealTime . . . 2
2.2 Fatigue Life Suspension Component Road Load Data . . . 4
2.2.1 Rainflow Method for Fatigue Life Calculation . . . 4
2.3 Tire Models . . . 4
2.3.1 Semi Empirical Models . . . 6
2.3.2 Physical Models . . . 6
2.3.3 Finite Element models . . . 8
2.4 Vehicle Models . . . 8
2.4.1 Demo Model . . . 8
2.4.2 CEVT Model . . . 9
2.5 General Testing Sequence . . . 9
2.6 Tire Models Used in Simulation . . . 10

3 Theoretical Analysis 11
3.1 Theoretical Validation . . . 11
3.1.1 Theory . . . 11
3.2 Road Profiles . . . 14
3.3 Power Spectral Density . . . 14

4 Demo Vehicle Results 17
4.1 Integration Step Size Comparison . . . 17
4.1.1 VI-CarRealTime . . . 17
4.1.2 ADAMS/Car . . . 19
4.1.3 Cleat Test Integration Step Size: VI-CarRealTime versus ADAMS/Car . . . 19
4.2 Demo Model with Pacejka Tire Results . . . 21
4.2.1 Flat Road . . . 21
4.2.2 Cleat Road . . . 22
4.3 Demo Model with Demo F-tire . . . 25
4.4 Ftire Specific Settings in VI-CarRealTime . . . 26
4.4.1 Flat Road . . . 28
4.4.2 Cleat . . . 30
4.4.3 Washboard . . . 30
4.5 Pacejka Tire versus FTire Comparison on Demo Model . . . 37
4.6 Demo Model with CEVT FTire . . . 38
4.6.1 Flat Road . . . 38
4.6.2 Cleat . . . 38
4.6.3 Washboard . . . 38
4.7 Washboard Track: Force Discrepancies and Workarounds . . . 42

4.7.1 Washboard Road Profile Analysis . . . 42
4.7.2 Vibration Dynamics: One Dimensional Model with Two Degrees of Freedom . . . 42
4.7.3 Vibration Dynamics: Simplified Model . . . 51
4.7.4 VI-CarRealTime and ADAMS/Car Driver Model Differences . . . 52
4.7.5 Additional Initial Flat Road . . . 53
4.7.6 Unsprung Mass . . . 55

5 CEVT Control Model Results **59**
5.1 CEVT Control Model Issues . . . 59
5.1.1 ADAMS/Car 2015 Setting . . . 59
5.1.2 Ftire Setting . . . 59
5.1.3 Powertrain . . . 59
5.1.4 Suspension Compliance Map . . . 59
5.2 2D Flat Road . . . 62
5.2.1 Pacejka Tires . . . 62
5.2.2 Continental - 225-40R19 . . . 62
5.3 Cleat Road . . . 65
5.3.1 Pacejka Tire . . . 65
5.3.2 Continental 225-40R19 Ftire . . . 65
5.4 Washboard Road . . . 68
5.4.1 Continental Ftire - Maintain Velocity . . . 68
5.4.2 Continental Ftire - Coasting . . . 68
5.4.3 CEVT model - Suspension Compliance Investigation . . . 74
5.4.4 Pirelli Ftire - Maintain Velocity . . . 74
5.5 Belgian Block . . . 74
5.5.1 Belgian Block - Coast . . . 74
5.5.2 Belgian Block - Compliance Setting . . . 77
5.6 Time Comparison and trade-off . . . 84

6 Conclusion **86**

7 Future Work **87**
Appendices . . . 88
A.1 Resreader Matlab Code . . . 88
A.2 Tire Properties . . . 90
A.2.1 Pacejka Tire . . . 90
A.2.2 Demo FTire . . . 90
A.2.3 CEVT FTire: Pirelli . . . 90
A.2.4 CEVT FTire: Continental . . . 91
A.3 Supporting Figures . . . 93
A.4 Tire Force Results . . . 105
A.4.1 Demo Model Result Tables . . . 105

References **109**

1 Introduction

The concept of platform sharing is quite common among today's automakers where certain components such as suspension, brakes, powertrain, etc. are shared between different vehicle models and only the necessary components are modified to suit specific vehicle requirements and differentiate models and brands. This encourages an increase in the number of variants and is quite obvious if one observes the various models among the major OEMs (Original Equipment Manufacturer) today. With increased number of variants, one cannot afford the luxury of extensive testing periods for each variant. Although platform sharing has its own benefits, the risk of recall rates are higher due to significant similarities within the variants. This is where CAE (Computer Aided Engineering) plays an important role by minimising the risks of recall to the maximum extent possible.

CAE software tools for FEA (Finite Element Analysis), MBD (Multibody Dynamics) aid in reducing development time and enables one to easily evaluate the performance of a certain design change without having to build a physical prototype. CAE today is integral to the iterative vehicle development process where continuous exchange of data takes place at different design stages.

This thesis work titled "Accelerated Road Load Simulation" is carried out at the Chassis and Powertrain CAE group of China Euro Vehicle Technology AB (CEVT) in Gothenburg. CEVT is a joint R&D venture catering to the vehicle platform requirements of both Volvo Cars and Geely Auto.

Full-vehicle dynamic simulations for various driving scenarios are widely conducted in the automotive industry by using multibody dynamics simulation tools. The comprehensiveness of these tools range from test rig data analysis to emergency lane change maneuvers and much more. ADAMS/Car is a simulation software that is predominantly used by car manufacturers. While the simulation offers high fidelity in load prediction, the downside is the demand for high computational power. On the other hand, tools like VI-CarRealTime enable real time computation of the same driving scenarios. Moreover it comes with added advantages of simpler and model specific solver, which can be used for design of experiments and conceptual level design [11].

This thesis will attempt to use the aforementioned benefits of VI-CarRealTime to derive wheel center loads with comparable accuracy as achieved by ADAMS/Car. VI-CarRealTime results, once deemed acceptable, can be used to evaluate damage analysis and assess fatigue life of suspension components. Thereby, complementary usage of VI-CarRealTime and ADAMS/Car will speed up vehicle development time.

1.1 Purpose

The purpose of this thesis is to answer whether VI-CarRealTime can provide fast, yet sufficiently accurate load approximations. The accuracy is attested by comparing the results with ADAMS/Car. To what extent is the accuracy level acceptable for downstream calculations and any other limitations will be established in the latter stages of this thesis work. Assuming acceptable accuracy levels are achieved, loading history on suspension components will be established and thereby damage and fatigue life can be obtained.

From a high-level process point of view, this thesis will enable easier evaluation of concept level parameter changes, such as weight distribution and centre of gravity, which will ultimately cut down development time at the conceptual stage. Since there will be a lack of decisive information available to build detailed models during the concept stage, this is a huge benefit especially taking into account the concept of platform sharing and the number of variants. It also has the potential to enforce a more data driven approach to component design, where the CAE group will drive the need for a component design change based on fatigue estimations of the different conceptual variations instead of the the reverse methodology.

1.2 Scope and Limitations

VI-CarRealTime was originally developed for hardware-in-the-loop testing and control system optimisation. Another intention was to provide a simplified vehicle model that can act as an easy interface for vehicle dynamics and control engineers. Although co-simulations with Simulink-implemented controllers seem easily possible, the effect of control parameters or active control on component loading will not be covered in the scope of this work. VI-CarRealTime is chosen due to its compatibility with ADAMS/Car in terms of common database and generated events file formats [10]. Other commercial software with similar functionalities to VI-CarRealTime and ADAMS/Car are not considered for this thesis work.

2 Background

2.1 Road Load Simulation In ADAMS/Car

2.1.1 Multibody Simulation

Multibody simulation deals with dynamic simulation of rigid or flexible bodies. Solid bodies and links interconnected by joints constitute a multibody dynamics (MBD) system. MBD equations in general are derived from Newton's equations of motion or the more elegant Lagrange equations. Specific to the automotive industry various software are used for MBD simulations. These software are usually derived from a general purpose platform and customised to automotive industry.

Usage of these software vary between OEMs: Audi is using ADAMS/Car along with VI-CarRealTime for ride and handling simulations and Dymola for mechatronic and multi-domain vehicle dynamics simulations [14]; BMW uses ADAMS/Car for ride and durability and also SIMPACK for driveline simulations; Volvo Cars relies mainly on ADAMS/Car but recently purchased the VI-Grade DriveSim platform, which uses VI-CarRealTime for its vehicle models.

2.1.2 ADAMS/Car

ADAMS stands for Automated Dynamic Analysis of Mechanical Systems and is provided by MSC Software. Nastran and MARC (for non-linear simulation) are some of the other software part of its product line. The ADAMS/Car vertical, which can be claimed as the current automotive industry standard for vehicle dynamics simulations, was developed in consultation with the consortium of OEMs, such as Audi, BMW, Volvo and Renault, who provided inputs such as type of suspensions and standard maneuvers. ADAMS/Car builds individual bodies in the system and incorporates properties in a detailed manner be it linear or non-linear. Each body is then assigned six degrees of freedom and the equations are solved based on the simulation conditions. As a result the effects of the system dynamics on the individual bodies can also be studied in detail. Two user modes exist - Expert User and Standard User, where the former can modify templates and create test procedures. ADAMS/Car 2015 version is used in this thesis.

2.1.3 VI-CarRealTime

VI-grade is a spin-off company from MSC Software with varying product lines, including standalone solutions such as VI-CarRealTime, VI-Motorsport and driving simulator platforms such as VI-DriveSim.

VI-CarRealTime 17.0 *(vicrt17)* is the software version used in this thesis. It is a real time simulation software that utilises a simplified vehicle model. It thereby provides an interface that is enabling easy usage for vehicle dynamics engineers and control engineers. The gap is bridged by enabling easy model exchange between OEM and suppliers, and enabling controller developers to visualise the effects of their iterations from a system perspective, which will yield in better and faster vehicle integration.

VI-CarRealTime follows the ISO 8855 *(Road vehicles - Vehicle dynamics and road-holding ability - Vocabulary. 1991)* reference co-ordinate system and uses a vehicle modeling approach, where the suspension linkages, bushings, steering parts are absent. This is in contrast to ADAMS/Car which has all the detailed bodies in its model. The VI-CarRealTime suspension properties are determined when the model is exported from ADAMS/Car. A series of analyses are done and the properties are extracted and expressed within VI-CarRealTime domain as look-up tables and DAE.

The vehicle model has 14 Degrees of Freedom and can be extended up to 20 upon including compliance [16]. The vehicle model is made up of one sprung mass and four wheel masses as shown in Figure 2.1. The vehicle chassis with 6 DOF and the four wheels with 2-DOF each constitute the 14 DOF. Figure 2.2 shows the software work flow chart for VI-CarRealTime. The vehicle models can be an ADAMS/Car exported model or built by the user within VI-CarRealTime. Within the VI software package, options for animations, post-processing, road editing are also available.

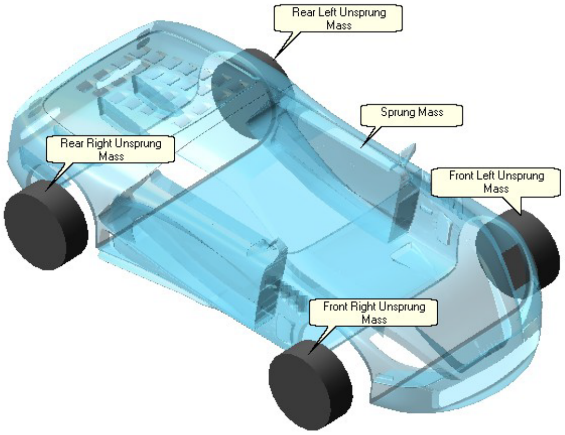


Figure 2.1: *VI-CarRealTime Sprung and Unsprung Masses*

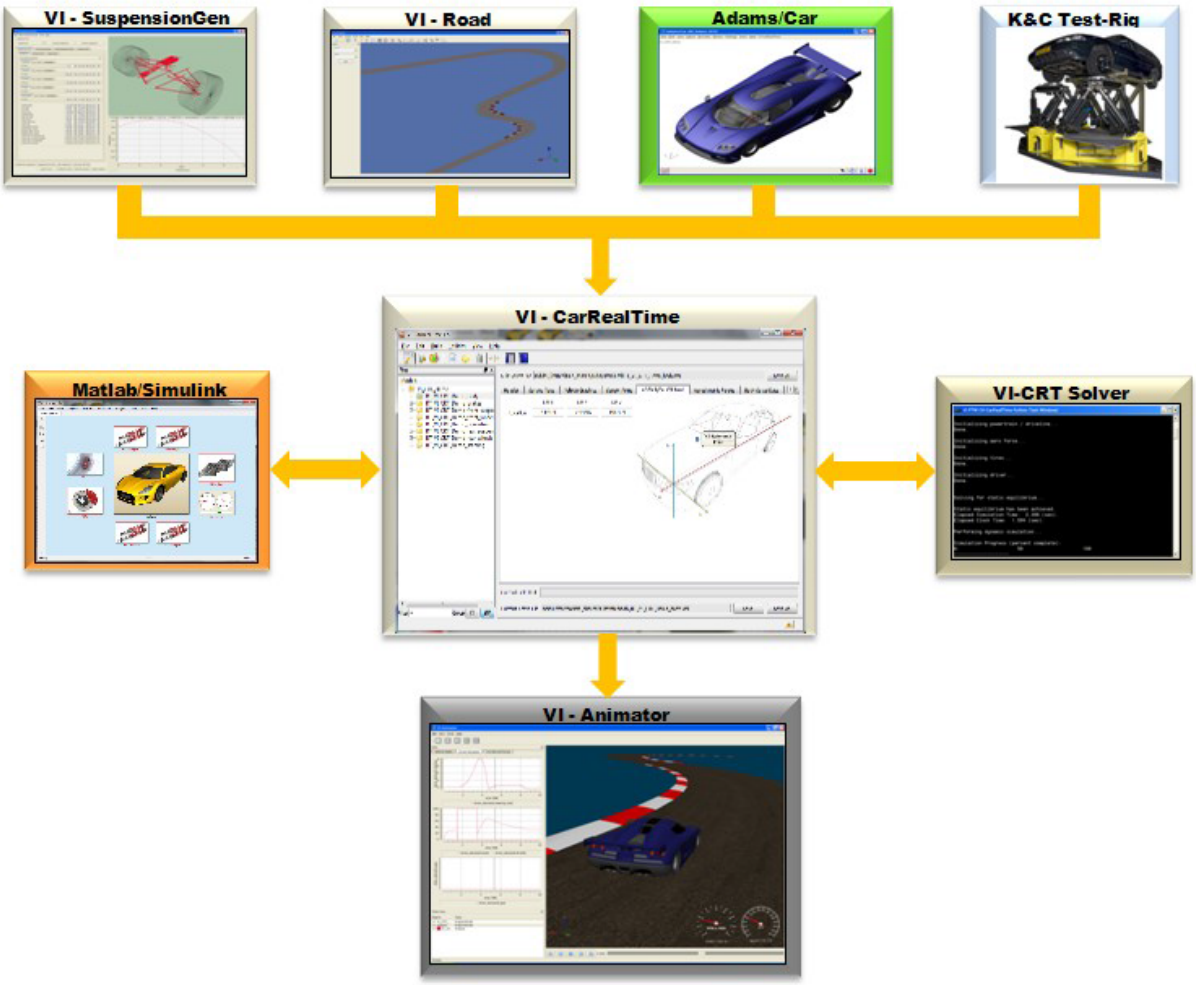


Figure 2.2: *VI-CarRealTime process flow*

2.2 Fatigue Life Suspension Component Road Load Data

2.2.1 Rainflow Method for Fatigue Life Calculation

Rainflow counting method is a widely adopted way to summarize load history and to estimate fatigue life of a component. Rainflow diagram is characterized by a time versus stress plot. Combined stresses, such as tensile and bending stress, at a point of interest can still be analyzed, but must be first converted into equivalent stresses.

The cycle counting procedure described in this thesis is the ASTM E1049-85 Standard Practice. The standard contains many cycle counting techniques. Only Section 5.4.5 of standard - "Simplified Rainflow Counting for Repeating Histories" will be described here. This technique is suitable for various chassis and suspension components that are subjected to repeated spectrum loading. Spectrum Loading, or Various Amplitude Loading, occurs when acting forces are not constant, and thus the stress amplitude are continuously varying. An example of spectrum loading stress history and related terminologies are illustrated in Figure 2.3. The cycle counting steps are highlighted below.

1. Plot stress as a function of time. Locate point with the highest stress magnitude.
2. Stress signal before the highest reversal point is shifted to the end of the signal, as shown in Figure 2.4
3. The modified stress history shall start and end with the highest absolute stress.
4. Perform Rainflow counting. A Rainflow cycle is counted when $|\sigma_{i-1} - \sigma_i| \leqslant |\sigma_i - \sigma_{i+1}|$
5. Mean Load: the algebraic average of the peak and valley stress values, i.e. $\sigma_{mean} = \frac{\sigma_{i-1}+\sigma_i}{2}$
6. Range: the algebraic difference between the absolute values of peak and valley, i.e. $\sigma_{range} = |\sigma_{i-1}| + |\sigma_i|$

2.3 Tire Models

Tires, contrary to their looks are arguably some of the most complex components in the vehicle. Tire design is a complex task balancing between performance, stability, and durability, while satisfying safety requirements. With numerous components involved in tire manufacturing, modeling of a tire is a mammoth task. However, attempts have been made to simulate tire behaviour with the help of various modeling methods, a few of which are reviewed briefly in this section.

Based on the type of approach to modeling, models varying from simple physical models *(theoretical)* to semi-empirical models to complex finite element models are discussed below. Tire models are not limited to the ones listed in this thesis work. Many other approaches and models exist but are beyond the scope of this thesis. The VI-CarRealTime tire coordinate system is presented in Figure **??** for reference.

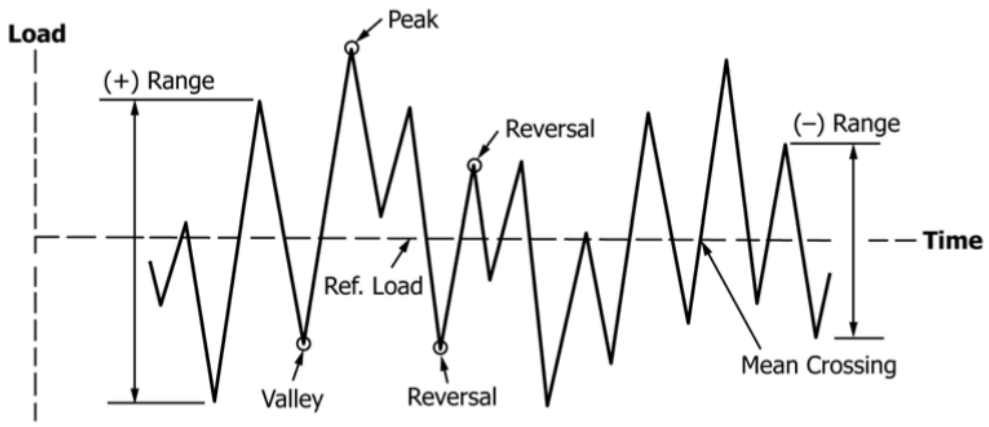


Figure 2.3: *Basic Fatigue Loading Parameter [1]*

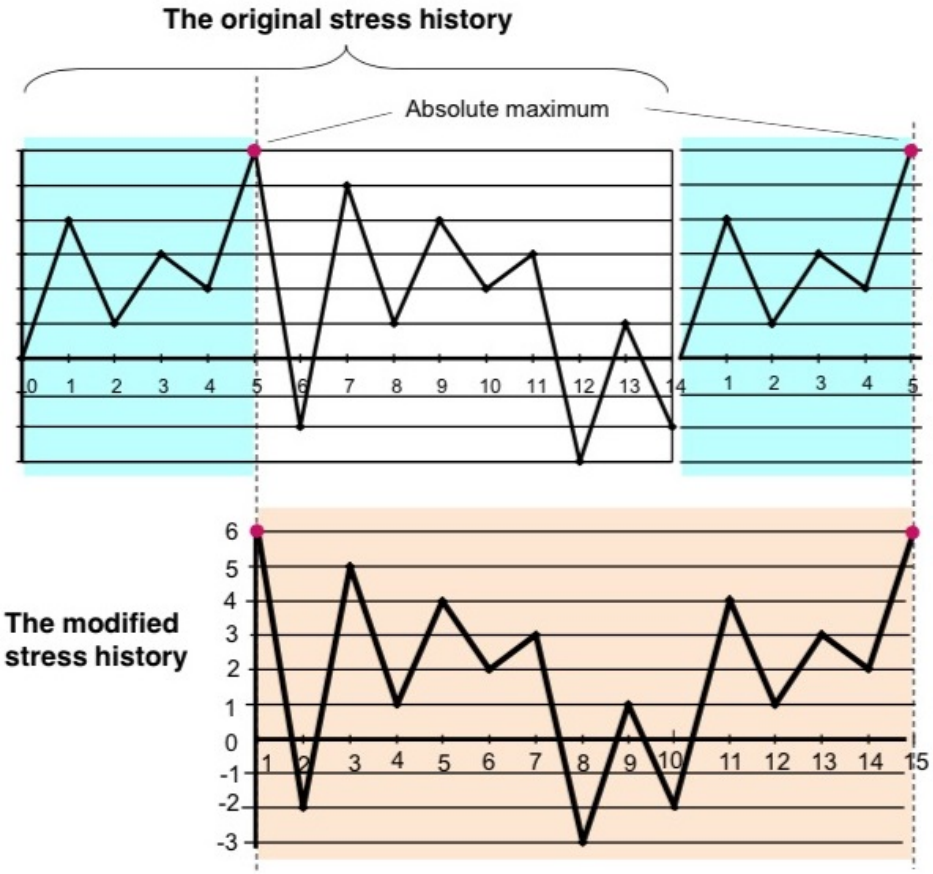


Figure 2.4: *Stress History Modification [7]*

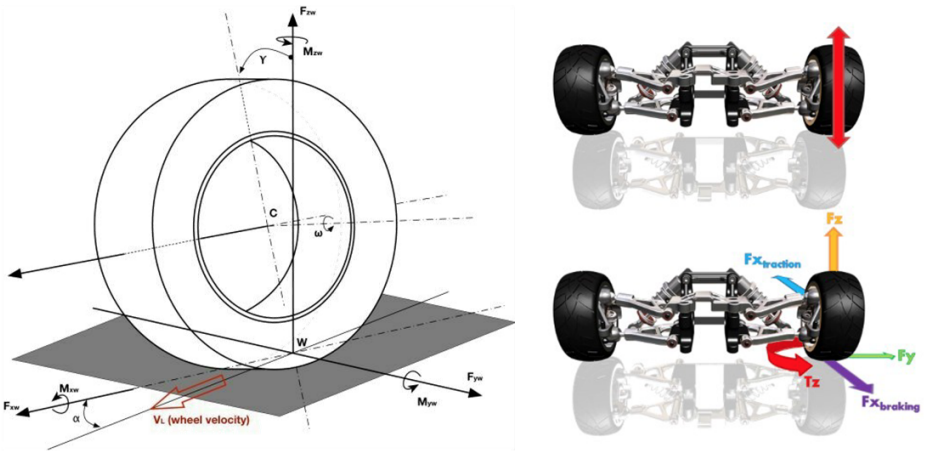


Figure 2.5: *VI Tire Model Coordinate System [16]*

2.3.1 Semi Empirical Models

These models are based on measured tire data and applying the technique of regression. However, some of the models' root structure can be traced back to simpler physical models, and thereby resulting in the name 'semi-empirical'.

Magic Tire Formula

Developed by Volvo Cars and Delft University, it is one of the most widely used tire models. Trigonometric functions are utilised for curve fit calculations of the measured tire data. This formula provides values of side force, longitudinal force and aligning moment with acceptable accuracy compared to the actual measured data. The trigonometric function considers slip ratio or slip angle as input and it is presented in Equation 2.1.

$$Y = D * sin(C * \arctan B * x - E * (B * x - \arctan(B * x))) \tag{2.1}$$

Here "x" and "Y" are the input and output respectively with variations in calculation methods of B,C,D,E for the different outputs i.e lateral and longitudinal forces and aligning moment. B,C,D,E are the stiffness factor, shape factor, peak value and curvature factor, respectively. Note that the ply steer and conicity can also be included in the model but are not illustrated in the above equation. Other models which fall under this category are the Burckhardt and the Kiencke and Daiss models [2].

Similarity Models

This model is usually utilised when very fast computation times are required. This is based on the idea that the tire characteristics will be similar to the reference characteristic even if the conditions are altered. Nominal tire load at zero camber and zero side slip is the usual reference. New relations are obtained for special conditions via rescaling. An example multiplication factor includes the ratio of the wheel load to nominal wheel load, F_z/F_{z_0}, to the slip angle, α, in order to obtain an equivalent slip angle. Fast computation times of this model is a result of its simplicity, although the accuracy comes into question when higher values of combined slip is introduced.

2.3.2 Physical Models

Brush Model

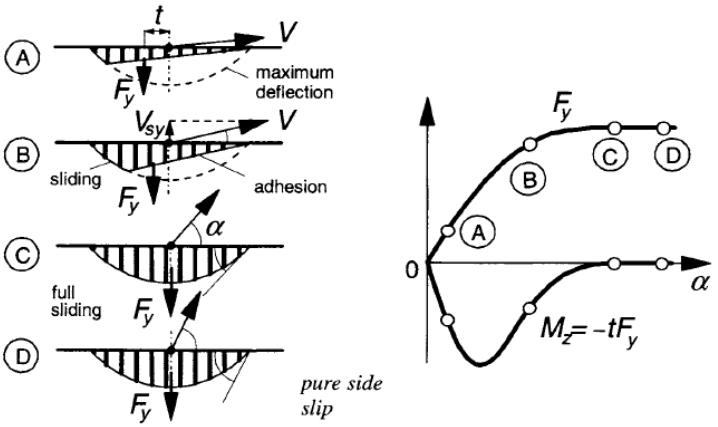
It is a simplified physical model that considers a parabolic pressure distribution. Elastic bristles are assumed to be arranged along the circumference of the wheel center. The bristle's mechanical properties are an accumulation of the properties of the belts, carcasses and other tread elements. This model can be used for situations of pure side slip, pure longitudinal slip and also combined slip. Details and extensions to the brush model exist and can be found in literature [12]. Figure 2.6a shows the variation of the tire force and aligning moment with increase in slip angle.

Stretched String Model

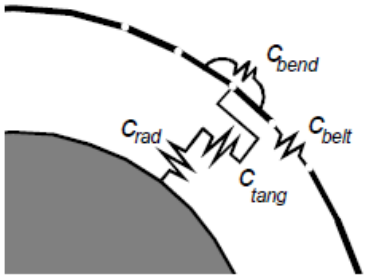
An endless string pre-tensioned by a uniform radial force and connected elastically to the wheel center plane in the axial direction gives an indication of the construction of the stretched string model. This model can be extended to many strings in parallel with numerous tread elements along the circumference. As a result of this extension, there is a contact width in addition to only a contact length with the basic version of the model as seen in Figure 2.6c. The finite contact length version is useful in considering short path wavelength situations, where the contact width requirement are needed for moment calculations.

Beam Model

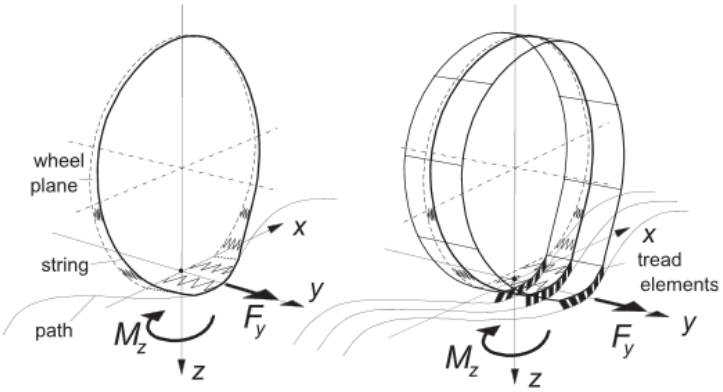
The Magic Formula model cannot be implemented when there is deformable terrain, such as soil. The beam model is a more physical model based approach. It consists of thin beams with no mass and stiffness in lateral and axial directions. Multiple beams that are connected to each other emanate from the rim to form a web like structure as seen in Figure 2.6d. The tire is considered a force element and the forces due to beam deflections are of importance. Literature study suggests the beam model can be better applied to construction vehicles moving over soft grounds [13].



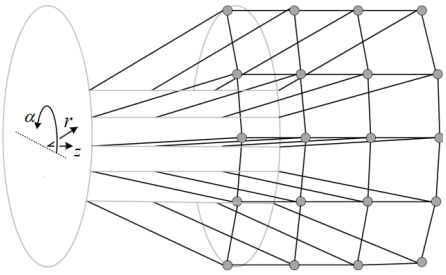
(a) *Tire model taken from [12])*



(b) *Simplified illustration of Ftire model (Taken from [5])*



(c) *Single string and extended string model. Taken from [12]*

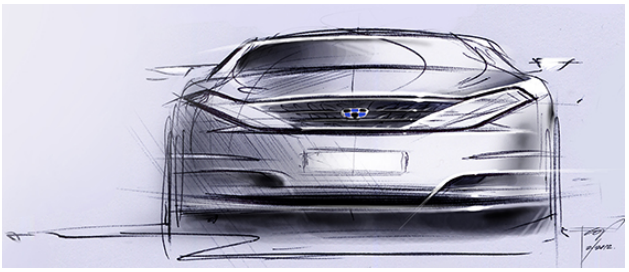


(d) *Tire Model as per Beam Theory [13]*

Figure 2.6: *Tire Models*



(a) *Koenigsegg Demo Model*



(b) *CEVT Model*

Figure 2.7: *Vehicle Models*

2.3.3 Finite Element models

FTire

FTire *(Flexible Ring Tire Model)* is the tire model used in some of the simulations. It is a non-linear structural dynamics based model, where a slim ring capable of being deflected longitudinally, laterally and vertically is chosen as representation for the tire belt. The model structure consists of nodes connected by stiffness and damping elements representing the steel cords. A simple representation can be viewed in Figure 2.6b. FTire requires certain tire and rim parameters like rim translational velocity, rim diameter, tread width and other tire related parameters [6] as input and provides the tire force vector and tire moment vector as output. In FTire, Newmark method is utilised for integration and it works well with the MSC ADAMS solver. Contrary to simpler empirical models, which are limited to steady state calculations, FTire can be used for higher frequency variations with good accuracy.

2.4 Vehicle Models

Two vehicle models concerned in this thesis work are the demo model and the CEVT control model, which are shown in Figure 2.7. The vehicle model simulation will start with the demo model and then proceed to the CEVT control model. This order is partly due to lack of availability of the CEVT model in VI-CarRealTime format at the beginning of the thesis, and partly in effort to eliminate as many model-related errors as possible. The demo model from VI-CarRealTime tutorial package is used for pilot testing. Once the software features are familiarized and the comparison procedure is streamlined, the next step is to take on the more detailed CEVT model and repeat the comparison tests.

The vehicle coordinate systems in VI-CarRealTime and ADAMS/Car are shown in Figure 2.8. VI-CarRealTime uses the ISO 8855 coordinate system with X forward, Y to the vehicle left side and Z upwards. ADAMS/Car's X coordinate system points backwards, Y pointing towards the right and Z pointing upwards.

2.4.1 Demo Model

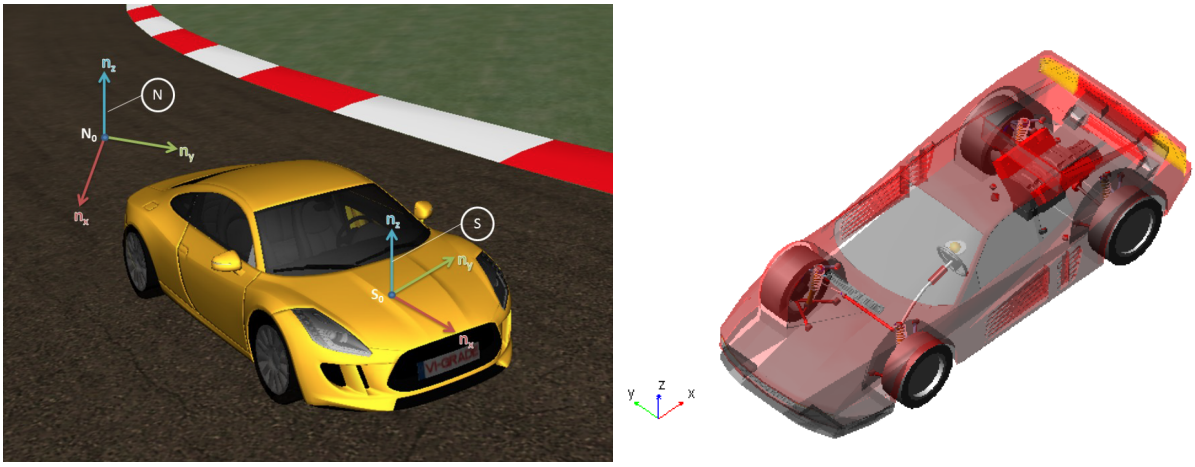
The demo model originates from the VI-CarRealTime example database. It exists in two formats - an ADAMS/Car (`.asy`) file and a VI-CarRealTime (`.xml`) file. The advantage of having files in both software's native format is that it avoids the need of exporting from one software to another. In addition, two versions of the demo model can be found in the example database - one containing subsystem compliance and the other one does not. The demo model without subsystem compliance is used given its simpler system settings. The demo model with compliance is only used in this thesis to compare system parameter values and compliance maps with the CEVT model.

Demo Model Variables

Some key variables for longitudinal vehicle dynamics studies are presented below.

L Wheelbase (2920 mm)

l_{front} Distance from front axle to vehicle center of gravity (1566.3 mm)



(a) *VI-CarRealTime [16]* (b) *ADAMS/Car*

Figure 2.8: *Vehicle Coordinate System*

m_{sprung} Sprung mass (1147.66 kg)

$m_{unsprung}$ Unsprung mass - sum of mass of front wheels and rear wheels

$m_{frontwheel}$ Front wheel mass with Pacejka 96 front tire (30.35 kg)

$m_{rearwheel}$ Rear wheel mass with Pacejka 96 rear tire (35.31 kg)

2.4.2 CEVT Model

The CEVT control model is exported through ADAMS/Car. A set of analyses are performed during the export and properties such as compliance, toe and camber variations are described as look-up tables and 3D splines in the VI-CarRealTime model. The CEVT control model also includes flexible bodies with the tie rod being an example.

The biggest difference between the CEVT model and the demo model is the use of compliance in the suspension system and the presence of flex bodies. The details regarding the CEVT model are confidential and hence are not specified in this thesis.

2.5 General Testing Sequence

Road load simulation is accelerated by using VI-CarRealTime, which has a simpler model compared to that of ADAMS/Car. The fidelity of the data produced by VI-CarRealTime is compared against the results of ADAMS/Car.

The general testing procedure is illustrated by the flowchart in Figure 2.9. The comparison between ADAMS/Car and VI-CarRealTime is accomplished in the following order:

1. Run simulation in ADAMS/Car and VI-CarRealTime
   (a) Determine the appropriate integration step sizes
   (b) Compare tire normal forces F_z
   (c) Compare tire longitudinal forces F_x
2. Extract tire forces from respective result files
3. Perform rainflow cycle counting
4. Estimate fatigue life

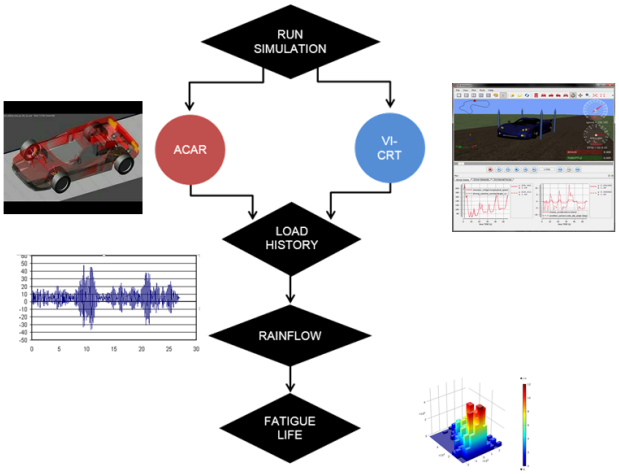


Figure 2.9: *Overall Process Flow*

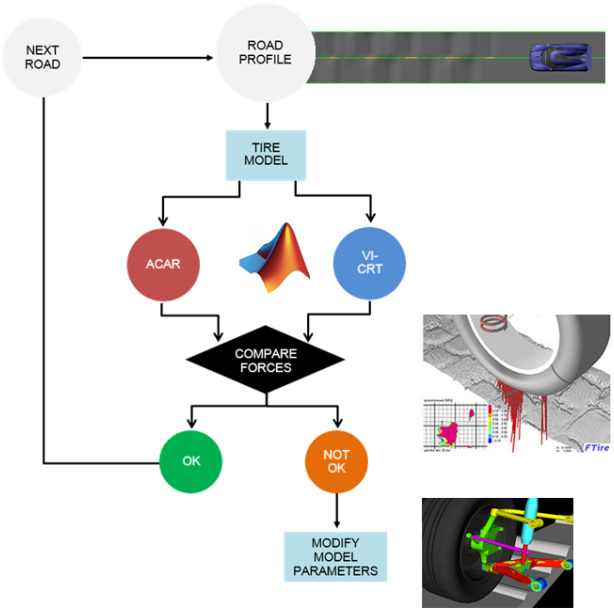


Figure 2.10: *ACAR and VI-CarRealTime Comparison Process Flow*

The simulations are performed according to the steps below. The process is also illustrated in the flowchart in Figure 2.10. The order of road surface complexities are further discussed in section 3.2. The order of tire testing sequence is elaborated in section 2.6.

1. Select road profile
2. Set up ADAMS/Car and VI-CarRealTime
   (a) Choose tire model in the assembly
   (b) Set up the driving scenario
3. Parameter Comparison
   (a) F_x and F_z: average force, root mean square average force, maximum and minimum force
   (b) Velocity versus displacement graph: to ensure vehicles in both simulations are travelling at the same velocity
4. If the forces are comparable, repeat simulation with a more sophisticated road surface if possible, otherwise test with a more complex tire model.

2.6 Tire Models Used in Simulation

A variety of tire models based on unique modeling approaches are available in the VI-CarRealTime, ADAMS/Car, and CEVT databases. In order to limit the number of simulations being performed, only Pacejka tire and FTire tire models are considered in this thesis. Table 2.1 summarizes the capability of the two tire types.

Pacejka tire is chosen for several reasons. First, Pacejka tire is the original tire used in the demo model. Not making any modifications to the demo model would allow the most basic comparison between ADAMS/Car and VI-CarRealTime with minimal chance of user error. However, there are limitations to Pacejka tires. For example, Pacejka tire fails during simulation initiation on complex `.rgr` roads and with high frequency inputs.

FTire is selected as it is the standard tire used for simulation at CEVT. Hence, the final goal is to compare the software with vehicle models using FTire. Demo FTire `ftire_205_55R16.tir` from ADAMS/Car database with two additional FTires from the CEVT database, the Pirelli `235_45R20.tir` and the Continental `225_40R19.tir`, are tested in this thesis. Details on these tire properties can be found in Appendix section A.2.

Table 2.1: Tires vs. Roads

	Pacejka	**FTire**
Flat 2D	Yes	Yes
Cleat	Yes	Yes
Washboard	No	Yes
Silver Creek	No	Yes
Tile Road *(Belgian Block)*	Yes	Yes

3 Theoretical Analysis

3.1 Theoretical Validation

This section attempts to provide a theoretical view regarding the results illustrated by both software. Since normal and longitudinal wheel forces are the two main output parameters considered throughout this thesis, theoretical validation is performed for these two outputs with the simplest test scenario: VI-CarRealTime Demo Model with Pacejka 96 tires driving on a flat road with a constant velocity of 40 kph.

3.1.1 Theory

The calculation of normal forces has been simplified to a static normal force distribution and the influence of drag force. The acceleration component reduces to zero since the velocity is constant. The following free body diagram illustrates the forces involved. For a more detailed understanding, it is recommended that one refers the Vehicle Dynamics Compendium [8].

It should be noted that the force calculations are considered per axle, not per wheel. The individual wheel forces have been calculated using the equations below where the drag force is assumed to be equally distributed among the wheels. All these assumptions and simplifications result in the following set of relations as in Equation 3.1 for normal forces.

$$\begin{aligned} F_{zf} &= m \cdot g \cdot l_r/L - F_{air} \cdot h_{air}/L \\ F_{zr} &= m \cdot g \cdot l_f/L + F_{air} \cdot h_{air}/L \\ F_{zfl} &= F_{zfr} = F_{zf}/2 \\ F_{zrl} &= F_{zrr} = F_{zr}/2 \end{aligned} \tag{3.1}$$

The longitudinal forces are calculated using the road load power relation as in Equation 3.2. In short it is the difference between propulsion force and resistance force, which includes the drag and rolling resistance. The vehicle in consideration is rear wheel driven.

$$\begin{aligned} F_{xfl} &= F_{xfr} = F_{roll} + 0.25 * F_{air} \\ F_{xrl} &= F_{xrr} = (0.5 * Power_{Engine}/v) - (F_{roll} + 0.25 * F_{air}) \end{aligned} \tag{3.2}$$

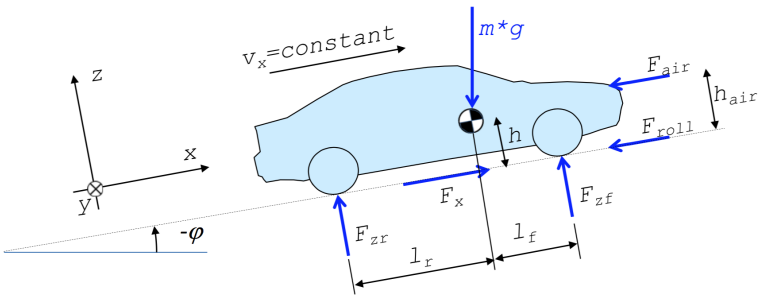


Figure 3.1: *Vehicle Free body diagram [8]*

Table 3.1: Vehicle Variables

Parameter	**Value**	**Unit**	**Description**
m	1279	kg	Total Vehicle mass
L	2920	mm	Vehicle Wheelbase
lf	1566.29	mm	Centre of gravity distance to front wheel
lr	1353.71	mm	Centre of gravity distance to rear wheel
h_{cg}	413.4	mm	Centre of gravity height
h_{air}	319.5	mm	Drag force location
F_{air}	51.3	N	Drag Force
g	9.81	m/s^2	Acceleration due to gravity
v	11.11	m/s	Vehicle velocity
$F_{z_{fl}}$, $F_{z_{fr}}$, $F_{z_{rl}}$, $F_{z_{rr}}$	–	N	Calculated Normal forces for individual wheels
$F_{x_{fl}}$, $F_{x_{fr}}$, $F_{x_{rl}}$, $F_{x_{rr}}$	–	N	Calculated Longitudinal forces for individual wheels
F_{roll}	–	N	Rolling resistance force

Figures 3.2 and 3.3 illustrate the variation of both normal and longitudinal forces using ADAMS/Car, VI-CarRealTime, theoretical calculation using ADAMS/Car output variables *(Theory ACAR)* and theoretical calculation using VI-CarRealTime output variables *(Theory VI)*. The differences between the theoretical and the software values are not significant. These can be attributed to the fact that the theoretical calculation is a simplified model and does not consider the effect of pitch and rotational inertia effects on the loads.

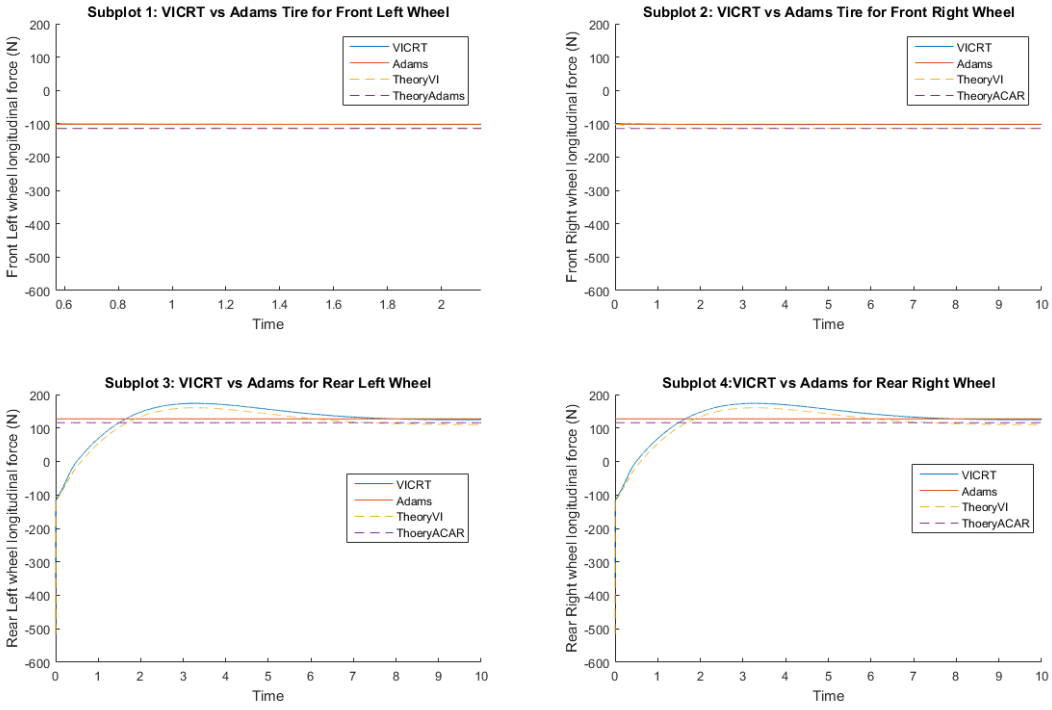


Figure 3.2: *Vehicle Longitudinal forces in Newton*

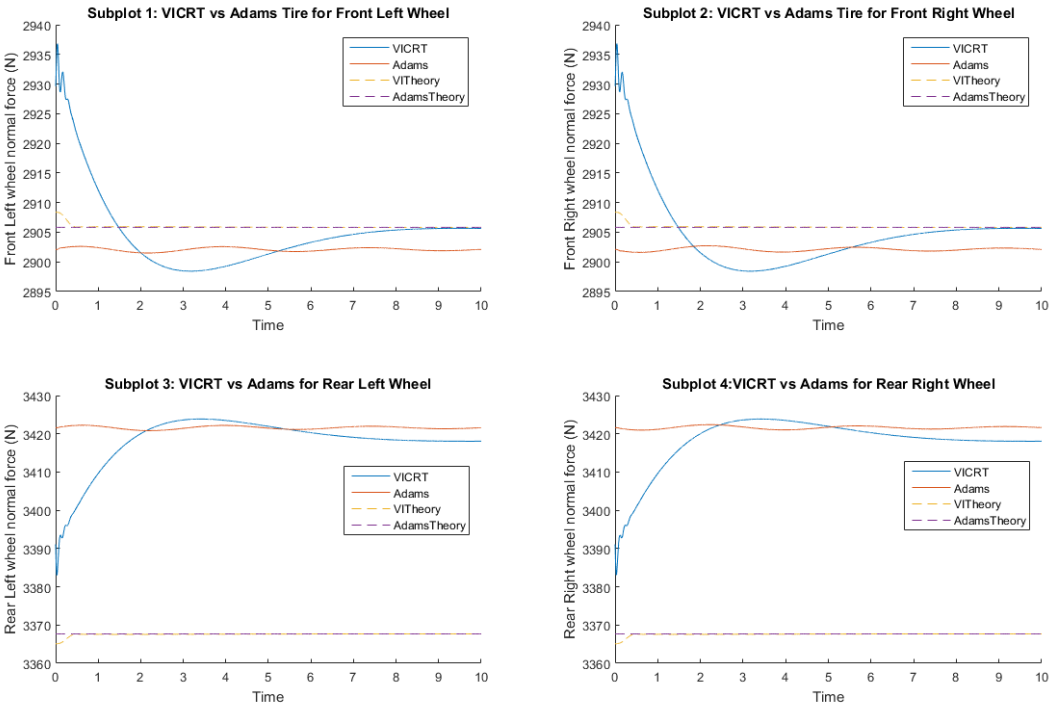


Figure 3.3: *Vehicle Normal forces in Newton*

3.2 Road Profiles

Simulations are performed in increasing order of road model complexity levels. Besides the obvious reasoning, if simple roads, such as flat and cleat, do not produce the expected forces, this gives strong indication that flaws in software setup or vehicle model exists. Moreover, simple roads are faster to compute than more complex roads.

The simplest road is the "Flat 2D", which is as the name suggest - a straight flat path, and given its simplicity simulation time is the shortest. Hence, this road profile is always used in initial testing to ensure simulation is correctly set up.

The cleat road is a flat road with a single 10 mm tall by 50 mm wide obstacle perpendicular to the path of the vehicle, as shown in Figure 3.4a. Since the two software have dissimilar driver models, results generated by the two software have slightly different starting time and offset starting point in the vehicle travel path. A spike in normal and longitudinal tire forces as the wheel travels over the bump can be easily identified, helping alignment of data sets for easier visual comparison.

Washboard road features continuous sinusoidal bumps. Two versions of the washboard road exists: in-phase and out-of-phase. In-phase washboard, shown in Figure 3.4c, means the left and right wheels are travelling up-and-down the ridge simultaneously, while out-of-phase washboard means the left and right wheels are traveling over a bump in opposite motion.

Silver Creek is a more advanced straight road. It contains both harmonic oscillation sections and stochastic sections. The stochastic section is presented in Figure 3.4d.

Lastly, the most complicated roads in this category are the Hipped Tile and the Belgian Block. Hipped tile consists of a short straight flat section followed by a circular track with stochastic tiled ground. Belgian Block is a S-curved road with tile surface.

3.3 Power Spectral Density

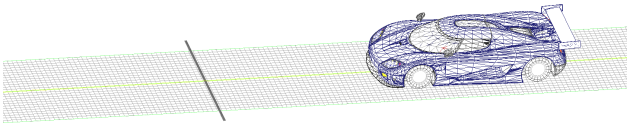
While single frequency road models are useful at understanding the harmonic behavior of the vehicles, multiple frequency roads resemble real world roads. To quantitatively classify various road surfaces tested in this thesis and to ensure a wide spectrum of road disturbances are covered in the simulation, a "Power Spectral Density" plot is shown in Figure 3.6b. The x-axis represents spatial angular frequency Ω and the y-axis is the the power spectral density Φ governed by Equation 3.3.

$$\Phi(\Omega) = \Phi_0 \cdot (\frac{\Omega}{\Omega_0})^{-w} \tag{3.3}$$

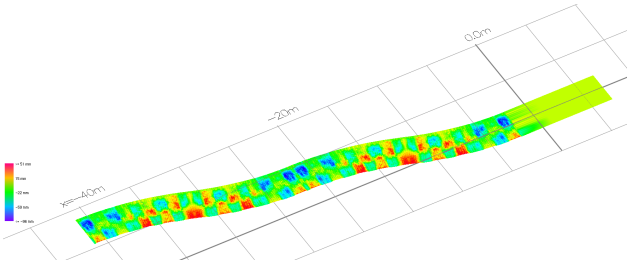
The power spectral density lines for the washboard and Silver Creek are derived using Matlab code "One dimensional surface roughness power spectrum" written by Mona M Kanafi [9]. "Smooth", "Rough", and "Very Rough" road lines from Figure 3.6a are translated into spatial frequency space with the following values [8]:

- Smooth Road: $\Phi_0 = 1 \cdot 10^{-6}$, $w = 3$
- Rough Road: $\Phi_0 = 10 \cdot 10^{-6}$, $w = 2.5$
- Very Rough Road: $\Phi_0 = 100 \cdot 10^{-6}$, $w = 2$
- $\Omega_0 = 1$

Using the road severity lines in Figure 3.6b as guidance, the washboard track shows a combination of smooth and very rough sections. This is because the spacing between the ridges is not consistent, as it will be demonstrated later in section 4.7.1. The rough road section is made up of close-together ridges, and the smooth section consists of peaks set far apart. On the other hand, the Silver Creek track mostly consists of rough and very rough roads according to the Power Spectral Analysis. This is in agreement with the photograph of the track in Figure 3.4d.



(a) *Cleat Road ISO view*



(b) *Belgian Block*



(c) *Ford Washboard Section*



(d) *Ford Silver Creek Test Track*

Figure 3.4: *Road Profiles*

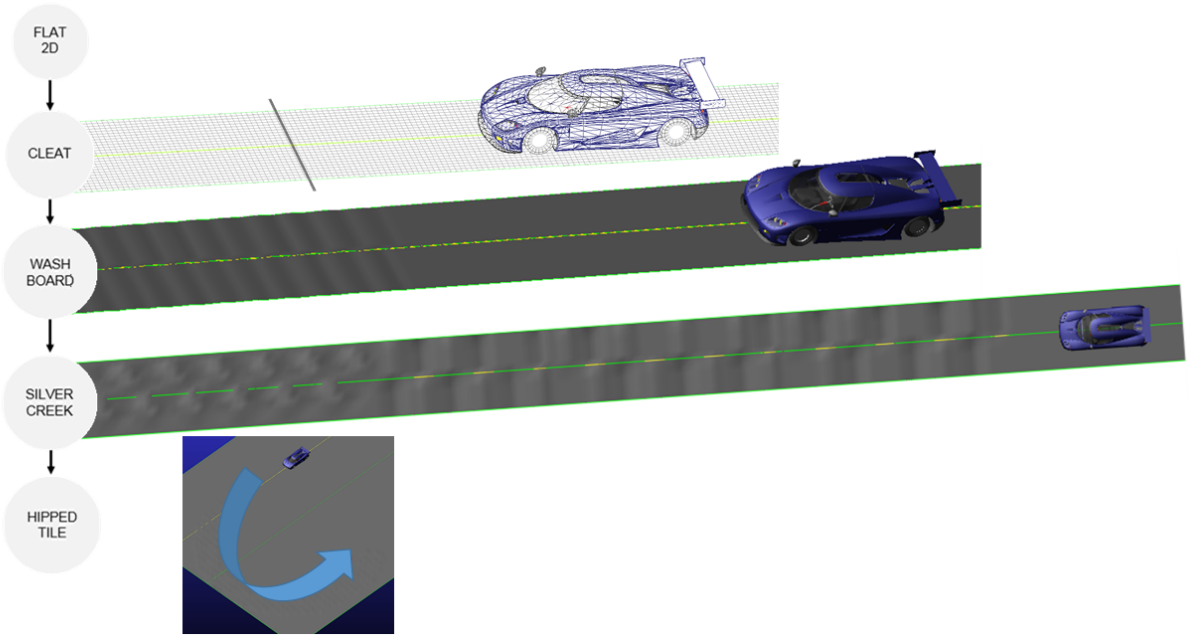
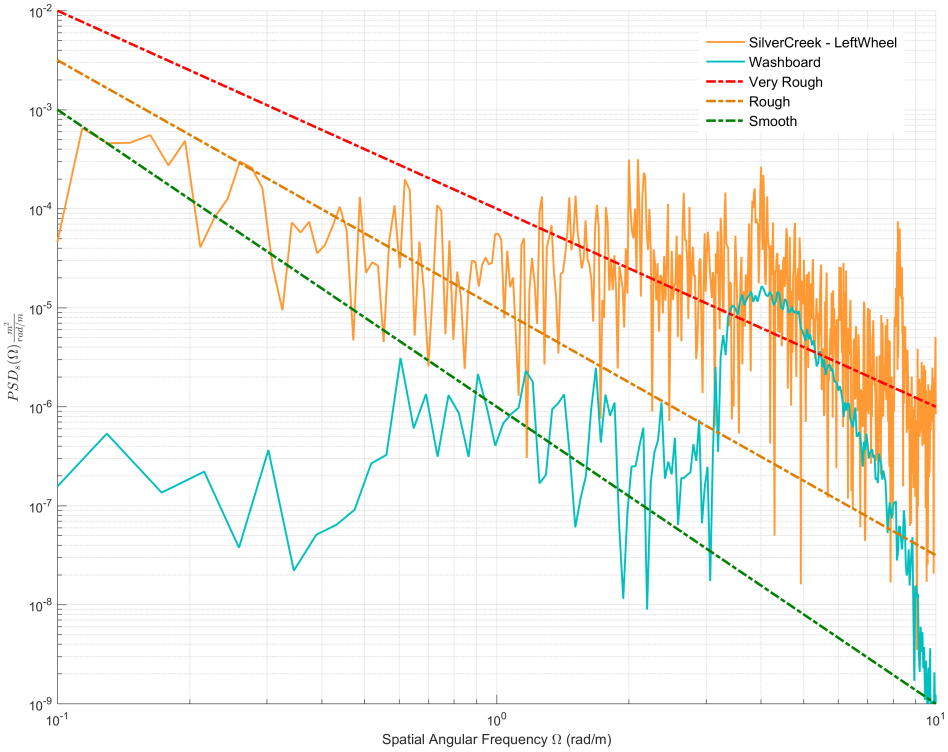


Figure 3.5: *Road Profiles Testing Sequence*



(a) *Four Typical Road Types [8]*



(b) *Power Spectral Density of Roads*

Figure 3.6: *Catagories of Road Surfaces*

4 Demo Vehicle Results

4.1 Integration Step Size Comparison

MBD system of equations are usually solved using numerical integration. Various integration methods exist which use a constant step size *(Runge Kutta)* or adaptive step size *(Runge Kutta Fehlberg)*. The choice of the right integration step size is important. Too large of a step size will not deliver the required detail and an extremely small step size will involve lengthy simulation times. ADAMS/Car uses the GSTIFF integrator as default while the Runge-Kutta method is used in VI-CarRealTime.

Simulation engineers at CEVT have been using 1000 steps per second for ADAMS/Car. Despite this standard, finer and coarser step sizes are checked to ensure the best results.

1. 10,000 steps (integration step size = 0.0001)
2. 1,000 steps (integration step size = 0.001)
3. 100 steps (integration step size = 0.01)

Integration step sizes will also be checked to determine the fastest permissible time step in VI-CarRealTime while still delivering accurate results.

VI-CarRealTime simulation provide users with the freedom of choosing both the integration step size and the output step size. In other words, calculation can be performed at a fine step size, but the results can be recorded at larger time interval. This way result file size can be cut down without sacrificing computation accuracy. Naturally, output step size must be larger or equal to simulation step size. Five different combinations of simulation and output step sizes are considered here.

1. Integration step = 0.0001, time output step = 0.0001
2. Integration step = 0.001, time output step = 0.001
3. Integration step = 0.01, time output step = 0.01
4. Integration step = 0.0001, time output step = 0.001
5. Integration step = 0.001, time output step = 0.01

The integration step size comparison tests are performed with the following simulation set ups. The cleat road is chosen since it includes only a single obstacle and the force peak can be easily analyzed in isolation.

- Road: Cleat road (`Cleat10x50mm.crg`)
- Model: Demo model
- Tire: Demo Ftire
- Driving Event: 3rd gear with no shifting, straight line, 3 seconds at 72 kph

4.1.1 VI-CarRealTime

First, integration time step in VI-CarRealTime is kept at a constant value of 0.0001, and output time step are varied between 0.01, 0.001, and 0.0001. As described previously, the primary motivation to keep a coarse output step size is to reduce the result file size, which lessens storage usage and improves post-processing time.

VI-CarRealTime does not permit combination of 0.0002 integration step size and 0.001 output step size. To avoid possible confusion during post-processing, both ADAMS/Car and VI-CarRealTime results output frequency is in powers of 10.

Figure 4.1 shows time output bigger than 0.001 seconds will not capture all the tire forces. Reducing the output time step size finer than 0.001 seconds will not capture any meaningful additional information. The simulation run time and file size comparison between different output step sizes are presented in Table 4.1.

Secondly, integration step sizes are also investigated. The comparison between 0.0001 second and 0.001 second integration step sizes is shown in Figure 4.2. Data line of the finer integration time step is slightly

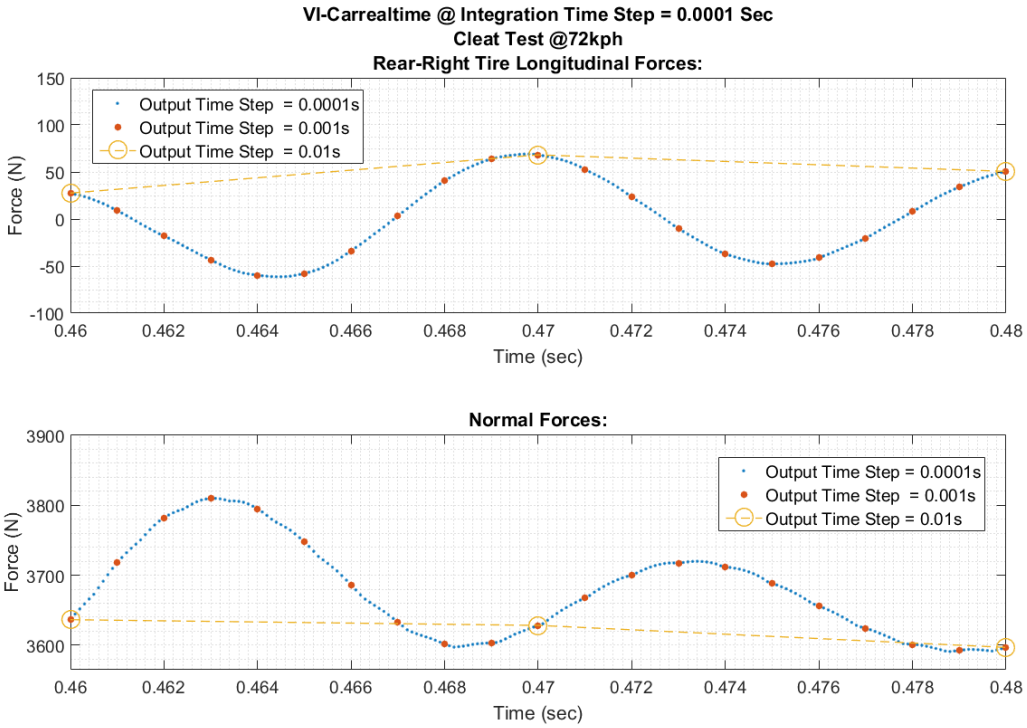


Figure 4.1: *Rear-Right Tire Center Forces*

Table 4.1: VI-CarRealTime Output Step Size vs. File Size Comparison

Integration Step Size	**Output Time Step**	**ADAMS/Car**		**VI-CarRealTime**	
		Run Time (s)	File Size (Mb)	Run Time (s)	File Size (Mb)
0.0001	0.0001	451	438.8	147	223
0.0001	0.001	N/A	N/A	124	22.4
0.0001	0.01	N/A	N/A	117	2.3

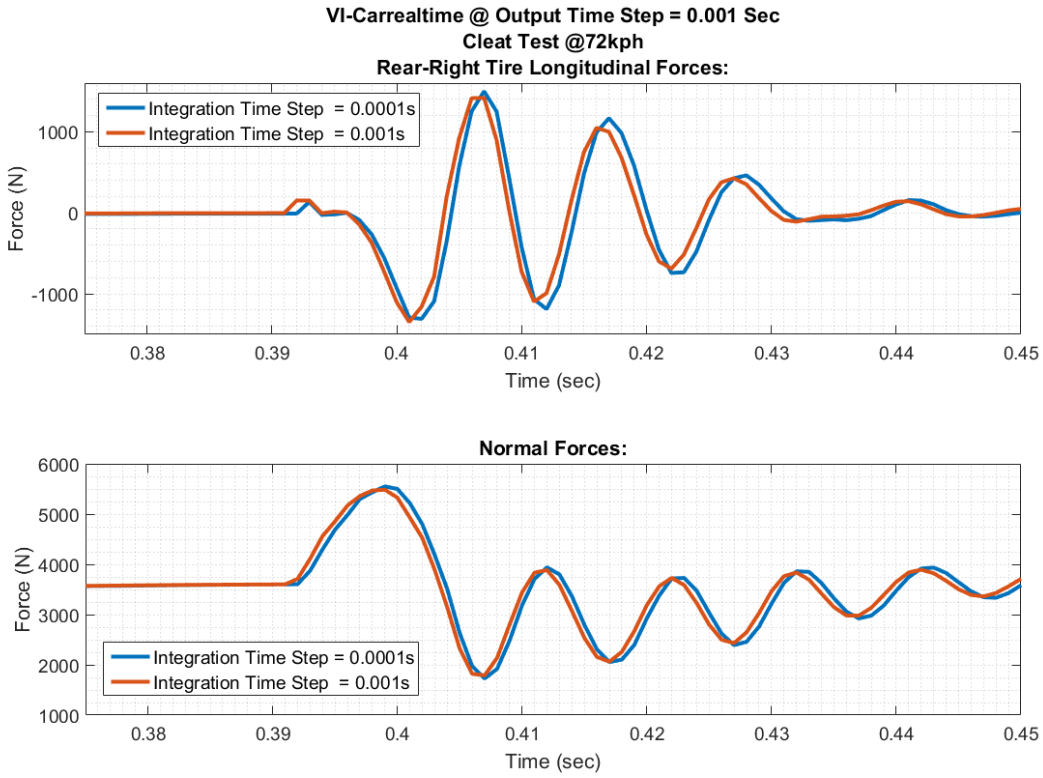


Figure 4.2: *Longitudinal Force*

lagging behind the 0.001 integration time step data line. The reason is likely due to the Pacejka tire model. The magnitude between the data lines are nearly identical. Integration step size and output step size of 0.001 seconds is recommended for VI-CarRealTime.

It is worth noting that according to VI-CarRealTime user manual, the integration step size should be no greater than the maximum time step indicated in the FTire `.tir` file. For the demo FTire the maximum allowable time step is 0.0002. Cosin Tire tool also indicates that using simulation step size larger than the maximum allowable time step will be ignored by the FTire solver.

4.1.2 ADAMS/Car

For ADAMS/Car, having an approperiate integration step size is just as important as it is for VI-CarRealTime, as the simulation time is much longer with ADAMS/Car. Any integration step size greater than 0.001 would not capture all the peak forces, as shown in Figure 4.3.

Integration time step size of "0.0001" and "0.001" captured highly comparable tire forces. Therefore using "0.001" step size is defended, as it avoids unnecessary computation time and large file size.

Unlike VI-CarRealTime, ADAMS/Car does not have the option to output results directly in Matlab data format. Given that Matlab is a more powerful and more convenient data analysis tool than ADAMS/Post-Processing or VI-Animator tool, ADAMS/Car results must be converted into Matlab format. Thankfully, ADAMS/Car and VI-CarRealTime shares the same result file format, and the `resreader.mex` function that is part of the VI-CarRealTime installation package has been used for file conversion. However, at the time of writing, the `resreader.mex` function cannot convert ADAMS/Car `.res` file larger than 2GB due to a software bug. Consequently, numerous hours have been devoted into programming a Matlab script that would convert larger `.res` files. The full code can be found in the Appendix section A.1.

4.1.3 Cleat Test Integration Step Size: VI-CarRealTime versus ADAMS/Car

The experimented simulation time logs and `.res` file sizes are tabulated in Table 4.2. Tire forces computed by VI-CarRealTime and ADAMS/Car, both using the suggested 0.001 time step size, are plotted in Figure

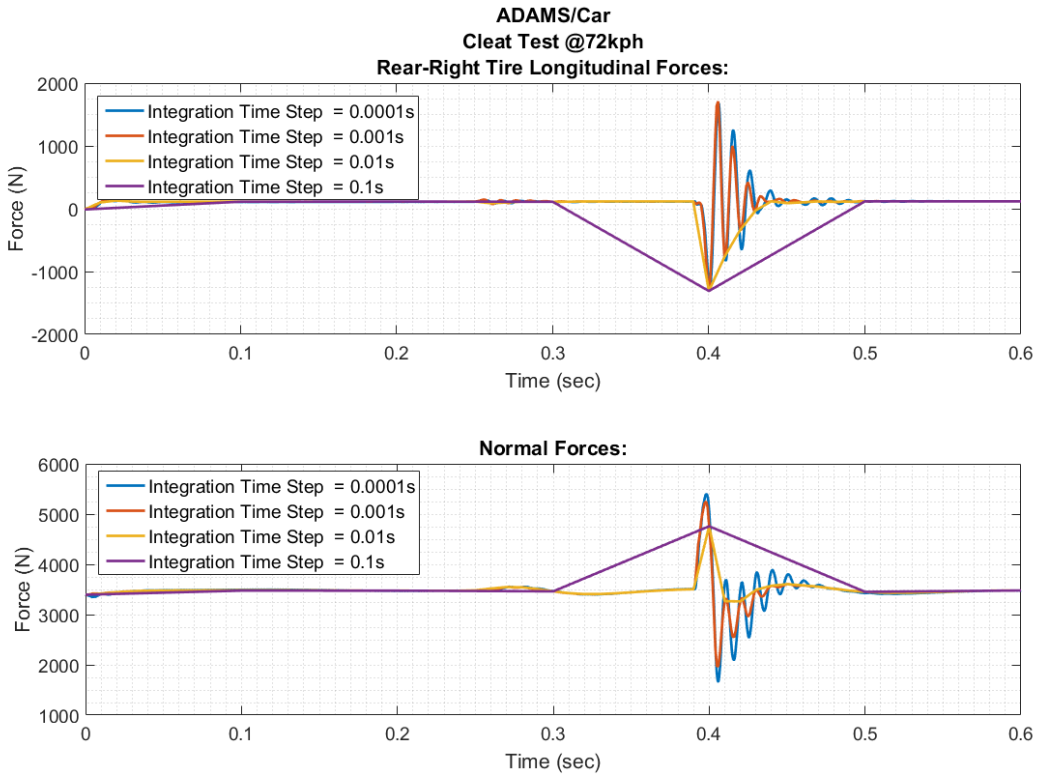


Figure 4.3: *ADAMS/Car Integration Steps Sizes*

Table 4.2: ADAMS/Car and VI-CarRealTime Output Step Size vs. File Size Comparison

Integration Step Size	**Output Time Step**	**ADAMS/Car**		**VI-CarRealTime**	
		Run Time (s)	File Size (Mb)	Run Time (s)	File Size (Mb)
0.0001	0.0001	451	438.8	147	223
0.001	0.001	??	45.5	52	22.4
0.001	0.01	N/A	N/A	49	2.3
0.01	0.01	??	4.8	N/A	N/A
0.1	0.1	??	0.5	N/A	N/A

4.4. Noting the shape and magnitude of the force graphs, the step size chosen has managed to capture the necessary force data.

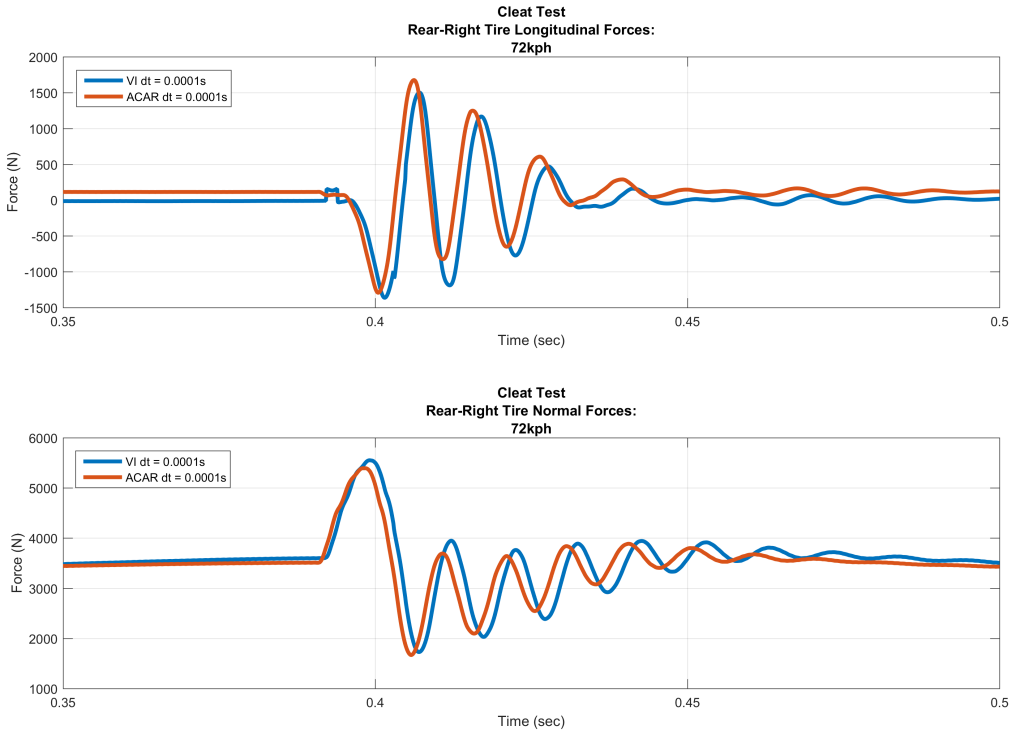


Figure 4.4: *ADAMS/Car vs. VI-CarRealTime with 0.001 Integration Step Size*

4.2 Demo Model with Pacejka Tire Results

In this section, the Demo model is paired up with the Pacejka 2002 tire model instead of the Pacejka 96 tires, which have already been tested on the flat road and the results are presented in section 3.1.

- Model: Demo model
- Tire: Pacejka 2002, front wheel: 30.35 kg, rear wheel: 35.31 kg
- VI-CarRealTime
  - Integration step size: 0.001
  - Output step size: 0.001
- ADAMS/Car
  - Step size: 0.001

4.2.1 Flat Road

The demo vehicle is simulated in VI-CarRealTime and in ADAMS/Car with the following event settings. This is the most basic simulation comparison between ADAMS/Car and VI-CarRealTime and it has several important advantages.

- Road: Flat road (`flat.rdf`)
- Driving Event: 3rd gear with no shifting, straight line, 10 seconds at 40 kph (11111.11 mm/s), maintain initial velocity

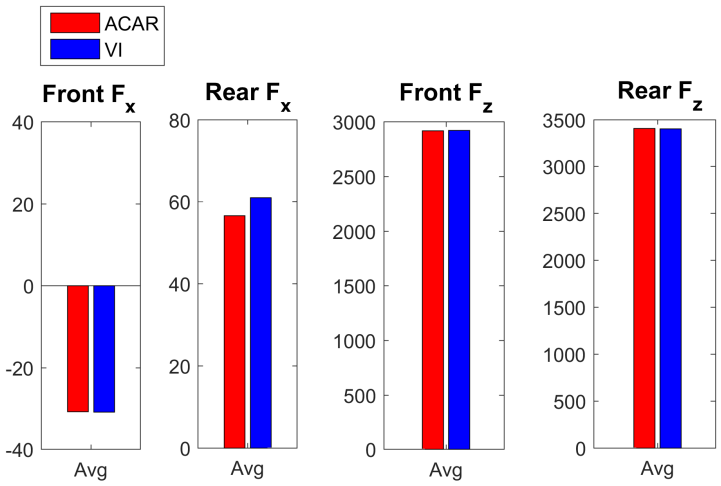


Figure 4.5: *Demo Model with Pacejka Tires: Flat Road Force Comparisons*

Firstly, the demo model exists in both ADAMS/Car (`.asy`) and VI-CarRealTime format(`.xml`). This is highly desirable as it avoids having to export the model from ADAMS/Car to VI-CarRealTime. An attempt was made later to export the demo model. The process is not straightforward. To correctly carry out the export procedure, which entails a series of static and dynamic suspension test rig analysis, it requires in depth understanding of the process and prior experience. It is assumed that the demo model does not contain any error.

The second motivation behind this simulation is to understand the work process and grasp a basic understanding in the differences between ADAMS/Car and VI-CarRealTime. For example, Figure 4.7 presents the differences between driver models. While ADAMS/Car maintained the velocity at 40 kph, the vehicle in VI-CarRealTime started at 40 kph but slowed down before accelerating back to the target velocity. This can be explained due to the different parameters of the longitudinal velocity controller.

The force differences between the software are small but not entirely negligible. For the given driving task, although not pushing the vehicle's performance envelope, yet the longitudinal forces between ADAMS/Car and VI-CarRealTime matched very well. The longitudinal force averages differed by less than one newton on the front axle and four newtons on the rear axle. Figure 4.7 also shows that on average ADAMS/Car has produced 2 N lower and 3 N higher normal forces on the front and rear axle than VI-CarRealTime respectively. Although both ADAMS/Car and VI-CarRealTime considers aerodynamic forces, difference in downforce calculations between the software could account for some of the discrepancies.

To improve graph's clarity and thanks to the vehicle model's high level of lateral symmetry, only forces from the left side of the vehicle is illustrated in Figure 4.7 and for the remainder of the thesis. The F_x and F_z results are compared in Figure 4.5, and results for all four tires are tabulated in Table 1 the Appendix.

4.2.2 Cleat Road

Simulation setting in VI-CarRealTime and in ADAMS/Car:

- Road: Cleat road (`Cleat10x50mm.crg`)
- Driving Event: 3rd gear with no shifting, straight line, 3 seconds at 40 kph (11111.11 mm/s), maintain initial velocity

The same driving event set up for the flat road is repeated on a cleat road. As aforementioned, the cleat road is a flat road with a 10 mm tall, 50 mm wide obstacle lying across the road. This road disturbance is reflected by the sharp force peak in Figure 4.8. Overall the forces between ADAMS/Car and VI-CarRealTime is highly comparable. Observations made from the flat road in section 4.2.1 can also be seen on the cleat road. Normal forces in ADAMS/Car are higher than those in VI-CarRealTime simulation.

In Figure 4.8 ADAMS/Car simulation also sees the longitudinal force on the rear wheel being 30 N higher than VI-CarRealTime's result. At first this appears contradictory to the longitudinal force results from the flat

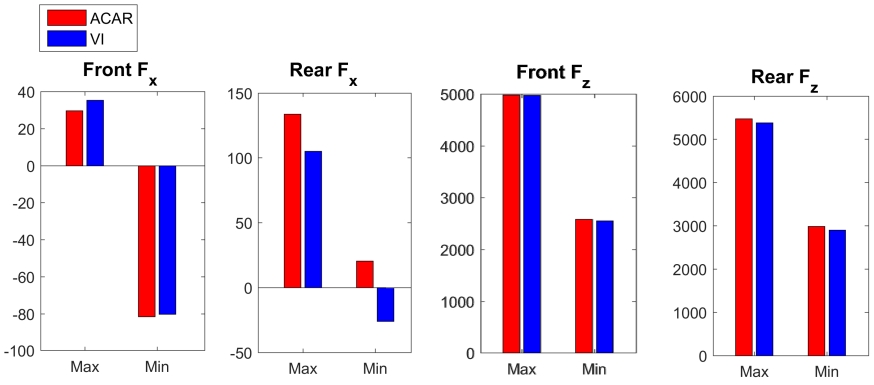


Figure 4.6: *Demo Model with Pacejka Tires: Cleat Road Force Comparisons*

road, but this is only a scaling issue. Closely examining the flat road results between the 4.5 to 9.5 m distance travelled, similar force differences are found.

The F_x and F_z results are plotted in Figure 4.5 and the exact values are stored in Table 4 in the Appendix.

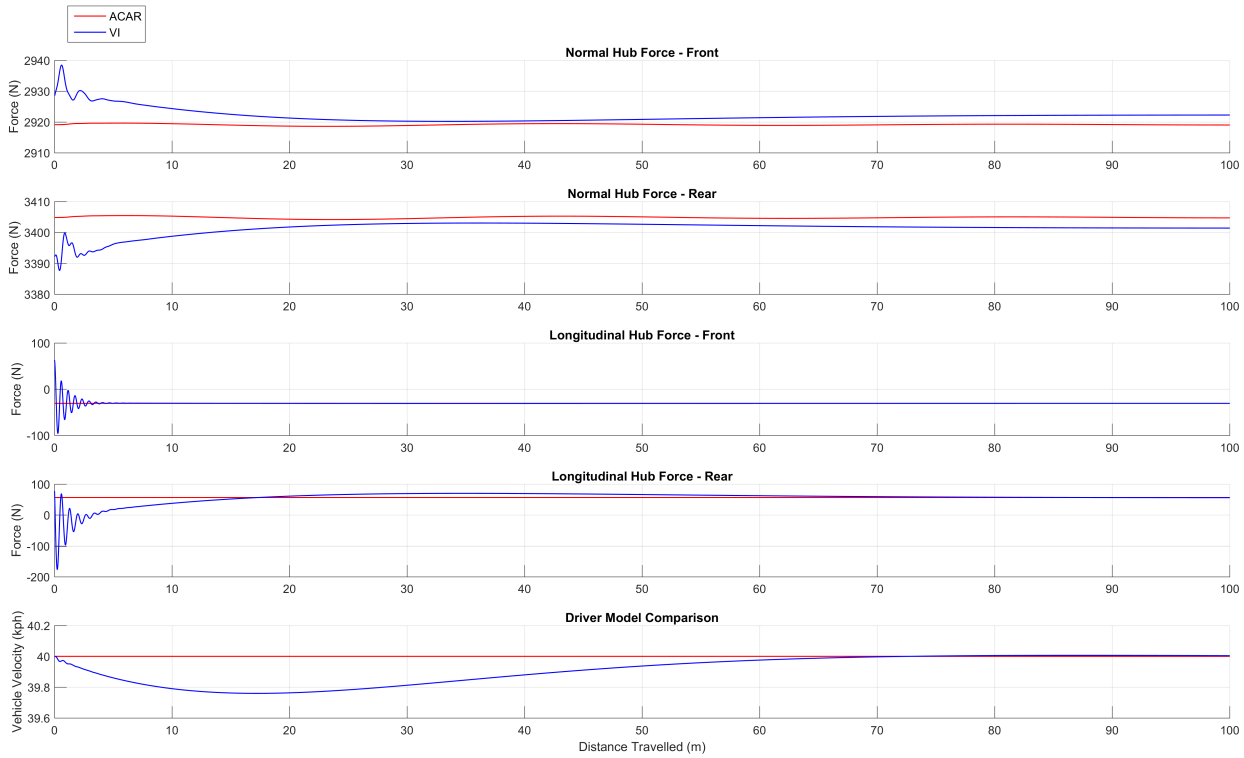


Figure 4.7: *Demo Model with Pacejka Tires: Flat Road Tire F_x and F_z Forces*

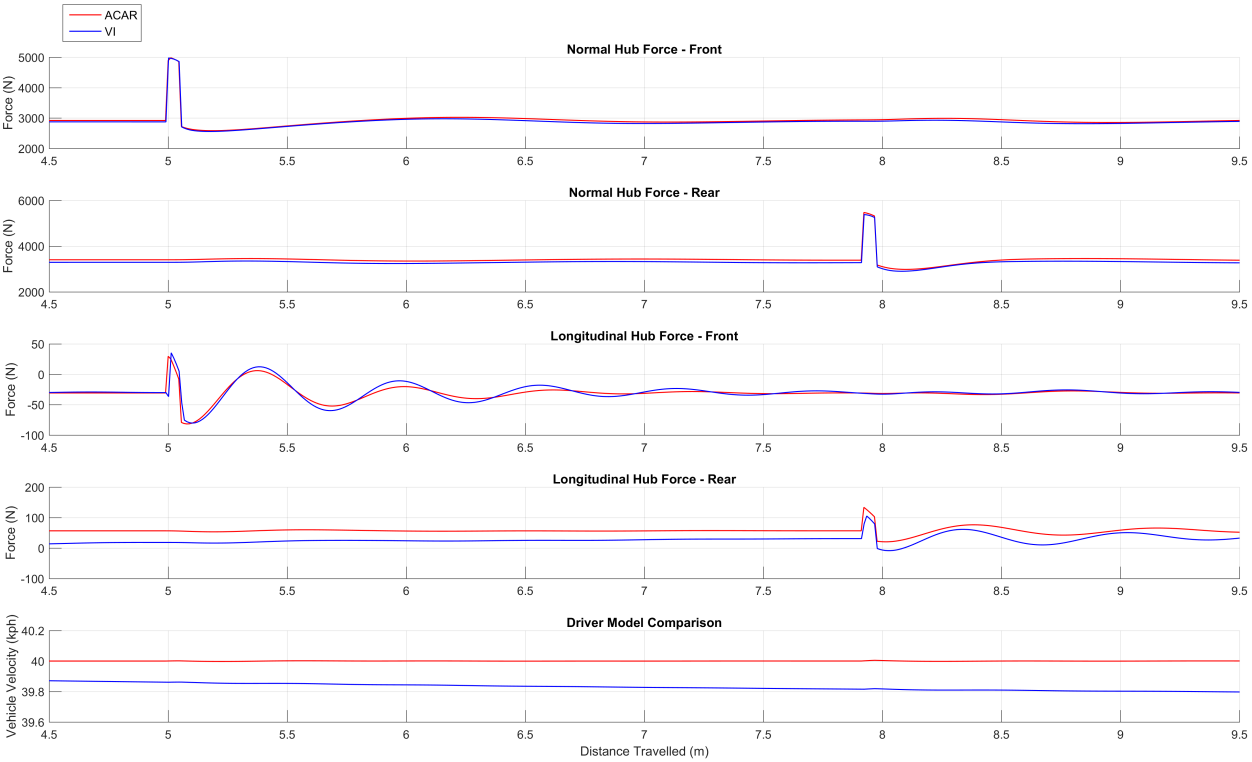


Figure 4.8: *Demo Model with Pacejka Tires: Cleat Road Tire F_x and F_z Forces*

4.3 Demo Model with Demo F-tire

- Model: Demo model
- Tire: `ftire_205_55R16.tir`
- VI-CarRealTime
  - Ftire run mode: 0
  - Integration step size: 0.001
  - Output step size: 0.001
- ADAMS/Car
  - Ftire run mode: 0
  - Step size: 0.001

Changing the tire model in ADAMS/Car is simply accomplished by pointing the tire model to a new file. When changing the tire model in VI-CarRealTime, in addition to selecting the new file, the wheel mass also need to be manually adjusted. The unsprung mass in VI-CarRealTime is the sum of the tire, rim and a proportion of suspension components, such as drive shaft, upper and lower control arm, and tie rod. Unsprung mass from the VI-CarRealTime user manual is defined below:

```
Unsprung Mass
It includes the mass of a single wheel and the portion of suspension masses
not belonging to sprung part.
```

According to the VI-CarRealTime user manual the unsprung mass is determined through a parallel wheel travel test on ADAMS/Car suspension test rig simulation. The test is carried out with and without gravity, and the difference in vertical load at zero jounce is the static unsprung mass. Unfortunately, this test could not be performed in accordance to the manual. Instead, Static Vehicle Characteristic analysis in ADAMS/Car is performed.

```
FRONT SUSPENSION CHARACTERISTICS
Suspension Description:
<carrealtime_shared>/subsystems.tbl/VI_FrontSusp.sub
------------------------------------------------------------------------

(PARAMETER) (UNITS) (AVERAGE) (LEFT) (RIGHT)
------------------------------------------------------------------------
Unsprung mass (total) kg 50.00
Wheel hop natural freq. Hz 17.19 17.19 17.19

REAR SUSPENSION CHARACTERISTICS
Suspension Description:
<carrealtime_shared>/subsystems.tbl/VI_RearSusp.sub
------------------------------------------------------------------------

(PARAMETER) (UNITS) (AVERAGE) (LEFT) (RIGHT)
------------------------------------------------------------------------
Unsprung mass (total) kg 50.00
Wheel hop natural freq. Hz 16.40 16.40 16.40
```

An excerpt of the analysis is shown here, and the results indicate the wheel mass for all four wheels should be 25 kg. The accuracy of the result from the Static Vehicle Characteristic analysis is disputable. From the tire file data, the tire mass is 9.37 kg + 7.51 kg of 'free tire mass', which adds up to 16.88 kg, and based on Table 4.3 the front and rear suspension components weights are 9.96 kg and 24.42 kg, respectively. Since rear

Table 4.3: Demo Vehicle Suspension Component Weight

	Front Suspension *(kg)*	Rear Suspension *(kg)*
tripot		1.99
drive_shaft		4.22
spindle	1.1	1.1
lower_strut	1	5
upper_control_arm	1.03	1.03
tierod	0.67	1
upper_strut	1	5
upright	1.4	1.33
lower_control_arm	1.71	1.71
arb	1.68	1.68
droplink	0.37	0.37
Total	**9.96**	**24.42**

suspension components are much higher than the front due to heavier upper and lower struts, higher rear unsprung mass was expected.

Trial and error method was used to guess the correct unsprung mass. A Matlab script was written to loop VI-CarRealTime simulation on the washboard track while changing the wheel mass by three kilogram each time. The sweep was carried out with the following parameters:

- Road: sine road, maximum amplitude 10 mm, distance between peaks (λ) 1000 mm
- Model: Demo model
- Tire: Demo Ftire
- Front and Rear Wheel Mass: from 16 to 40 kg at an increment of 3 kg
- Driving Event: 3rd gear with no shifting, straight line, 5 seconds at 45 kph (12500 mm/s), maintain initial velocity

The results from the wheel mass sweep is presented in Figure 4.9. Visually inspecting the figure it can be seen that 22 kg and 25 kg wheel masses produced close match to ADAMS/Car simulation's tire normal forces. Wheel mass lesser than 22 kg will result in mismatch with ADAMS/Car's tire normal force. Increasing the rear wheel mass above 25 kg will create a significant jump in rear tire forces. 25 kg was used for both front and rear wheels in VI-CarRealTime, as it produced good results, especially on the washboard track, as shown in upcoming section 4.4.3.

```
ftire_205_55R16.tir

 $----------------------------------------------------------------MASS_CORRECTION
[MASS_CORRECTION]
$these data are not used by FTire, but only by the calling solver
 free_tire_mass =                  7.51307               $ kg

 $-----------------------------------------------------------------------------DATA
[FTIRE_DATA]
$.....................................................basic data and geometry
 tire_mass =                       9.37                  $ kg
```

4.4 Ftire Specific Settings in VI-CarRealTime

Ftire specific VI-CarRealTime settings were not realized early enough, and thus it resulted in great productivity loss. In order to properly run simulations with Ftire in the VI-CarRealTime model, these settings are described

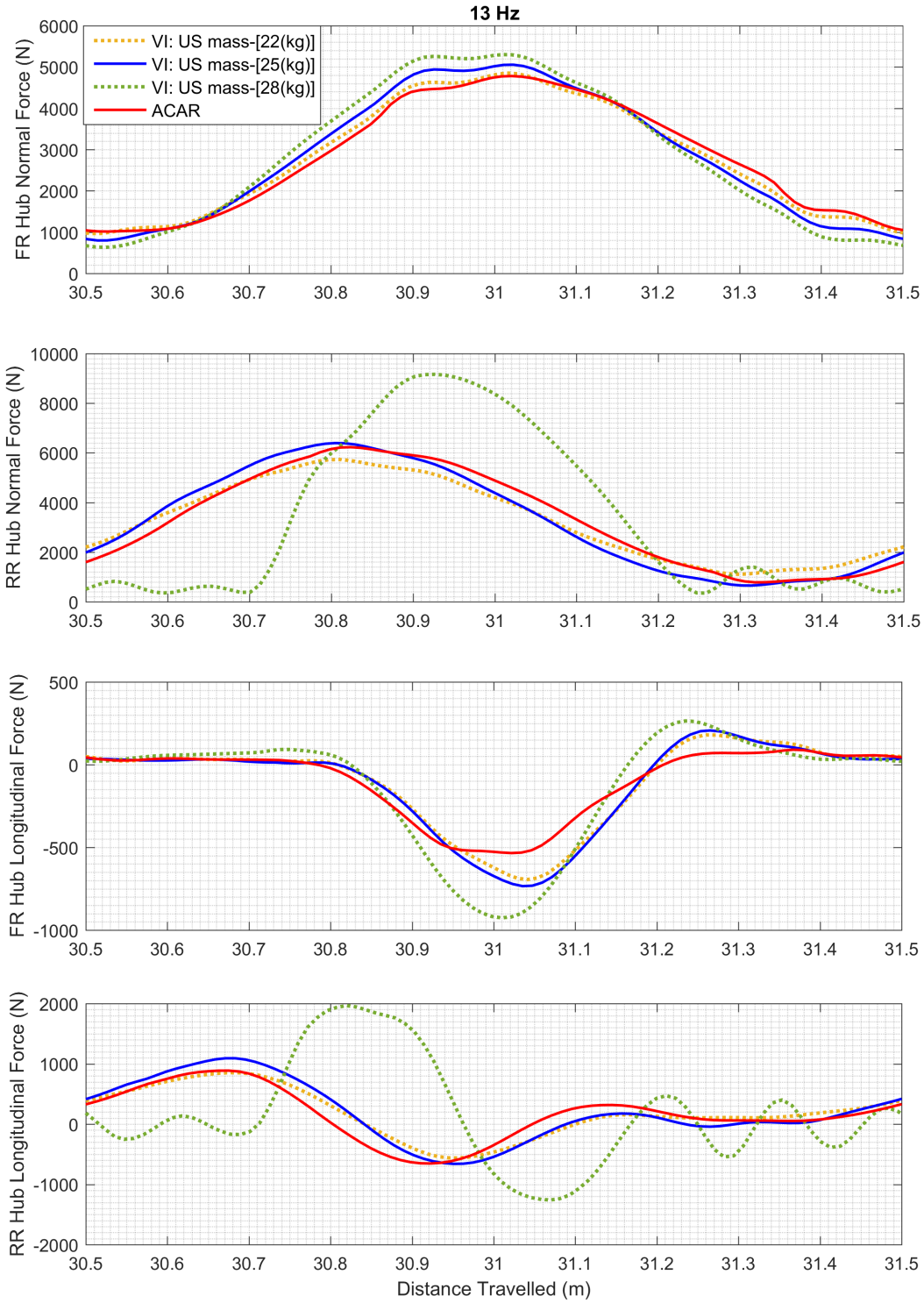
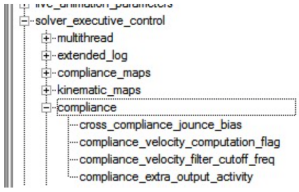


Figure 4.9: *VI-CarRealTimeUnsprung Mass Sweep*



Name	Value
cross_compliance_jounce_bias	1.0
compliance_velocity_computation_flag	1
compliance_velocity_filter_cutoff_freq	20.0
compliance_extra_output_activity	0

Figure 4.10: *VI-CarRealTime Ftire Settings: Compliance Model*

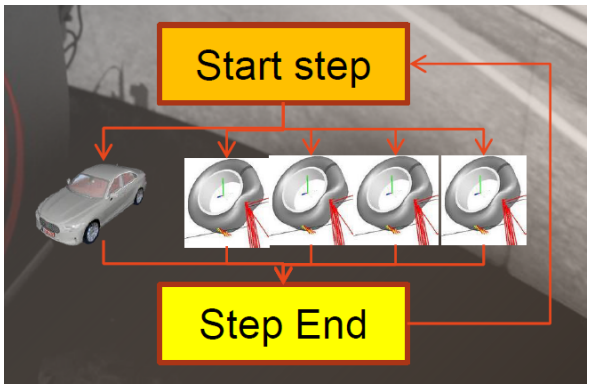


Figure 4.11: *Ftire Parallel Computation*

under Chapter 5.15 - "Using FTire At Best In VI-CarRealTime" in the VI-CarRealTime user manual. The key parameter changes are highlighted here:

- Compliance Model: see Figure 4.10
  - `compliance_velocity_flag` is set from "0" to "1"
  - `compliance_velocity_filter_cutoff_freq` is reduced from 100 Hz to 20 Hz
- Parallel Computation:
  - `tire_calc_active_flag` is set from "0" to "1". This allows parallel ftire computation, meaning several time instances of the simulation can be solved simultaneous, as shown in Figure 4.11.
  - This switch reduces run time on washboard road from 367 seconds to 170 seconds.
  - This plays a major factor at improving the plausibility of real-time simulation.
- FTire Execution Mode:
  - `run_time_mode` is set from "0" to "3". Five run modes are available from "0", standard mode, to "4", maximum acceleration.
  - "3" is the recommended setting per VI-CarRealTime user manual. Run mode acceleration is not possible in ADAMS/Car. A more in depth explanation from the Cosin Ftire user manual is provided in Figure 4.12.
  - Without parallel computation the simulation time is 64.7 seconds using run mode "3".
  - A combined utilization of parallel computing and run mode "3" reduced the simulation time to 49 seconds.
  - The forces measured on the washboard track varies slightly between the different run time modes as illustrated in Figure 4.13. Since tire force generated by run mode "0" matched most closely with that of ADAMS/Car and the simulation clock time is not significantly prolonged, run mode "0" is chosen instead of "3" for the demo Ftire.

4.4.1 Flat Road

Flat road simulation is performed using the same set up as the Pacejka tire, and the parameters are listed below:

- Road: Flat road (`flat.rdf`)
- Driving Event: 3rd gear with no shifting, straight line, 10 seconds at 40 kph (11111.11 mm/s), maintain initial velocity

run_time_mode	0,1,2,3,4	Set run-time speed mode (for speed modes > 1, an extra license key is required): **0** standard mode **1** acceleration level 1: no model extensions **2** acceleration level 2: no model extensions, no extra output **3** acceleration level 3: no model extensions, no extra output, coarse mesh **4** real-time mode: no model extensions, no extra output, coarse mesh, no TYDEX output

Figure 4.12: *Ftire Run Time Modes*

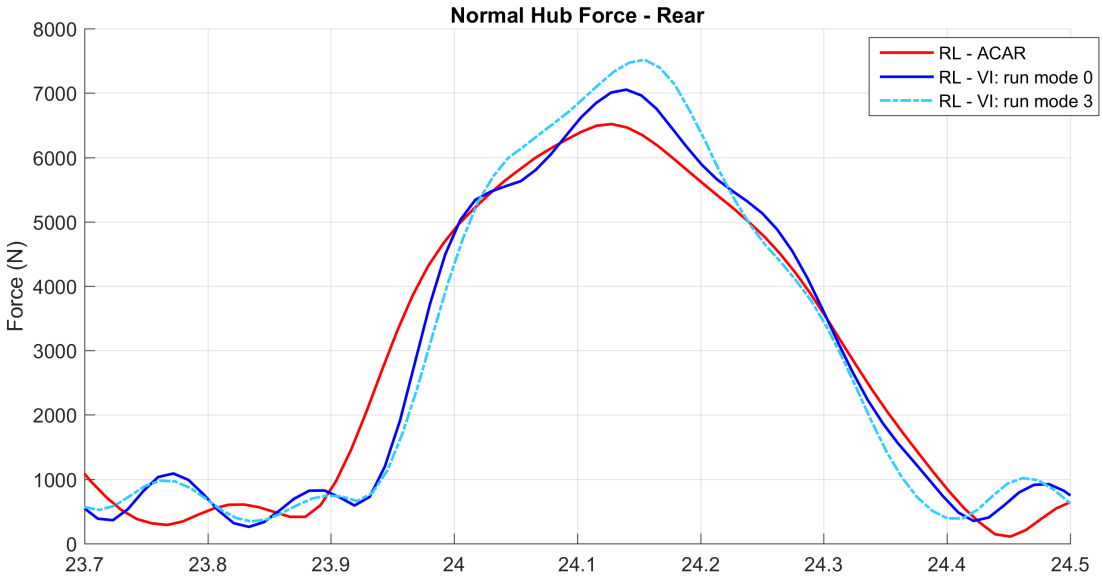


Figure 4.13: *Run Mode Comparison*

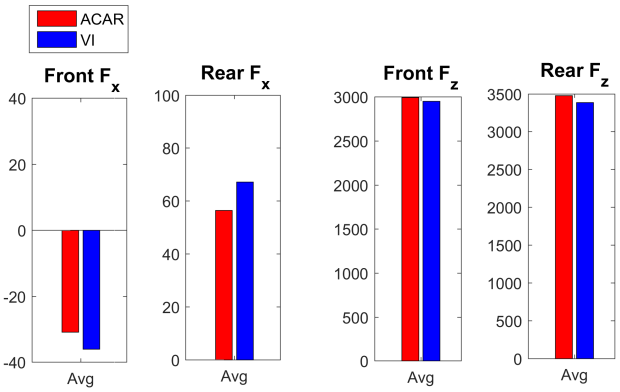


Figure 4.14: *Demo Model with Demo FTires: Flat Road Tire F_x and F_z*

Focusing on the normal tire forces, the values are similar to those observed with the Pacejka tires. Switching from Pacejka tire to Demo Ftire saw front wheel average normal force increased from 2919 N to 2993 N in ADAMS/Car and 2869 N to 2950 N in VI-CarRealTime. Similarly for the rear wheels, the normal forces rose from 3405 N to 3478 N and 3301 N to 3387 N for ADAMS/Car and VI-CarRealTime respectively. As shown in Figure 4.15 ADAMS/Car simulation found higher vertical loads than VI-CarRealTime on front and rear wheels. Overall, tire forces raised 79 N on average. The discrepancy between the software is 43 N for the front wheel and 91 N for the rear wheel, which does not pose as a concern for concept stage evaluations.

Likewise, differences on longitudinal tire force between ADAMS/Car and VI-CarRealTime grew slightly. Taking average tire F_x, the difference is 5 N and 11 N for front and rear wheels, respectively, which is negligible.

The force comparison are shown in Figure 4.14, and the results for all four tires are tabulated in Table 2 in the Appendix.

4.4.2 Cleat

Demo vehicle is simulated with demo Ftire on the cleat road with the following parameters:

- Road: Cleat road (`Cleat10x50mm.crg`)
- Driving Event: 3rd gear with no shifting, straight line, 3 seconds at 40 kph (11111.11 mm/s)

The tire force plots are presented in Figure 4.17. The x-axis of the plot has been cropped to show vehicle displacement from 4.5 m to 9.5 m, making it more clear that the distance between force peaks on the front wheel and rear wheel is approximately 3 m and corresponds to the wheel base of the vehicle. The shapes as well as the magnitude of the forces between the software resemble each other well. VI-CarRealTime captured slightly higher peak forces across the cleat. The complete results are tabulated in Table 5 in the Appendix.

4.4.3 Washboard

The washboard event is one of several dozen simulation cases at CEVT. An event is different from a simple test cases, such as driving straight on flat or cleat roads. It consists of one or more maneuvers, such as acceleration followed by braking. The event is originally stored in ADAMS/Car Event Builder `.xml` format.

Since ADAMS/Car and VI-CarRealTime have many shared file formats and other cross-software capabilities, one can utilize VI-Driver plug-in to use the VI driver model in ADAMS/Car, and conversely one can use the ADAMS/Car Driving Machine to use the ADAMS/Car driver model in VI. However, through communication with VI-CarRealTime technical director Christoph Ortmann it is strongly advised to avoid using ADAMS/Car Driving Machine in VI-CarRealTime. Therefore, the original event is reconstructed in VI-EventBuilder `.vdf` format.

The content of the VI-Driver Input `.vdf` file on the washboard track is summarized below:

- Road: Washboard road (`washboard_in_phase_ccw.rdf`)
- Driving Event: Maneuver 1

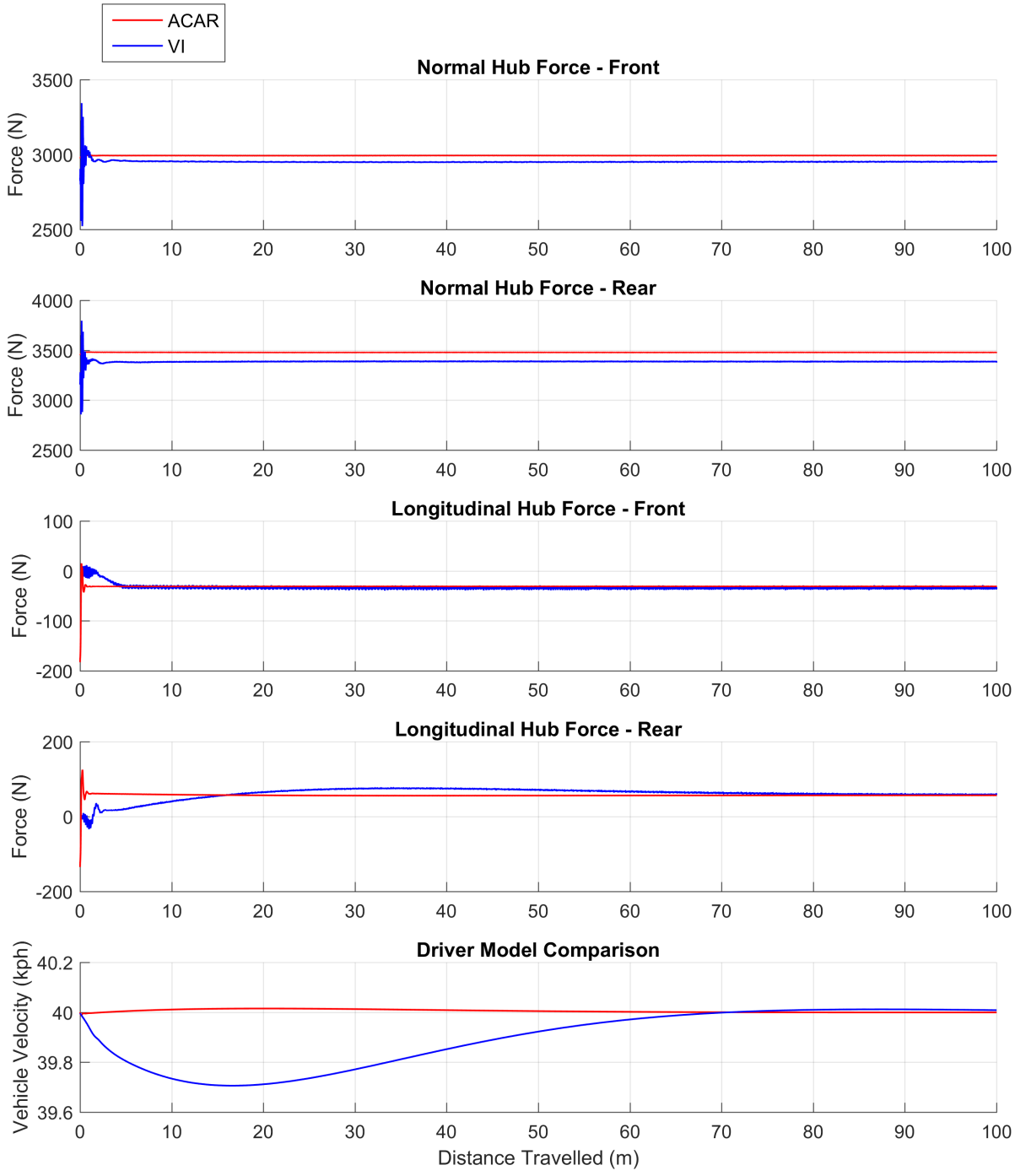


Figure 4.15: *Demo Model with Demo FTires: Flat Road Force Comparisons*

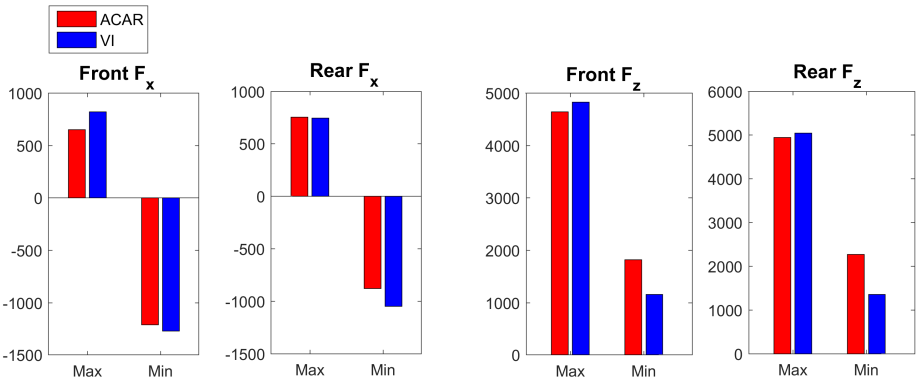


Figure 4.16: *Demo Model with Demo FTires: Cleat Road Tire F_x and F_z*

- 3rd gear with no shifting
- No clutch actuation
- Zero steering input
- Maintain velocity at 45 kph (12.5 mm/s)
- Throttle and braking machine controlled
- End condition when simulation time reaches 14.6 seconds

The washboard road has a sinusoidal road profile with increasing distance between consecutive peaks. This test track essentially performs an input frequency sweep on the vehicle and checks how well ADAMS/Car and VI-CarRealTime matches across the spectrum of frequencies.

The tire forces for the entire washboard track is presented in Figure 4.19, and forces from two parts of the washboard are displayed in Figure 4.20a and Figure 4.20b to allow closer examination. The overview figure indicates longer distance between consecutive peaks λ give rise to conforming ADAMS/Car and VI-CarRealTime tire forces. While maintaining constant vehicle velocity, increasing λ lowers road input frequency, and vice versa. Tire forces in ADAMS/Car and VI-CarRealTime are very comparable when λ is longer than approximately 1 m to 1.2 m for the front wheel and rear wheels, respectively. It should be noted that the washboard tire forces were matching poorly initially. The figures shown here are the results after long period of meticulously debugging and rectifying various software parameters as well as lengthening the washboard track's initial flat section. Detailed explanations behind these setting changes and road file modifications are found in section 4.7.

Average force plays an important roles in fatigue life estimations. In the washboard case the difference in average normal forces is less than 1%, while the average longitudinal forces differs by 36%. However, the longitudinal force differences are 25 N and 40 N on the front and rear wheels, respectively. The complete results are tabulated in Table 10 in the Appendix.

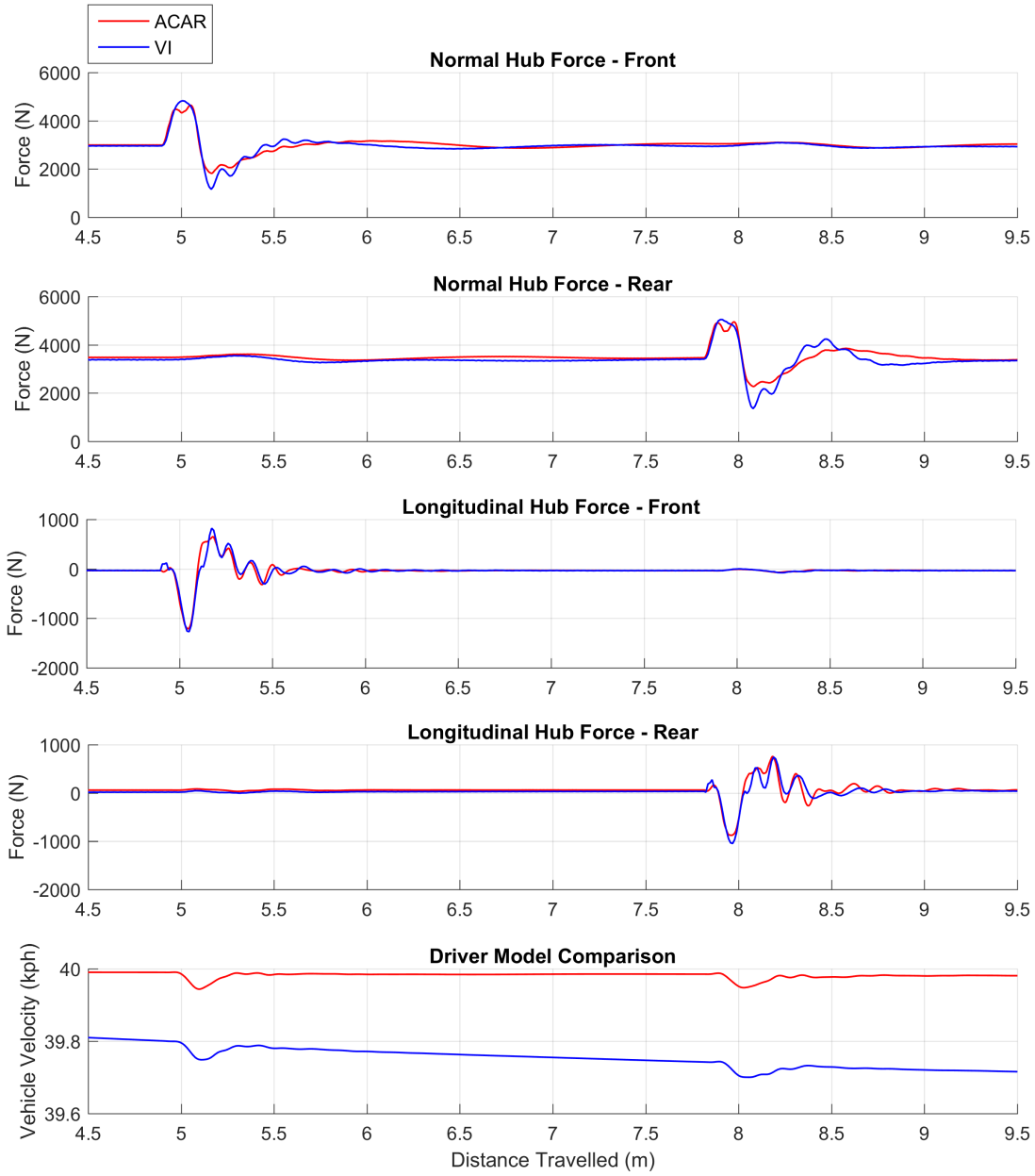


Figure 4.17: *Demo Model with Demo FTires: Cleat Road Force Comparisons*

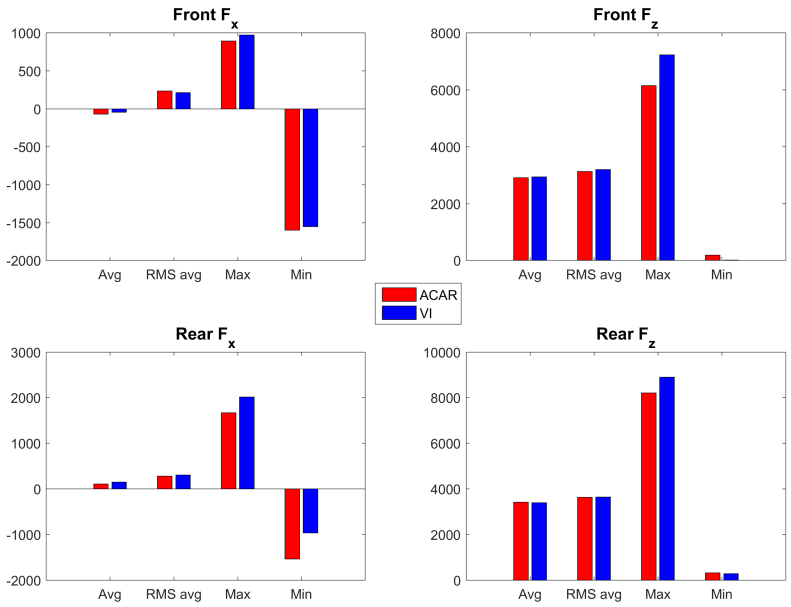


Figure 4.18: *Demo Model with Demo FTires: Washboard Road Force Comparisons*

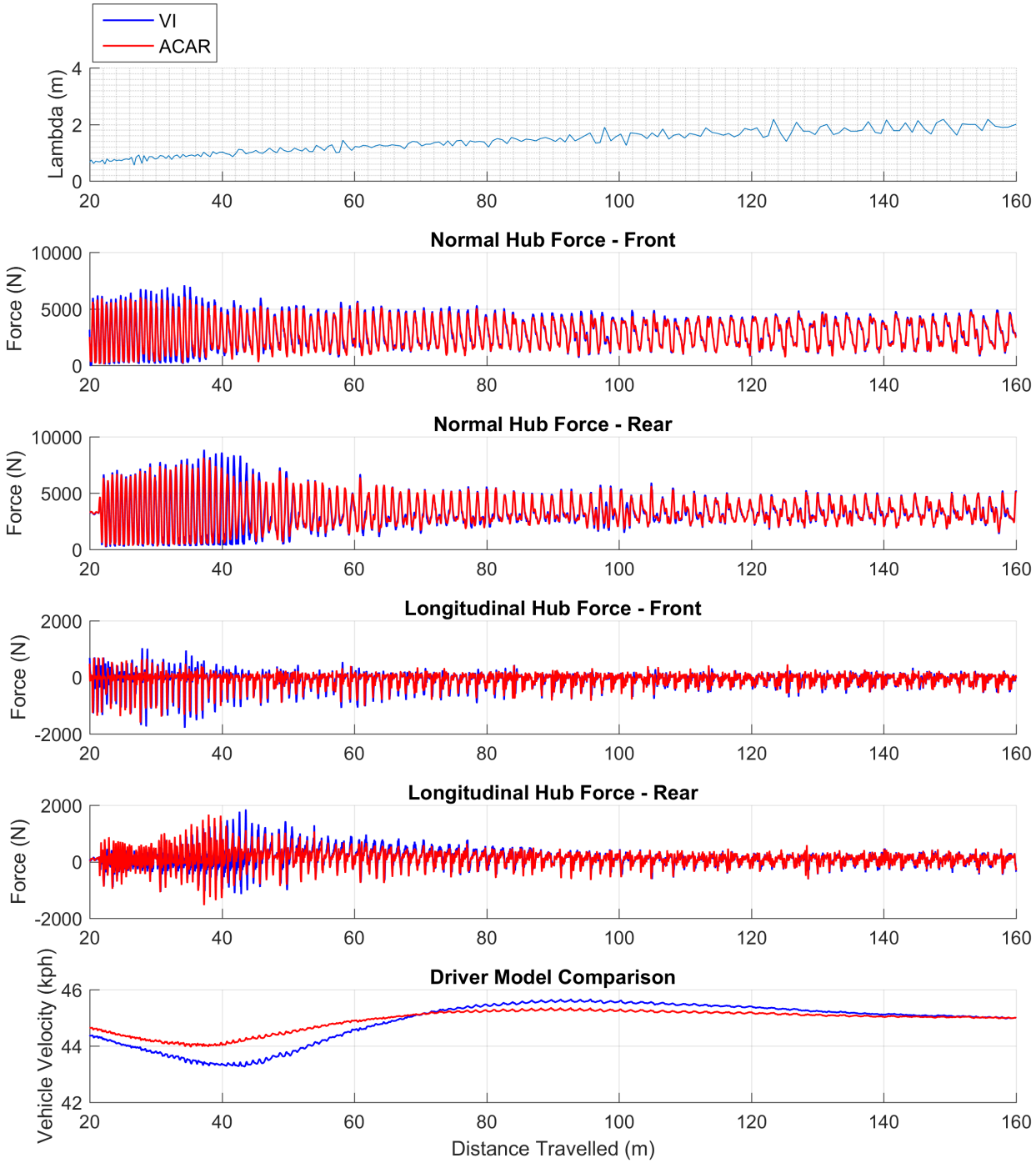
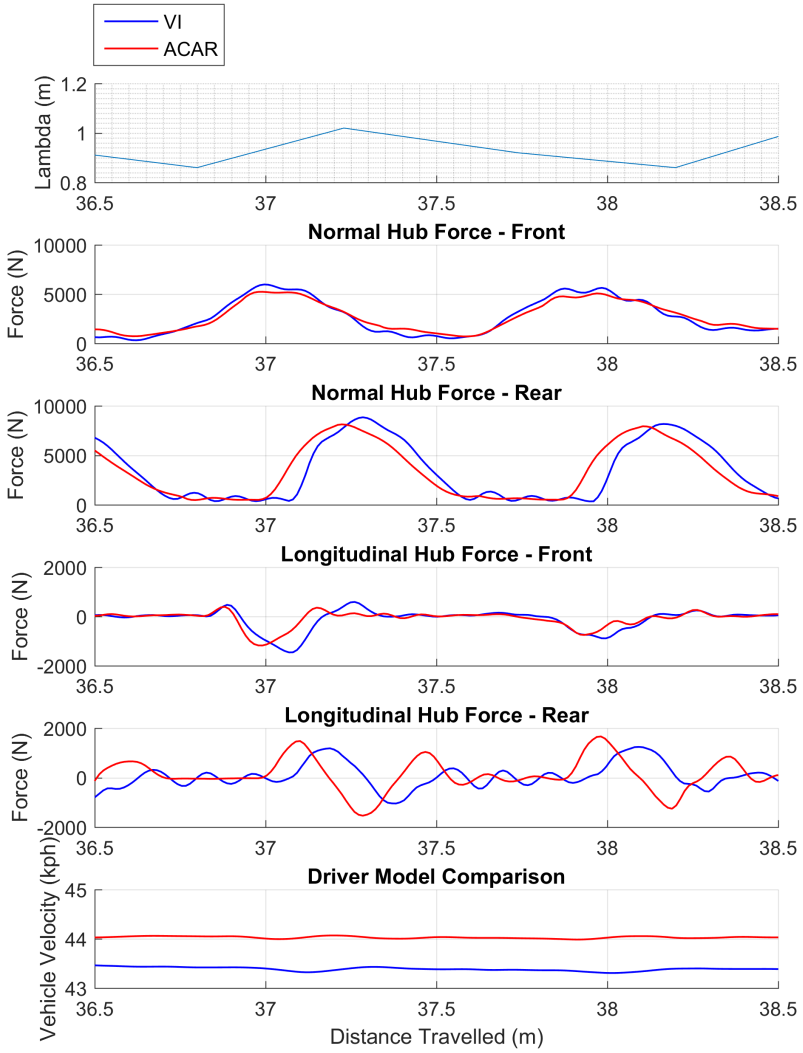
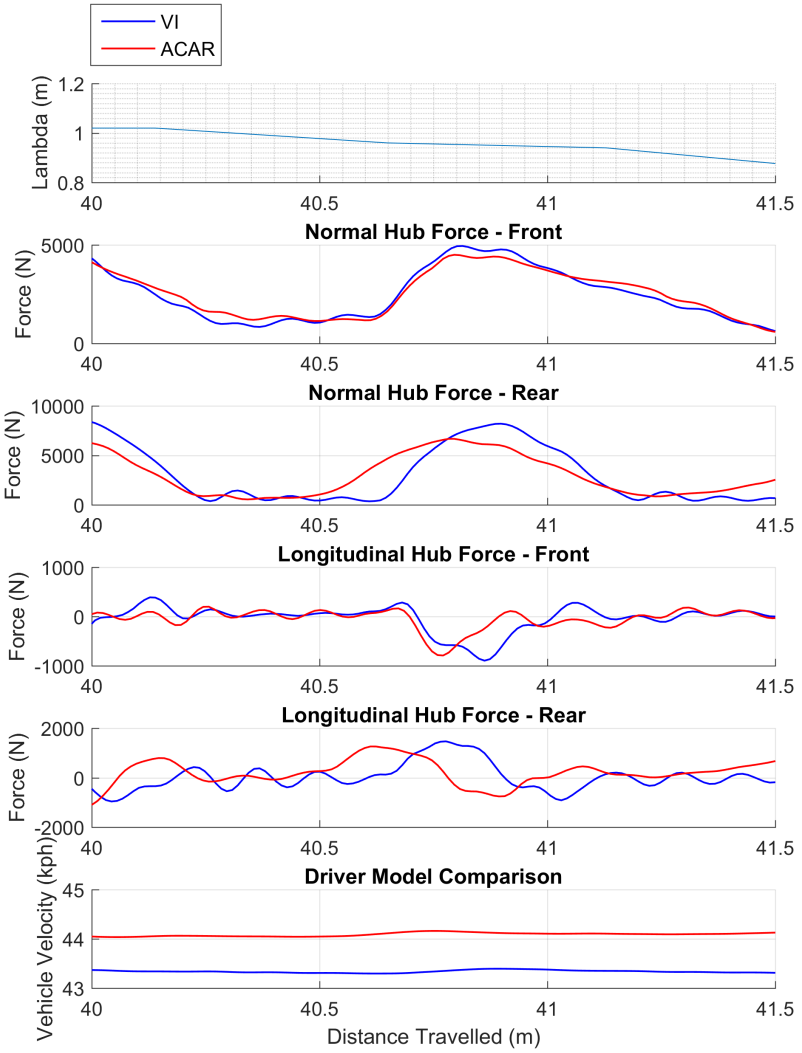


Figure 4.19: *Demo Model with Demo FTires: Washboard Overview*



(a) *36.5 - 38.5 m*



(b) *40 - 41.5 m*

Figure 4.20: *Demo Model with Demo FTires: Washboard Road*

4.5 Pacejka Tire versus FTire Comparison on Demo Model

As previously mentioned in the background section that Pacejka tire and FTire have two distinct modelling approach. To understand the differences in simulation results between the two tires, the demo vehicle is driven on a cleat road with the following event set up:

- Road: Cleat road (`Cleat10x50mm.crg`)
- Tire: Pacejka 2002 (`pac2002_235_60R16.tir`) and Demo FTire (`ftire_205_55R16.tir`)
- Driving Event: 3rd gear with no shifting, straight line, 3 seconds at 40 kph (11111.11 mm/s), maintain initial velocity

The force differences between the two tire models from the aforementioned simulation is illustrated in Figure 4.21. Interestingly, the peak normal forces measured on the front and rear wheels are very similar between the two tire models. However, the FTire model captured significantly larger longitudinal force than the Pacejka model.

From a computational intensiveness point of view, the FTire model with 0.001 second integration step took 156 seconds, while the Pacejka tire model took only 35 seconds with the same integration step. Pacejka tire is simpler and it is no surprise that it is nearly five times faster than FTire.

This exercise showed the Pacejka tire's strength and limitations. Pacejka tire is useful in the preliminary stage at identify any flaws in the vehicle model or tire model. A custom FTire normal force should resemble that of the Pacejka tire. On the other hand, while it is quicker to compute than FTire, it failed to capture the longitudinal tire forces.

Due to different tire properties and time restraint, further comparison between FTire and Pacejka tire on other road surfaces is not pursued. However FTire is used for high frequency while Pacejka tires cannot be used for the same.

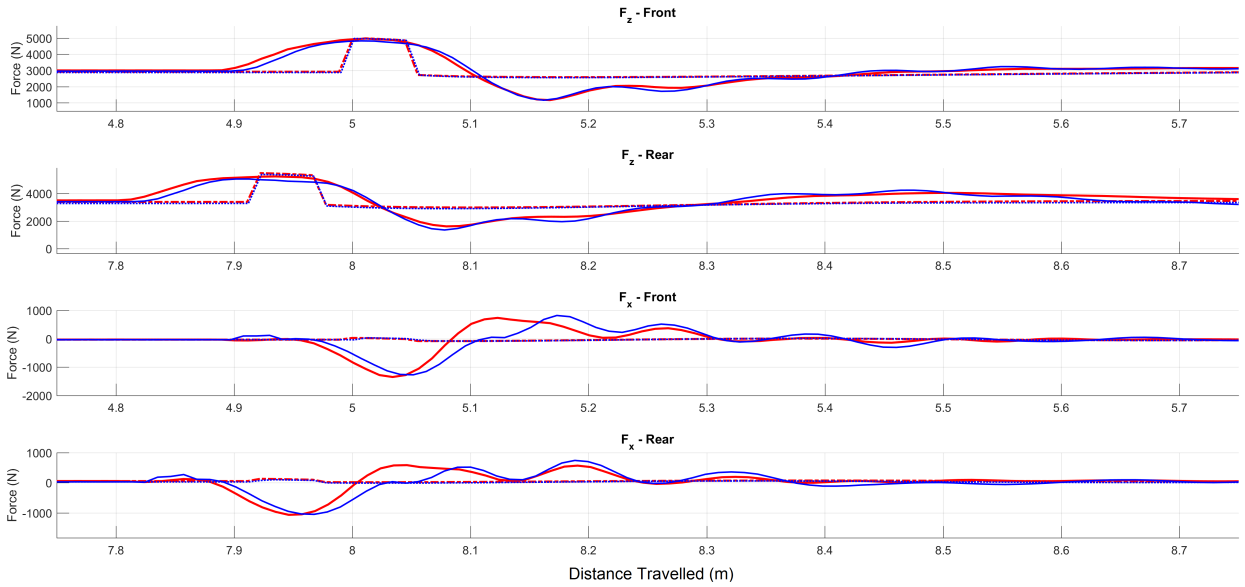


Figure 4.21: *Pirelli FTire vs. Pacejka*

4.6 Demo Model with CEVT FTire

- Tire: `235_45R20.tir`
- VI-CarRealTime
  - FTire run mode: 3
  - Integration step size: 0.0001 (VI-CarRealTime recommended setting)
  - Output step size: 0.001
- ADAMS/Car
  - FTire run mode: 0
  - Step size: 0.001

4.6.1 Flat Road

To keep the report succinct, simulation results on the flat road is not presented. The tire forces while driving on the flat road is the same as the forces after clearing the cleat and having stabilized. The tire forces observed from the cleat road is described in the following section.

4.6.2 Cleat

The same Matlab script is used to sweep through different wheel mass with Demo FTire is again used here to estimate the wheel mass with CEVT Pirelli FTire. Wheel masses from 16 to 40 kg at 3 kg increments are tested in VI-CarRealTime. It is visually determined from Figure 2 in Appendix A.3 that 25 kg wheel masses produced best match with ADAMS/Car results. This outcome is the same as the sweep performed with the Demo FTire.

The cleat is simulated with 25 kg front and rear wheel mass. The tire force comparisons can be found in Figure 4.23a. The normal tire forces captured by the two software follow each other closely, while the longitudinal forces differ more. Maximum longitudinal force difference is 84 N or 11.4% on the front wheels and 157 N or 26.6% on the rear wheels. It is also noticed that the VI-CarRealTime average front tire normal force is 52 N lower than that of ADAMS/Car, and 102 N lower for the rear wheel.

Taking the force difference into consideration, as an experiment 5.4 kg is added to the front wheel and 10.4 kg to the rear wheel. Cleat road is ran with 30.3 kg front wheel and 35.4 kg rear wheel, and the results are analyzed in Figure 4.23b. The comparison between the two different set of tire masses are shown in Figure 4.22. The change in wheel mass improved the normal tire forces. The average normal forces vary by 0.1% and the peak force is less than 1% apart between the software. Yet, the longitudinal force comparison worsened, especially for the rear tire, where the maximum force difference grew from 26.6% to 35%. Thus, changing wheel masses did not bring significant improvement to tire forces. Trusting the aforementioned wheel mass sweep, 25 kg is set for all four wheels.

4.6.3 Washboard

The demo vehicle is simulated on the washboard track with the CEVT Pirelli FTire. The tire force behavior resemble that of the demo FTire in section 4.4.3. The tire forces for the whole washboard is presented in Figure 3 in the Appendix A.3. A closer look at the 35 - 50 m region on the washboard, where the biggest force discrepancies are found, is shown in Figure 4.25a. The magnitude of the force peaks between the software are congruent throughout the washboard except around the 45 m mark, where the rear tire forces, both F_x and F_z, are greater for VI-CarRealTime.

To further assess 30 kg front wheel and 35 kg rear wheel masses, the washboard simulation is also ran with these values in VI-CarRealTime and the forces are plotted in Figure 4.25b. Heavier wheel masses produced dissimilar tire forces between ADAMS/Car and VI-CarRealTime from the 42 m to 60 m region on the washboard (not shown in the figure), which is worse than the 25 kg.

For a vehicle traveling at constant velocity over the washboard, road input frequency ranging from 8 to 21 Hz can be observed. Wheel mass varies in a inversely proportional way to the system's natural frequency. As expected, changing the wheel mass resulted in differences in tire forces over specific sections of the washboard track.

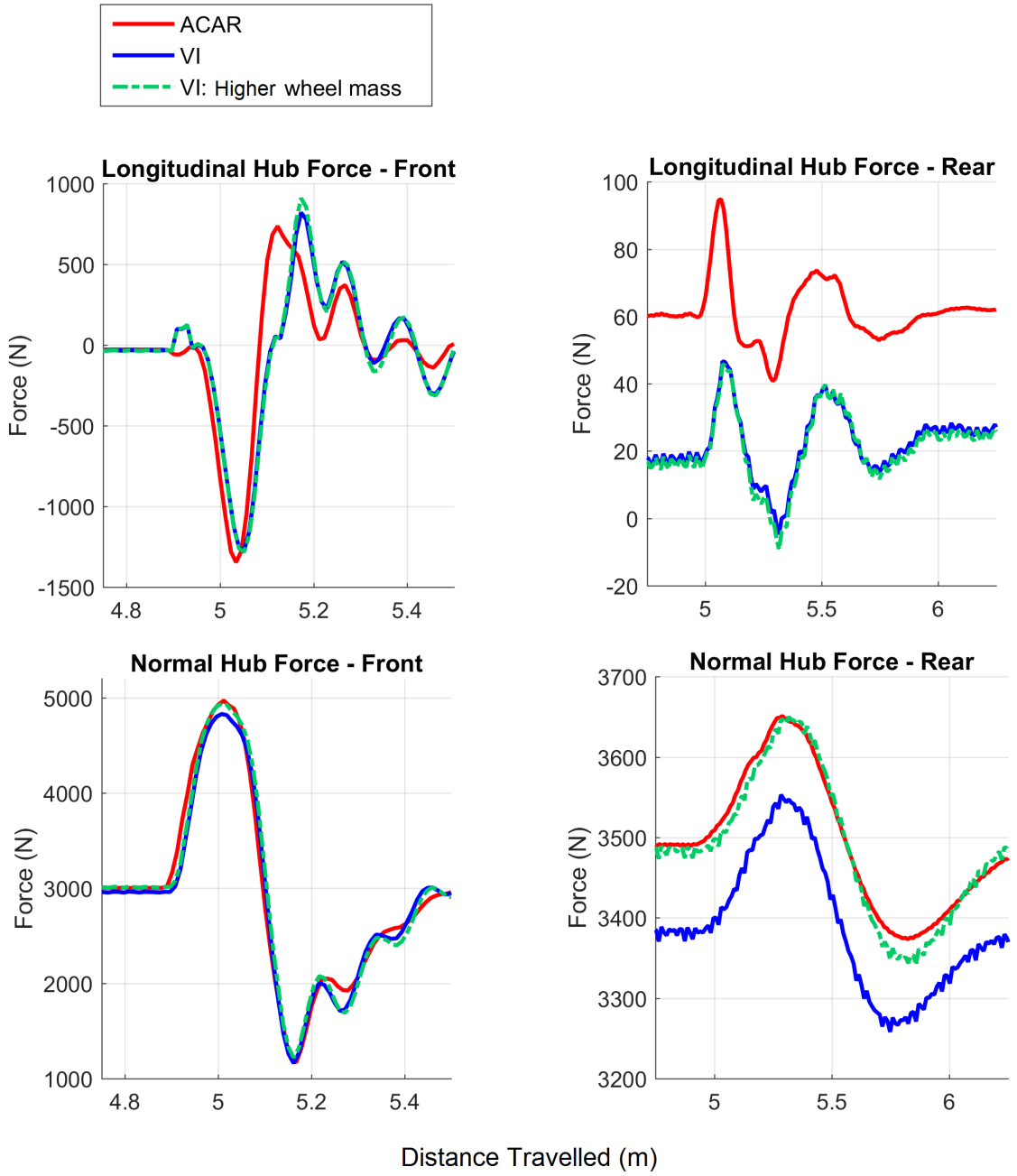
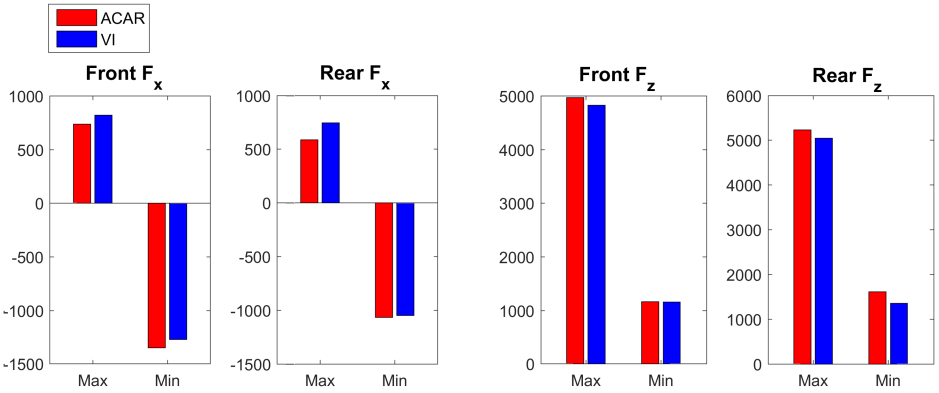
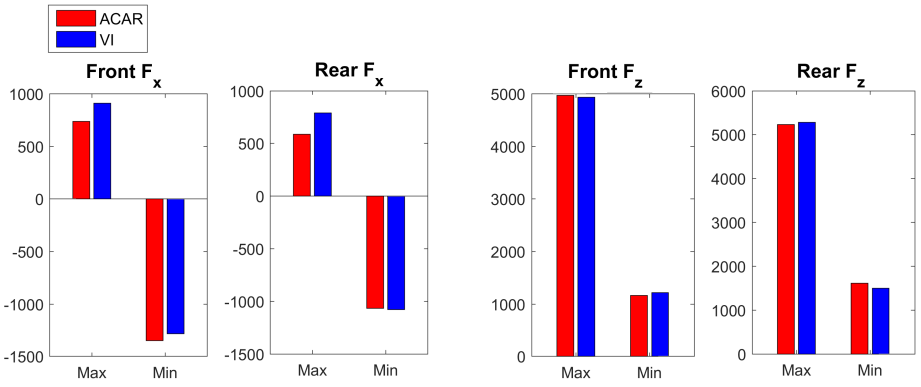


Figure 4.22: *Front/Rear Wheel Masses: 25kg/25kg vs. 30kg/35kg*



(a) *All Wheels: 25 kg*



(b) *Front Wheels: 30.3 kg, Rear Wheels: 35.4 kg*

Figure 4.23: *Demo Model with Pirelli FTires: Cleat Road Force Comparisons*

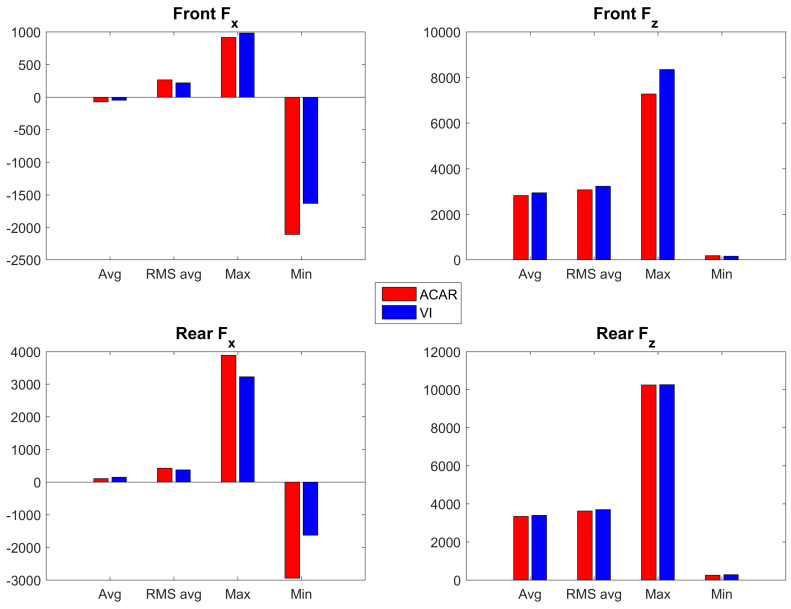
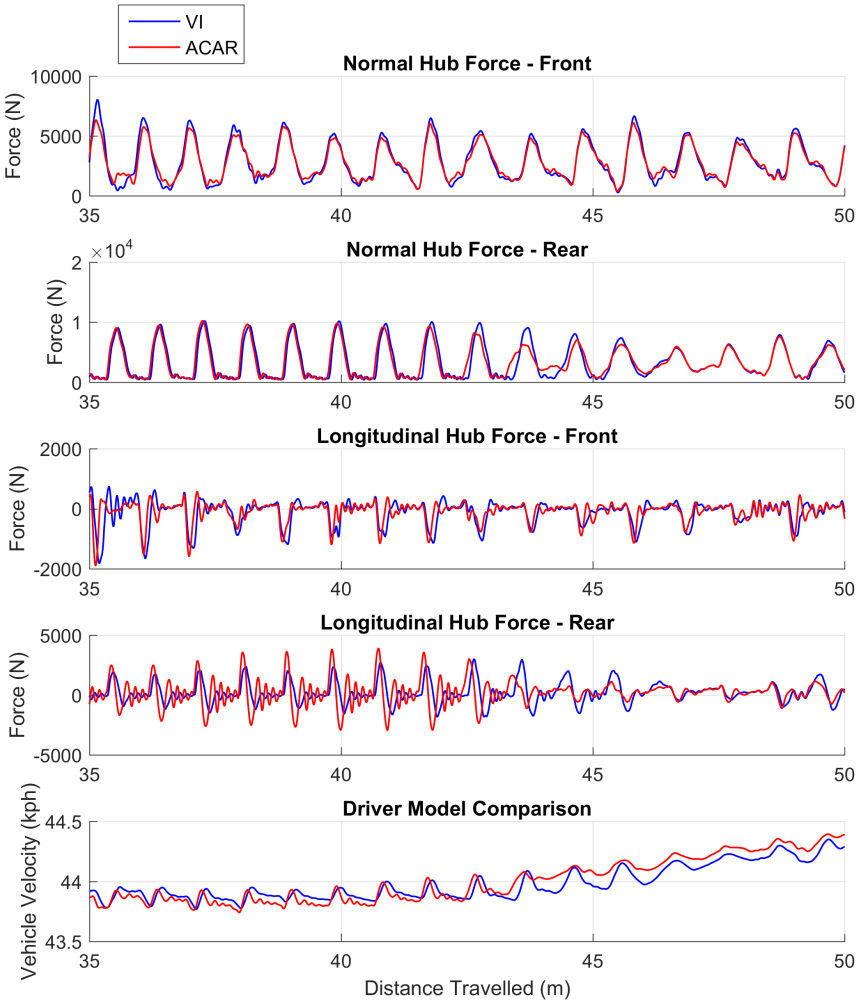
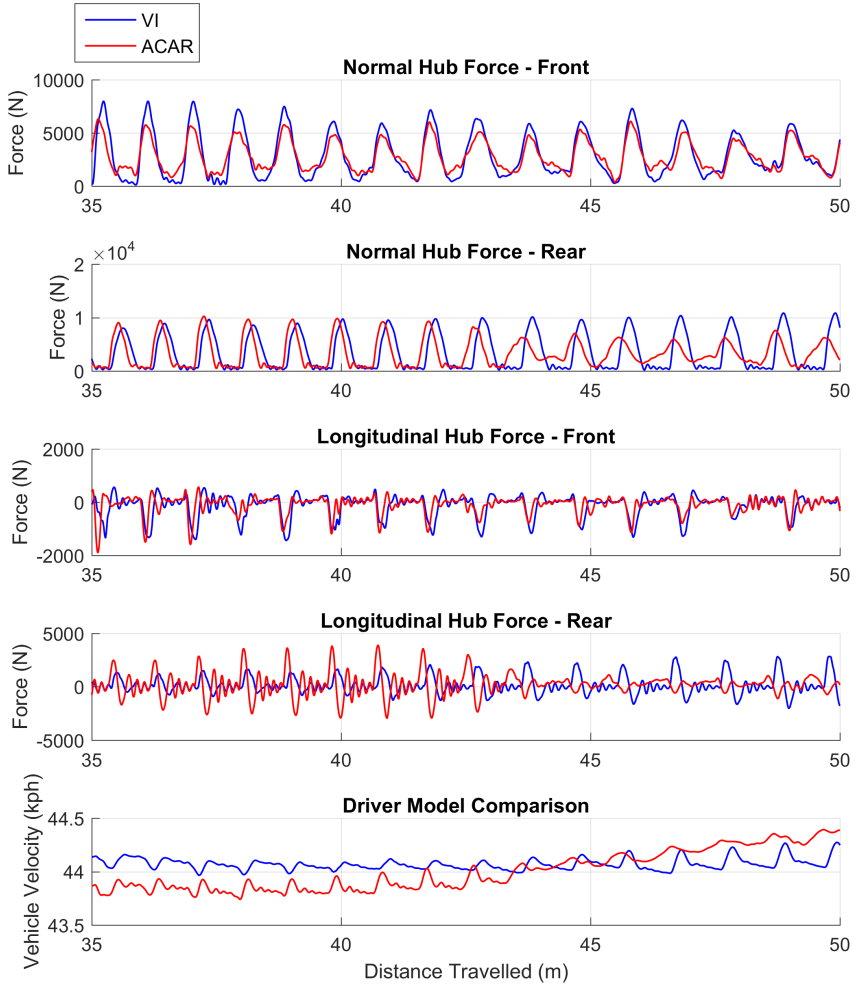


Figure 4.24: *Demo Model with Pirelli FTires: Washboard Force Comparisons*



(a) *Front and Rear Wheels: 25 kg*



(b) *Front Wheels: 30.3 kg, Rear Wheels: 35.4 kg kg*

Figure 4.25: *Demo Model with Pirelli FTires: Different Wheel Masses Comparison*

4.7 Washboard Track: Force Discrepancies and Workarounds

At early stage of this thesis work when demo FTire was selected for the wheel assemblies, large discrepancies in tire forces were observed between the 35 m and 45 m mark on the washboard track. For reference, the initial tire forces is shown in Figure 4.26. This applies not only to the demo FTire, but it also affects the Pirelli FTire. A series of investigations have been done to understand the root cause behind such large force differences. This section discusses various software setting changes implemented in order for the Demo FTire tire forces to appear as in Figure 4.19 in section 4.4.3 and Pirelli FTire as in Figure 3 in the Appendix A.3. Despite the fact that ADAMS/Car and VI-CarRealTime tire forces are not identical, the results are acceptable for conceptual design use. It is worth mentioning that further improvements are possible, however, it is not pursued due to time restraint placed on this thesis work.

The potential root causes are hypothesised here:

1. Washboard road profile: different road heights
2. VI-CarRealTime and ADAMS/Car driver model differences
3. Incorrect wheel masses in VI-CarRealTime

Confirmed software setting changes:

1. Incorrect FTire setting in VI-CarRealTime: these setting changes are mentioned previously in section 4.4
2. Incorrect FTire free mass setting in ADAMS/Car

4.7.1 Washboard Road Profile Analysis

Since little was known about the washboard track initially, it was thought that the higher tire forces captured during the first 45 m of driving was caused by taller ridges. Bigger road irregularities generate larger wheel travel and hence higher wheel forces. This hypothesis was dismissed once the X-Z road data is extracted using the Cosin tool. The road amplitude data is plotted in Figure 4.27, where the yellow data line indicate the road height along the length of the track. It is worth mentioning that the height of the ridges on the washboard is very consistent.

On the other hand, vertical wheel travel is not always the same for the front and rear wheels. Figure 4.28 compares ADAMS/Car wheel displacement at two velocities: 3 kph and 45 kph. At lower velocity both wheel displacements are identical for any given bump. Moreover, the wheel movements are following the ups and downs of the ridges. As velocity increases the rear wheel vertical displacement becomes larger than that of the front wheel. Such increase in wheel travel correlates to the higher normal forces.

The same trend was found with VI-CarRealTime. The wheel displacement graph at 15 and 45 kph is shown in Figure 4.29. Yet, despite this trend, Figure 4.30 reveals that VI-CarRealTime's rear wheel vertical travel is much higher in comparison to ADAMS/Car's. The difference is most likely created by incorrect Ftire mass, and the discrepancy is magnified by vehicle velocity. At lower vehicle velocity, the wheel displacements matches the road profile in both software. Tire force comparisons between ADAMS/Car and VI-CarRealTime at 20 kph is presented in Figure 4.32, and the forces are nearly identical. As the velocity increases the difference in rear wheel vertical travel become more prominent, and subsequently the tire forces become less comparable. The comparison performed at 60 kph is illustrated in Figure 4 in Appendix section A.3.

Furthermore, VI-CarRealTime's chassis pitch values at 15, 45, and 55 kph vehicle speeds are plotted in Figure 4.31. Varying front and wheel travel leads to change in pitch. The chassis pitch at 55 kph is mostly out-of-phase compared to that of 15 kph. Such difference in body pitch will influence the tire forces.

4.7.2 Vibration Dynamics: One Dimensional Model with Two Degrees of Freedom

As already shown in Figure 4.27 the washboard track has a near-constant ridge height fluctuation while the road input frequency is changing. Hence, this section attempts to grasp on the basic relationship between road input frequency and tire forces.

VI-CarRealTime model only includes the masses of the body and the wheels, the vehicle spring-mass-damper schematics is presented in Figure 4.33. Since the objective here is to understand the general trend rather than

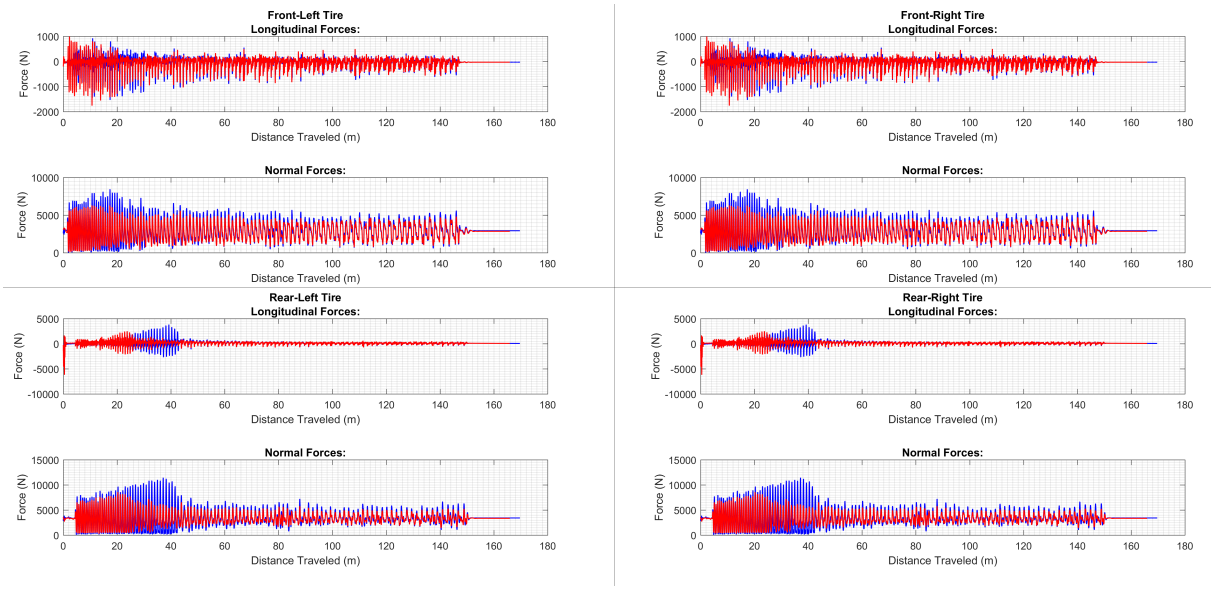


Figure 4.26: *Tire Forces on the Washboard Track Without Software Setting Changes*

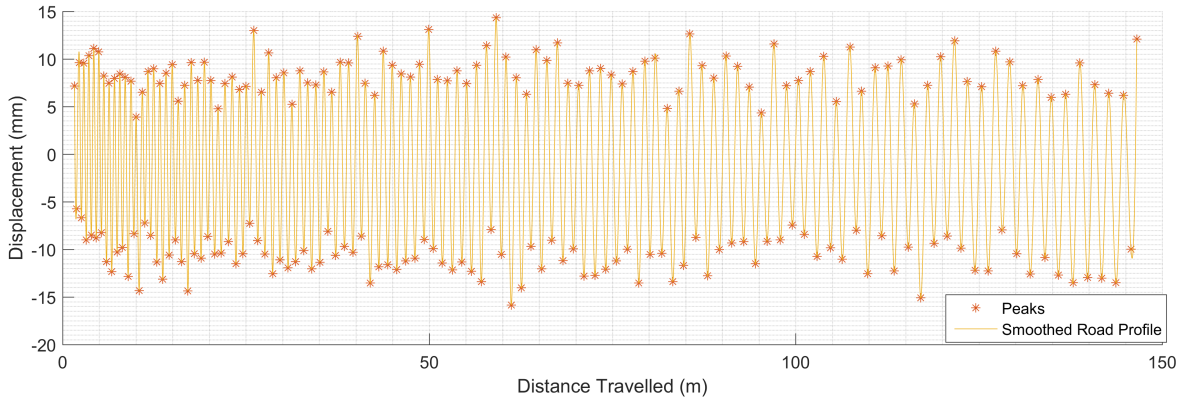


Figure 4.27: *Washboard Road Profile*

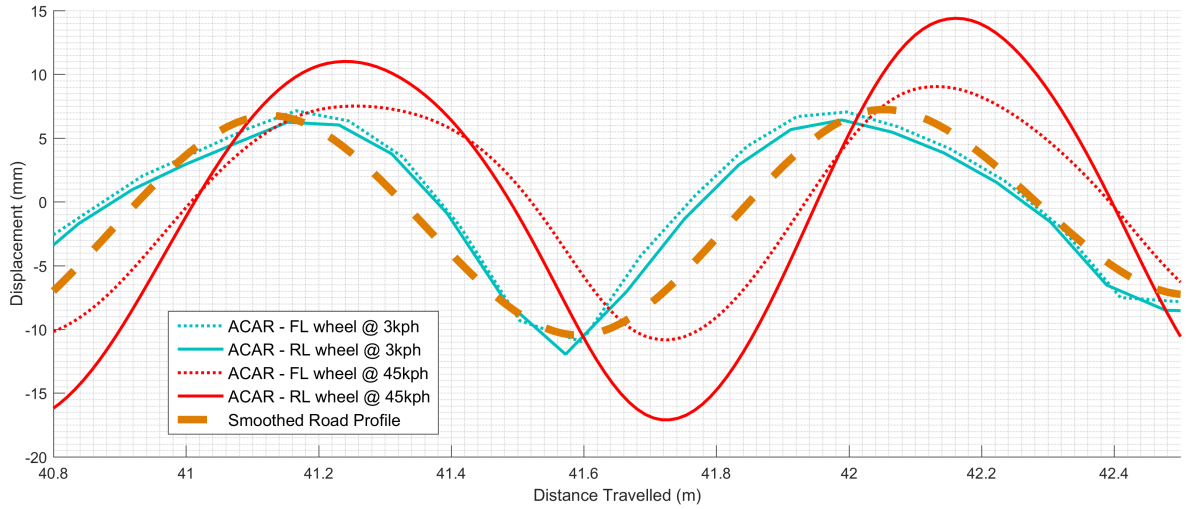


Figure 4.28: *ADAMS/Car Wheel Displacement*

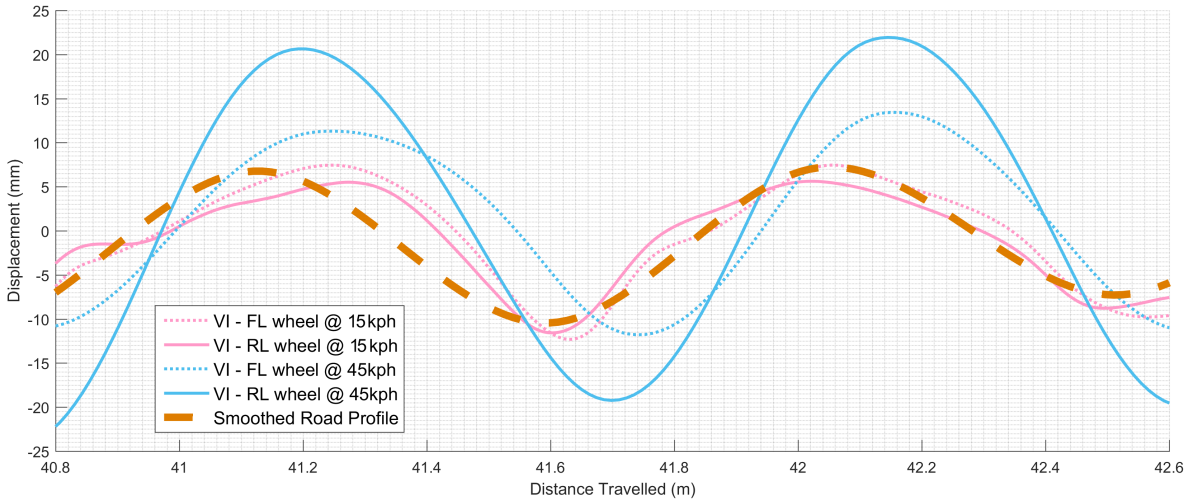


Figure 4.29: *VI-CarRealTime Wheel Displacement*

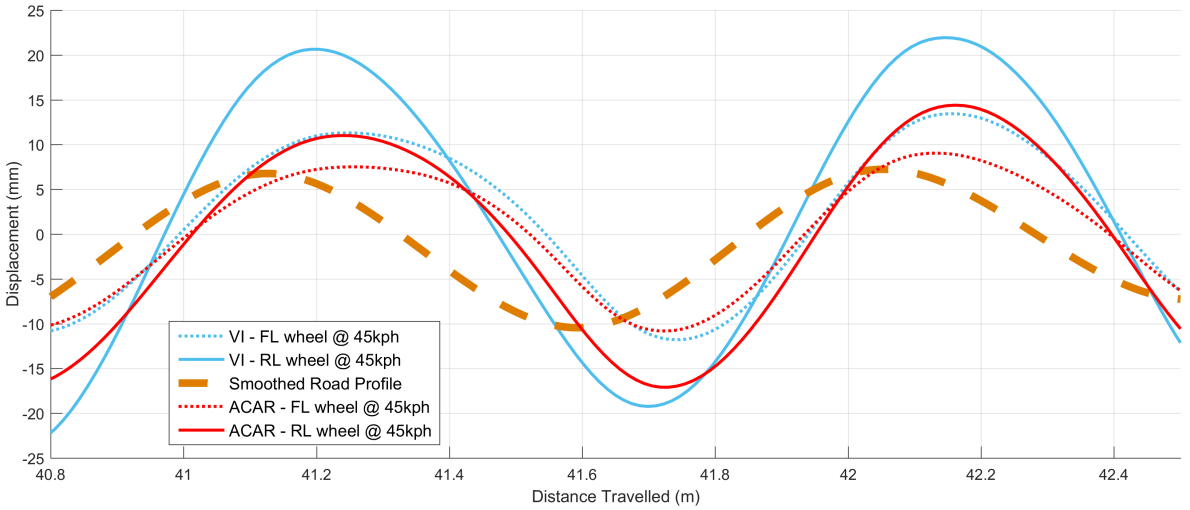


Figure 4.30: *ADAMS/Car vs. VI-CarRealTime Wheel Displacement*

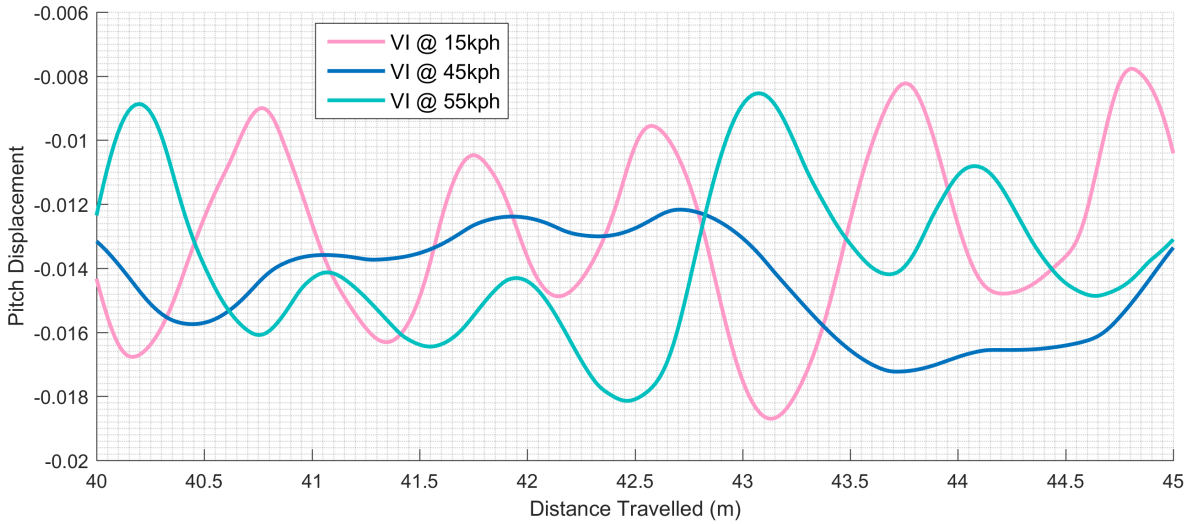


Figure 4.31: *VI-CarRealTime Chassis Pitch*

obtaining accurate results, complexity of this model is reduced into a One-Dimensional 2-Degree of Freedom (2-DOF) spring-mass damper system shown in Figure 4.34.

While the 1-DOF model only considers the spring-damper between the sprung and unsprung mass, the 2-DOF system also adds the tire's elasticity into the picture. In order to better understand the system's resonance behavior, tire stiffness also plays a major role. Although the results are no where near the fidelity of Ftire model, it still provides better insight than a 1-DOF model. For the rough force estimation, calculations will first be done on the 2-DOF system, and then a 2-DOF model split into two 1-DOF model will be used to verify calculated results.

This experiment gathers inspiration from a Structural Dynamics and Controls course project the author has done at Chalmers University of Technology [17]. Parts of the original Matlab code is modified and reused to save time.

List of Variables Vehicle properties, such as the damper, are non-linear. For simplicity reasons, typical passenger vehicle parameter values are chosen instead:

- z_u, z_1 - unsprung mass vertical displacement
- $\dot{z}_u$, $\dot{z}_1$ - unsprung mass vertical velocity
- $\ddot{z}_u$, $\ddot{z}_1$ - unsprung mass vertical acceleration
- z_s, z_2 - sprung mass vertical displacement
- $\dot{z}_s$, $\dot{z}_2$ - sprung mass vertical velocity
- $\ddot{z}_s$, $\ddot{z}_2$ - sprung mass vertical acceleration
- z_r - road disturbance
- m_u - unsprung mass
- m_u - Front Wheel Mass = 30 kg (VI demo model)
- m_u - Rear Wheel Mass = 35 kg (VI demo model)
- m_s - sprung mass
- F_{sz} - sprung mass vertical force
- F_{rz} - tire vertical force

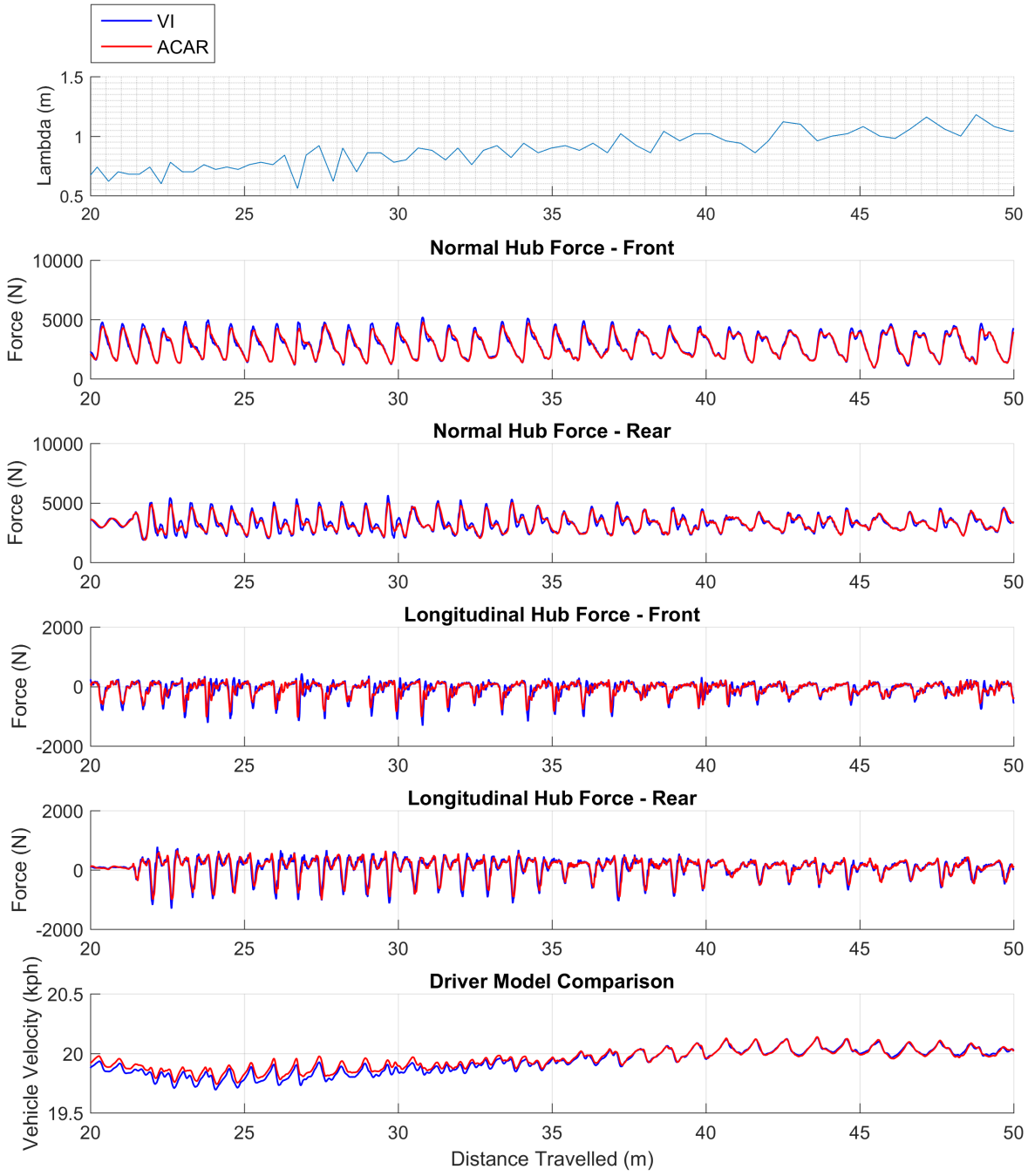


Figure 4.32: *ADAMS/Car vs. VI-CarRealTime at 20 kph: Tire Force Comparisons*

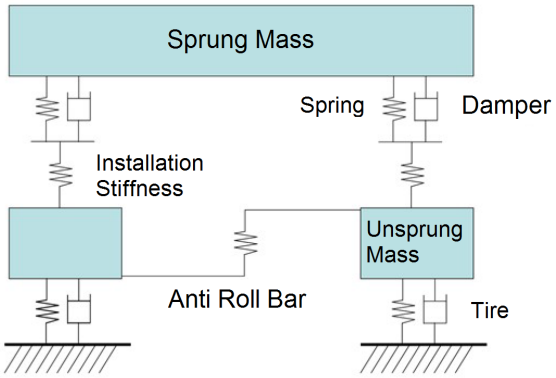


Figure 4.33: *VI-CarRealTime Model[16]*

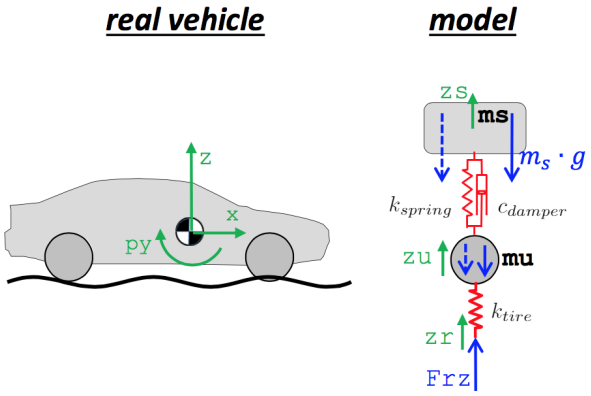


Figure 4.34: *Two DOF model*

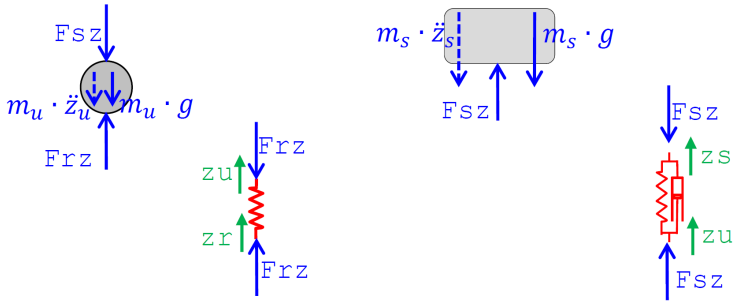


Figure 4.35: *Two DOF model Free Body Diagram*

- k_{tire} - tire stiffness
- k_{spring} - Spring Stiffness = 28.3 N/mm (1.5 Hz for passenger cars @ 318 kg per corner weight [4]
- c_{damper} - Damping Coefficient = 1300 Ns/mm (estimated based on maximum damper velocity over washboard, ca. 0.6 m/s: [3])

Equations of motion First, equations of motion are set up according the Free Body Diagram in Figure 4.35. The forces are described according to Equation 4.1 and 4.2. Road disturbance is acting on the unsprung mass through the tire spring. Unsprung mass and sprung mass is connected via a spring-damper.

$$m_u \ddot{z_u} = F_{rz} - F_{spring} - F_{damper} \tag{4.1}$$

$$m_s \ddot{z_s} = F_{spring} + F_{damper} \tag{4.2}$$

The spring and damper forces are described as below:

$$F_{rz} = k_{tire}(z_r - z_u)$$

$$F_{spring} = k_{spring}(z_u - z_s)$$

$$F_{damper} = c_{damper}(\dot{z}_u - \dot{z}_s)$$

By rearranging, the system of equation is presented in matrix form:

$$\boldsymbol{M}\ddot{\boldsymbol{x}} + \boldsymbol{C}\dot{\boldsymbol{x}} + \boldsymbol{K}\boldsymbol{x} = \boldsymbol{F}(t) \tag{4.3}$$

$$\begin{bmatrix} m_{unsprung} & 0 \\ 0 & m_{sprung} \end{bmatrix} \ddot{\boldsymbol{x}} + \begin{bmatrix} c_{damper} & -c_{damper} \\ -c_{damper} & c_{damper} \end{bmatrix} \dot{\boldsymbol{x}} + \begin{bmatrix} k_{tire} + k_{spring} & -k_{spring} \\ -k_{spring} & k_{spring} \end{bmatrix} \boldsymbol{x} = \begin{bmatrix} k_{tire} * z_r(t) \\ 0 \end{bmatrix}$$

Assuming the disturbance from the road, $z_r(t)$, is a sinusoidal input:

$$z_r(t) = z_0 * sin(2\pi * \frac{v}{\lambda} * t) \tag{4.4}$$

State Space Form The equations of motion can be rearranged by isolating $\ddot{\boldsymbol{z}}$:

$$\ddot{\boldsymbol{z}} = \boldsymbol{M}^{-1}(\boldsymbol{F}(t) - \boldsymbol{K}\boldsymbol{z} - \boldsymbol{C}\dot{\boldsymbol{z}}) \tag{4.5}$$

Taking $\boldsymbol{z} = [z_1, z_2, \dot{z}_1, \dot{z}_2]^T$, $\boldsymbol{y} = [\ddot{z}_1, \ddot{z}_2]^T$ and $\boldsymbol{F}(t) = [k_{tire}, 0]^T * z_r(t) = \boldsymbol{a}_h * z_r(t)$, Equation 4.5 can be re-written as:

$$\dot{\boldsymbol{z}} = \boldsymbol{A}\boldsymbol{z} + \boldsymbol{B}u \tag{4.6}$$

$$\dot{\boldsymbol{z}} = \begin{bmatrix} \boldsymbol{0} & \boldsymbol{I}_3 \\ -\boldsymbol{M}^{-1}\boldsymbol{K} & -\boldsymbol{M}^{-1}\boldsymbol{C} \end{bmatrix} \boldsymbol{z} + \begin{bmatrix} \boldsymbol{0} \\ -\boldsymbol{M}^{-1}\boldsymbol{a}_h \end{bmatrix} z_r(t)$$

$$\boldsymbol{y} = \boldsymbol{C}\boldsymbol{z} + \boldsymbol{D}u \tag{4.7}$$

$$\boldsymbol{y} = \begin{bmatrix} \ddot{z}_1 \\ \ddot{z}_2 \end{bmatrix} = \begin{bmatrix} -\boldsymbol{M}^{-1}\boldsymbol{K} & -\boldsymbol{M}^{-1}\boldsymbol{C} \end{bmatrix} \boldsymbol{z} + \boldsymbol{M}^{-1}\boldsymbol{a}_h z_r(t)$$

The values of the matrices are:

```
M =
          35            0
           0       309.87

K =
      310653      -28300
      -28300       28300
[N/m]

C_damping =
        1300       -1300
       -1300        1300
[Ns/m]
```

Matlab Simulation Matlab functions *rhsTwoMass* is used to describe the State Space Equation 4.6. Function *outputFun* is used to describe Equation 4.7. Matlab *ode*45 integrates the system of equation *zdot* in *rhsTwoMass* to find $\boldsymbol{z}$. Subsequently $\boldsymbol{z}$ is plugged into *outputFun* to derive displacement, velocity, and acceleration of the masses.

The Matlab function *rhsTwoCart*

```
function zdot = rhsTwoMass (t, z)
global A B a w1

u = a*sin(w1.*t)'; % z_r = amplitude * sin(freq*2*pi()/lambda);

zdot = A*z + B*u;
```

The second function *outputFun* describes $y = \boldsymbol{C}z + \boldsymbol{D}u$

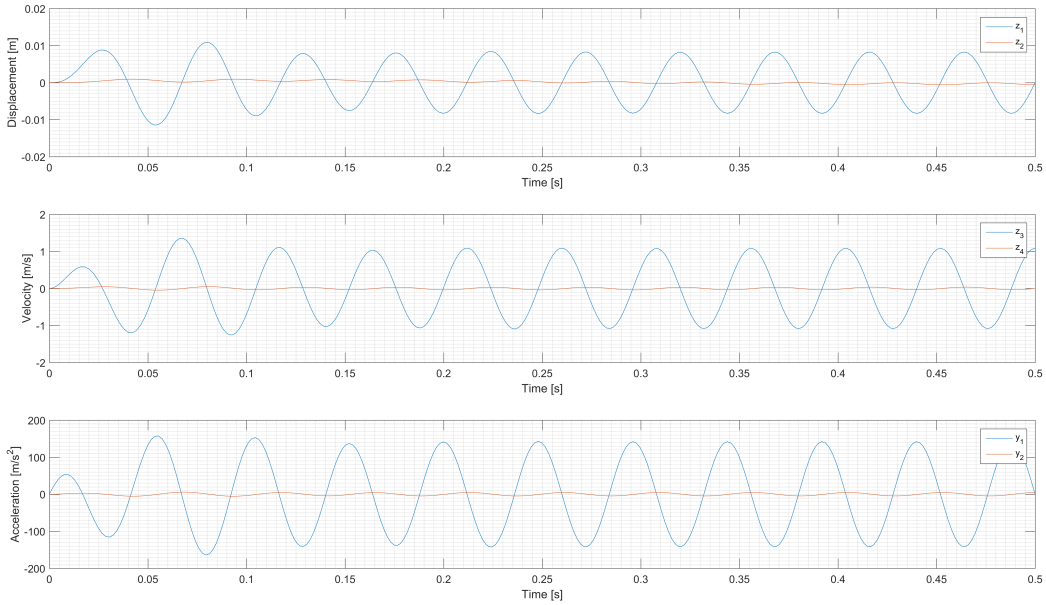


Figure 4.36: *Displacement, Velocity and Acceleration Results*

```
function y = outputFun (t,z)
global C D a w1

u = a*sin(w1.*t)'; % z_r = amplitude * sin(freq*2*pi()/lambda);

y = C*z' + D*u;
```

```
% integration ode
t0=0;
tf=5;
[t,Z] = ode45('rhsTwoMass',[t0 tf],z0);
Y=outputFun(t,Z)';
```

The initial state of the system is in equilibrium state, where $z_0 = [0, 0, 0, 0]$. The road profile is described by Equation 4.4, where the amplitude of the road disturbance, z_0, is 0.01 m, vehicle velocity, v, is 12.5 m/s, distance between consecutive bumps, λ, is 1 m, and time span, $t \in [1, 5]$ seconds. The road disturbance input is 12.5 Hz. For the given road disturbance, the simulated results are presented in Figure 4.36.

The identified eigenvalues are listed below, which match the peaks in the bode plot in Figure 4.37. Lambda values from 0.6 m to 2 m at 0.1 m increment has been tested. The sum of the static and dynamic rear tire force in relation to the road input frequencies are presented in Figure 4.38. According to the graph, tire force increases as the road input frequency approaches the 2-DOF system's natural frequency, and vice versa.

```
eigenvalues =
      -18.917 +     91.611i
      -18.917 -     91.611i
      -1.7519 +     9.0072i
      -1.7519 -     9.0072i
```

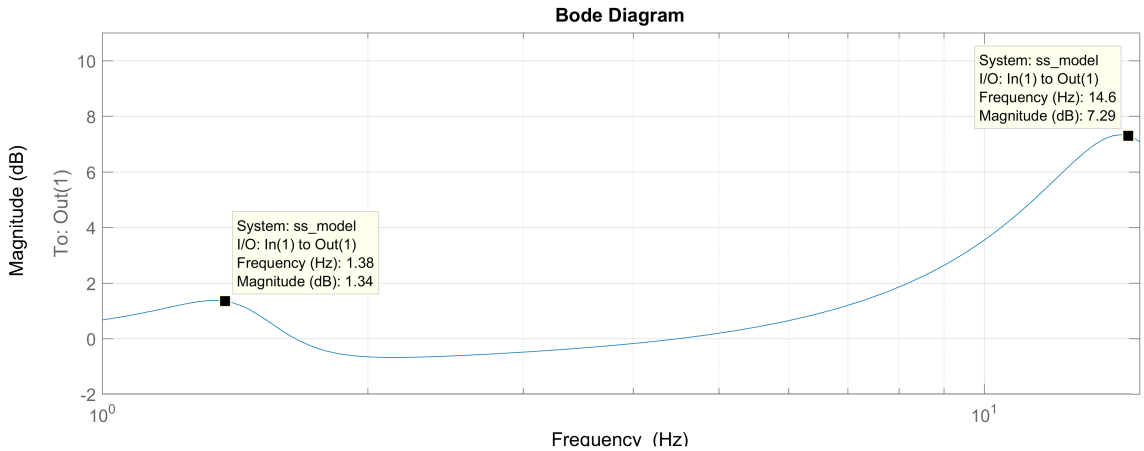


Figure 4.37: *Bode Plot*

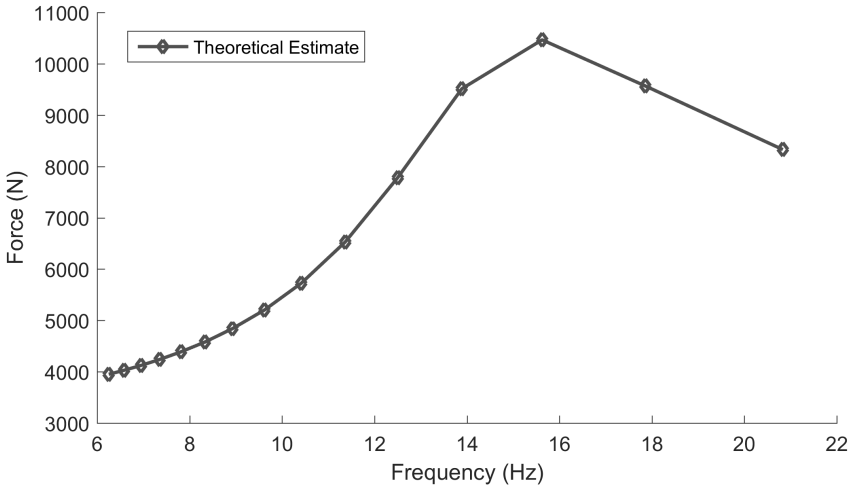


Figure 4.38: *Rear Wheel Tire Normal Forces*

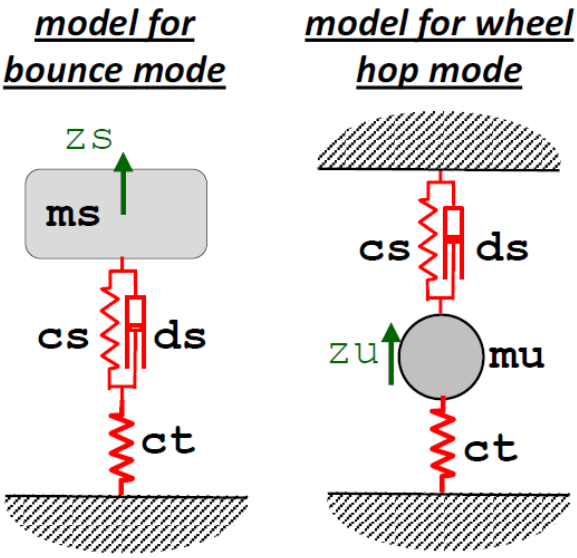


Figure 4.39: *Bounce and Wheelhop Modes*

4.7.3 Vibration Dynamics: Simplified Model

The simplified model takes advantage of the magnitude difference in sprung and unsprung masses and spring stiffnesses. As a result, the 2-DOF model is split into two 1-DOF models as shown in Figure 4.39.

The natural frequency of each sub-model can be solved according to Equation 4.8 and 4.9. The two particular frequencies are known as "bounce mode" and "wheel hop mode". Bounce mode refers to unsprung and unsprung masses travel in phase with each other, while wheel hop mode occurs when the two masses are moving out of phase. In wheel hop mode, sprung mass is nearly stationary.

Frequency of Modes:

$$\omega_{bounce} = \sqrt{\frac{1/(\frac{1}{K_{spring}} + \frac{1}{K_{tire}})}{m_{sprung_{RR}}}} \tag{4.8}$$

$$\omega_{wheelhop} = \sqrt{\frac{K_{spring} + K_{tire}}{m_{RearTire}}} \tag{4.9}$$

For the Rear-Right (RR) Corner Quarter Car Model:

$$m_{sprung_{RR}} = m_{sprung} * \frac{l_{front}}{L} * 0.5 = 309.87kg$$

$$\omega_{bounce} = \sqrt{\frac{1/(\frac{1}{28300} + \frac{1}{282353})}{309.87}} = 1.45Hz$$

$$\omega_{wheelhop} = \sqrt{\frac{28300 + 282353}{35.32}} = 14.99Hz$$

Similarly for the Front-Left (FL) Corner Quarter Car Model:

$$m_{sprung_{FL}} = m_{sprung} * \frac{l_{rear}}{L} * 0.5 = 263.96kg$$

Frequency of Modes:

$$\omega_{bounce} = \sqrt{\frac{1/(\frac{1}{28300} + \frac{1}{282353})}{263.96}} = 1.57Hz$$

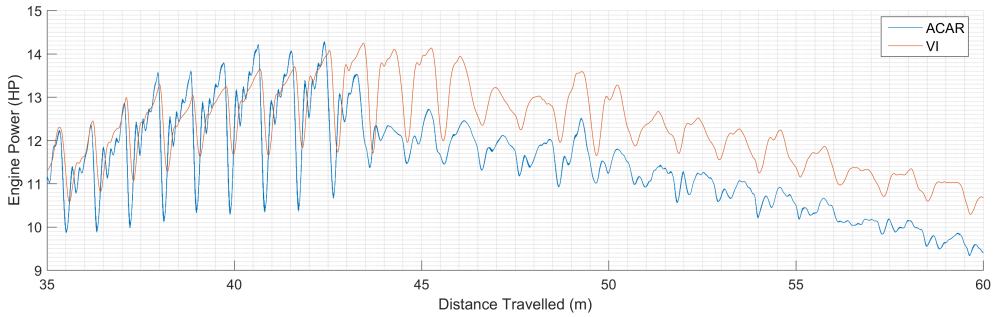


Figure 4.40: *Engine Output Power Comparison*

$$\omega_{wheelhop} = \sqrt{\frac{28300 + 282353}{30.35}} = 16.19Hz$$

The calculated values is similar to the numbers found in the 2-DOF model. They are also comparable to the values proposed by Bengt Jacobson [8], where passenger vehicle sprung mass resonance occurs at 1 Hz and wheel hop occurs at 10 Hz.

4.7.4 VI-CarRealTime and ADAMS/Car Driver Model Differences

As aforementioned, VI-CarRealTime and ADAMS/Car have their individual "driver models". Among numerous parameters, the model contains a PID controller that dictates throttle, braking, steering, and shifting commands in order to best meet the user specified driving maneuvers. Commonalities between the software allow possibilities of use other software's drive model with plug-ins. The combinations are listed below. Further discussions on driver model choice is described in section 4.7.5.

- VI-CarRealTime with VI-Driver
- VI-CarRealTime with ADAMS/Car driver model
- ADAMS/Car with ADAMS/Car driver
- ADAMS/Car with VI-Driver plug-in

Throttle and Braking Driver Demands

Since the demo vehicle is rear wheel driven, power delivered by the driving wheels may influence the rear hub forces. VI-CarRealTime has a system parameter setting that allows user to set torque reaction. The full description is extracted from the VI-CarRealTime user manual and shown here:

```
Driveline
torque_reaction_on_chassis_active flag
used to select the reaction part on which the driveline torque acts.
(1: chassis; 0: unsprung mass)
```

A test was done by changing the torque reaction part from unsprung mass to chassis. No major differences in longitudinal forces are noted, and this is likely due to the low power output from the driveline. The evidence is not conclusive enough to determine the correct setting, and thus the original setting is kept.

Engine speed fluctuation could be linked to the road disturbance input. Road surface irregularities slows down the vehicle, and as each driver models attempts to maintain target velocity, unique control algorithms lead to engine supplying different amounts of power to the wheel. The engine speed comparison can be seen in Figure 4.40. The region with the highest force differences saw highest differences in engine power. Subsequently, a set of tests, referred to as "coasting", have been done on the washboard track by having zero throttle and braking, in an effort to eliminate driver control all together. The analysis is presented in section 4.7.4.

Coasting Test - All Controls Off

In the driver event file, all control mechanisms are set to "open-loop" with zero input to see if driver control is what has caused force differences. As a result, the car is coasting from initial velocity. The VI-EventBuilder environment is presented in Figure 6 in Appendix A.3.

The driver model comparison plot indicates vehicles in both simulation software are slowing down. However, the rate of deceleration is different. After the 42 m mark ADAMS/Car vehicle becomes slower than VI-CarRealTime vehicle. This trend continues until the 95 m mark, where ADAMS/Car simulation stops with final speed as 5.5 kph, while VI-CarRealTime vehicle continue coasting at 32 kph.

The comparison between "coasting" and "maintaining velocity" is presented in Figure 4.41a and 4.41b. Vehicle velocities are closest between 30 m to 45 m portion of the track. By having distance travelled on the x-axis, time-independent analysis is permitted, allowing comparison of tire forces per "ridge". Naturally in contrast to "maintain", tire forces are lower without any driver inputs. Although the VI-CarRealTime front wheel longitudinal force peaks at the 35 m mark as seen in Figure 4.41a is no longer found at the same point in Figure 4.41b, rear wheel longitudinal force between 40 - 45 m remain higher for VI-CarRealTime than ADAMS/Car.

Eliminating driver model altogether brought forth improved ADAMS/Car and VI-CarRealTime tire force comparisons. Yet, not all divergences are eliminated. Braking comparison between ADAMS/Car and VI-CarRealTime using its own respective driver models is attempted. The motivation is to amplify the effect of ridges on tire longitudinal forces. Difficulty was encountered when tweaking to achieve the same rate of deceleration between the vehicles. The process was time consuming and abandoned due to lack of time.

4.7.5 Additional Initial Flat Road

Through communication with VI-CarRealTime technical support team, one of the recommendations was to increase the flat road section before the washboard. The motivation was to allow the vehicle to reach its target velocity before crossing the first ridge on the washboard.

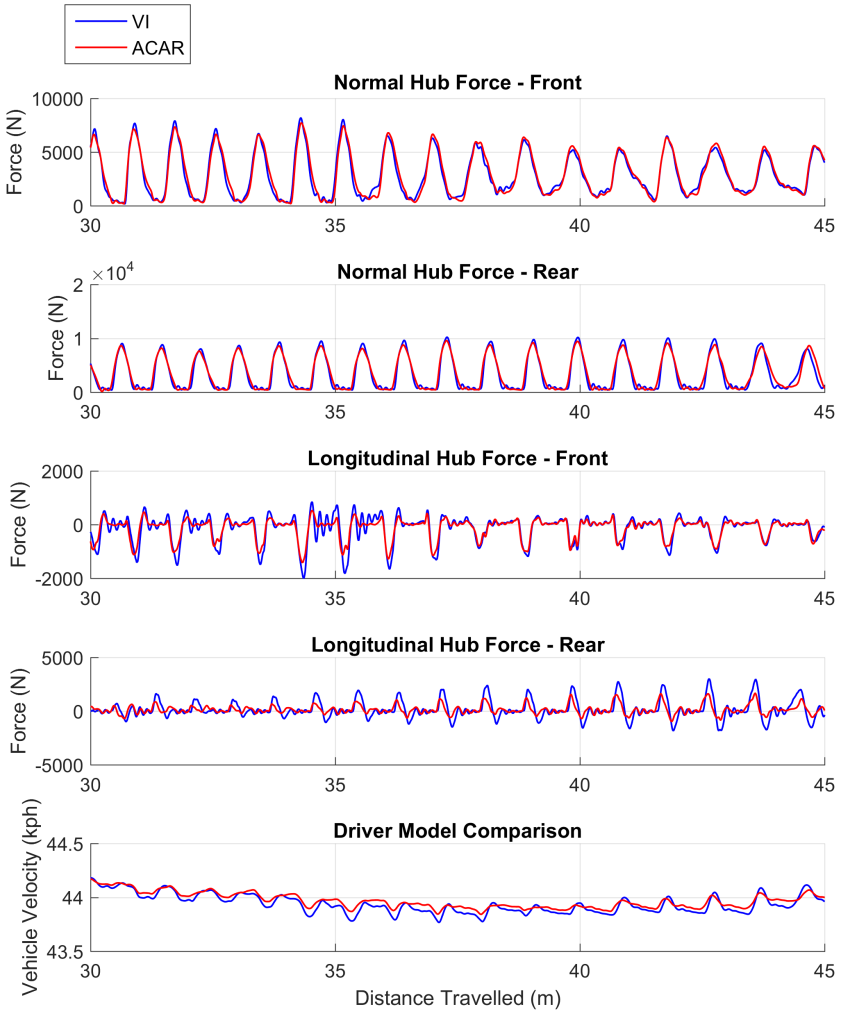
Two new roads are generated and are summarized below, and the added flat section of the washboard is visualized in Figure 4.42.

- Short Track: original road, 165 m total length, 3 m <flat road
- Medium Track: 17 m of flat track added (22 m flat road), 182 m track length
- Long Track: 47 m of flat track added (52 m flat road), 212 m track length

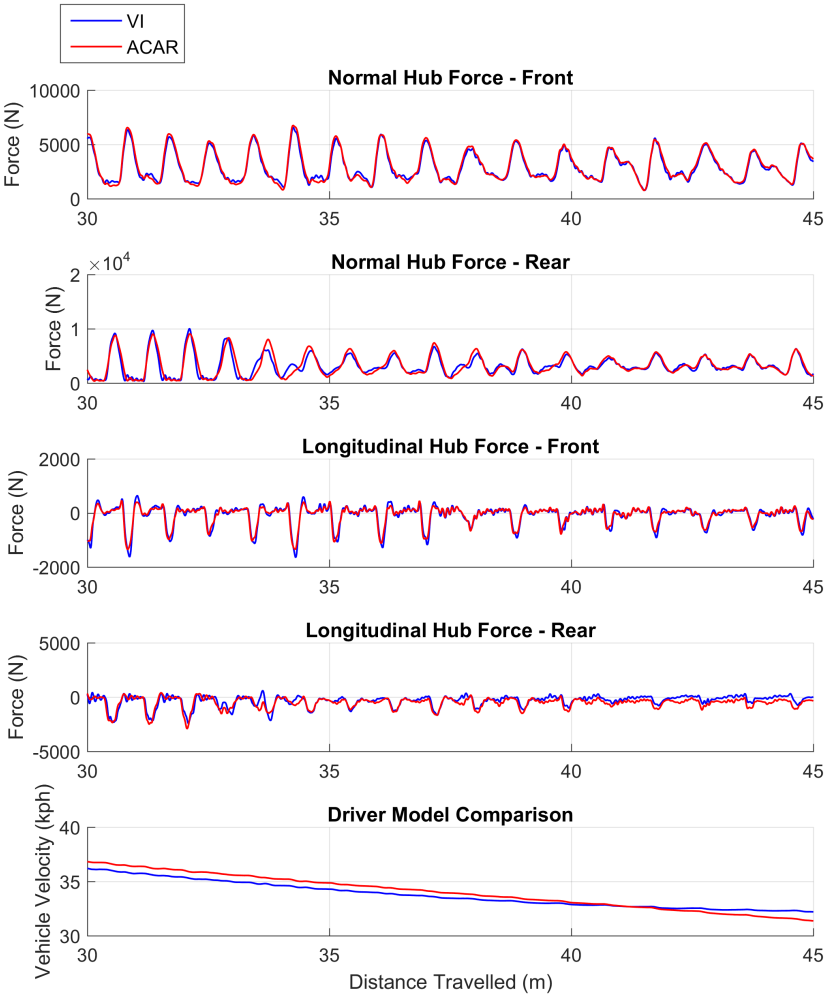
The flat section before the washboard road is extended from less than 3 m to 52 m, and consequently the vehicle velocity at the start of the washboard ridge are different. Without extending the flat section, 0.3 kph of initial velocity difference is observed between the software. On the 182 m washboard track, this variation is reduced to 0.1 kph. For the 212 m track, VI-CarRealTime vehicle reaches the target velocity, while ADAMS/Car model is less than 0.05 kph below the 45 kph target, and the velocity difference is less than 0.1 kph apart. The initial velocities are plotted in Figure 4.43

The three tracks are tested with eight combinations VI-CarRealTime, ADAMS/Car and driver models. The VI-CarRealTime and ADAMS/Car driver pair is not recommended by the VI-CarRealTime technical support team and hence not tested. These tests are:

1. VI-CarRealTime with VI-Driver:
    - Short, medium and long track
2. ADAMS/Car with ADAMS/Car driver:
    - Short, medium and long track
3. ADAMS/Car with VI-Driver:
    - Short and long track



(a) *Maintain*



(b) *Coast*

Figure 4.41: *Washboard: 30-45 m*

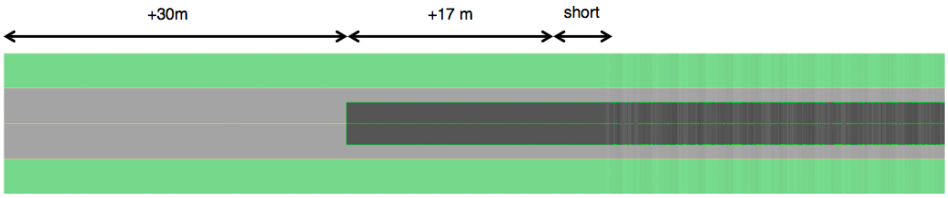


Figure 4.42: *Original and Modified Washboard Track*

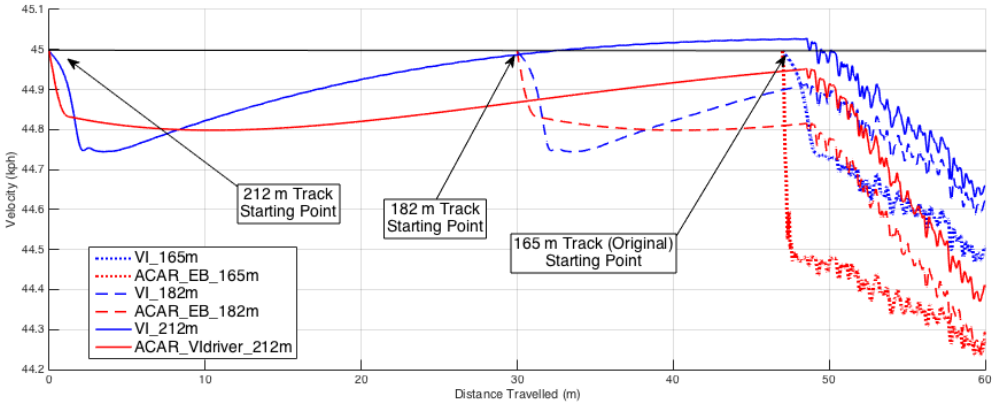


Figure 4.43: *Flat Track Length vs. Initial Velocity*

VI-CarRealTime simulation result is unaffected by the change in track length. On the other side of the coin, changing the driver model in ADAMS/Car affected its results. This observation is not further investigated due to lack of time, but moreover using VI-Driver plug-in in ADAMS/Car is not pursued for several reasons. One reason, it demands high workload associated with changing existing simulation script file format. Another reason is the limited VI-Driver plug-in licenses available. Furthermore, differences between ADAMS/Car results are observed with additional flat sections which could be attributed to the varied steady state values due to the varied distance. For the mere goal of reducing initial velocity difference between the software, the 182 m washboard track is used in this thesis work.

Having a longer test track (182 m) is favored over using VI-Driver plug-in despite increase in simulation computation time. Since VI-CarRealTime is supposed to complement ADAMS/Car, switching over to VI-Driver would result in significant change to the company's (CEVT) current work flow. As an example, all the ADAMS/Car simulation Event File would have to be converted from `.xml` into `.vdf` format.

4.7.6 Unsprung Mass

While ADAMS/Car and VI-CarRealTime have high compatibilities given that many file formats and system file setup are shared, differences between the two software and their versions are still present. This section briefly touches upon challenges brought by between different software versions.

VI-CarRealTime: Wheel Mass Setting

The process of estimating wheel masses is described in section 4.3. Yet, despite the straightforwardness of the mass sweeping process, it is crucial to have correct ADAMS/Car tire force data to compare against. Having had wrong tire force data in the beginning was not only misleading but also resulted in productivity losses.

ADAMS/Car: FTire Free Mass Setting

When starting up ADAMS/Car a user profile file `acar.cfg` is called and various user defined software environment settings are updated. Printed below, is one of the settings that determines the permission of ADAMS/Tire, the tire module associated with ADAMS/Car, to adjust wheel mass and inertia.

```
! Allows Adams/Tire to adjust wheel mass & inertia for belt properties
! of FTire and PAC2002
ENVIRONMENT    MSC_ADAMS_TIRE_DIS_M_AND_I   yes
```

Before 2015 version of ADAMS/Car, the default setting is "no", meaning no tire mass modification is allowed. This setting instructs ADAMS/Car to take "tire free mass" into account when loading the assembly. Since CEVT models are build on 2013 version and later converted to 2015 version, the setting is kept at "No". The opposite effect is true when the setting is "Yes". However, the demo model is based on 2015 version and therefore the switch must be reverted to "Yes".

To further clarify the effect, Static Vehicle Characteristic test is performed with both settings. The demo model is paired with the Pirelli FTire, which has a free tire mass of 8.58 kg as shown below.

```
 $----------------------------------------------------------------MASS_CORRECTION
[MASS_CORRECTION]
$these data are not used by FTire, but only by the calling solver
 free_tire_mass =                 8.58                  $ kg
 free_tire_jxx_jzz =              5.17e5                $ kgmm^2
 free_tire_jyy =                  1.034e6               $ kgmm^2
```

When the tire mass and inertia modification is disallowed, or the "No" setting, the total front unsprung mass is 50 kg, or 25 kg per wheel.

```
 FRONT SUSPENSION CHARACTERISTICS
Suspension Description:
<carrealtime_shared>/subsystems.tbl/VI_FrontSusp.sub
------------------------------------------------------------------------------
(PARAMETER) (UNITS) (AVERAGE) (LEFT) (RIGHT)
------------------------------------------------------------------------------
Unsprung mass (total) kg 50.00
```

Allowing ADAMS/Car to modify tire mass and inertia, or the "Yes" setting, the test saw the total front unsprung mass drop to 32.82 kg or 16.41 kg per wheel. The difference in mass between the setting change is the free tire mass, 8.58 kg. This mass is only added during simulation, where ADAMS/Car solver "modifies" the FTire mass and inertia.

```
 FRONT SUSPENSION CHARACTERISTICS
Suspension Description:
<carrealtime_shared>/subsystems.tbl/VI_FrontSusp.sub
------------------------------------------------------------------------------
(PARAMETER) (UNITS) (AVERAGE) (LEFT) (RIGHT)
------------------------------------------------------------------------------
Unsprung mass (total) kg 32.84
```

Sine Road Test

To replicate the washboard track, which has constant ridge height and increasing inter-ridge spacing (λ), 15 sine roads with λ from 0.6 to 2 m at 0.1 m increment are generated. The vehicle is driven over these roads at a constant velocity of 45 kph, the same speed as in the washboard track simulation, and the corresponding road input frequency is shown in Table 4.4.

Single obstacle is not the most effective method at determining the correct wheel mass. This is already shown in Figure 4.22 in section 4.6.2, where higher wheel masses in VI-CarRealTime did not produce noticeable increase in the front tire forces and rear tire longitudinal force. The influence of tire mass is more obvious when vehicle is tested with sinusoidal road inputs, as shown by the comparison between Figure 4.25a and 4.25b section 4.6.3. At 45 kph vehicle speed, the washboard segment with 1 m inter-ridge spacing (13 Hz input) is the sensitive region that led to the discovery of the FTire free mass modification setting.

Table 4.4: Inter-ridge Spacing λ to Road Input Frequency

Lambda (m)	0.6	0.7	0.8	0.9	1	1.1	1.2	1.3	1.4	1.5	1.6	1.7	1.8	1.9	2
Freq. (Hz)	20.8	17.9	15.6	13.9	12.5	11.4	10.4	9.6	8.9	8.3	7.8	7.4	6.9	6.6	6.3

Thus, to verify the correct FTire settings in ADAMS/Car and wheel masses in VI-CarRealTime, simulations are conducted with different road input frequencies ranging from 6.3 Hz up to 20.8 Hz per Table 4.4. Figure 4.44b shows the tire forces at 12.5 and 13.9 Hz road disturbance, while the remainder of the result plots can be found in Figure 7, 8, and 9 in the Appendix section A.3.

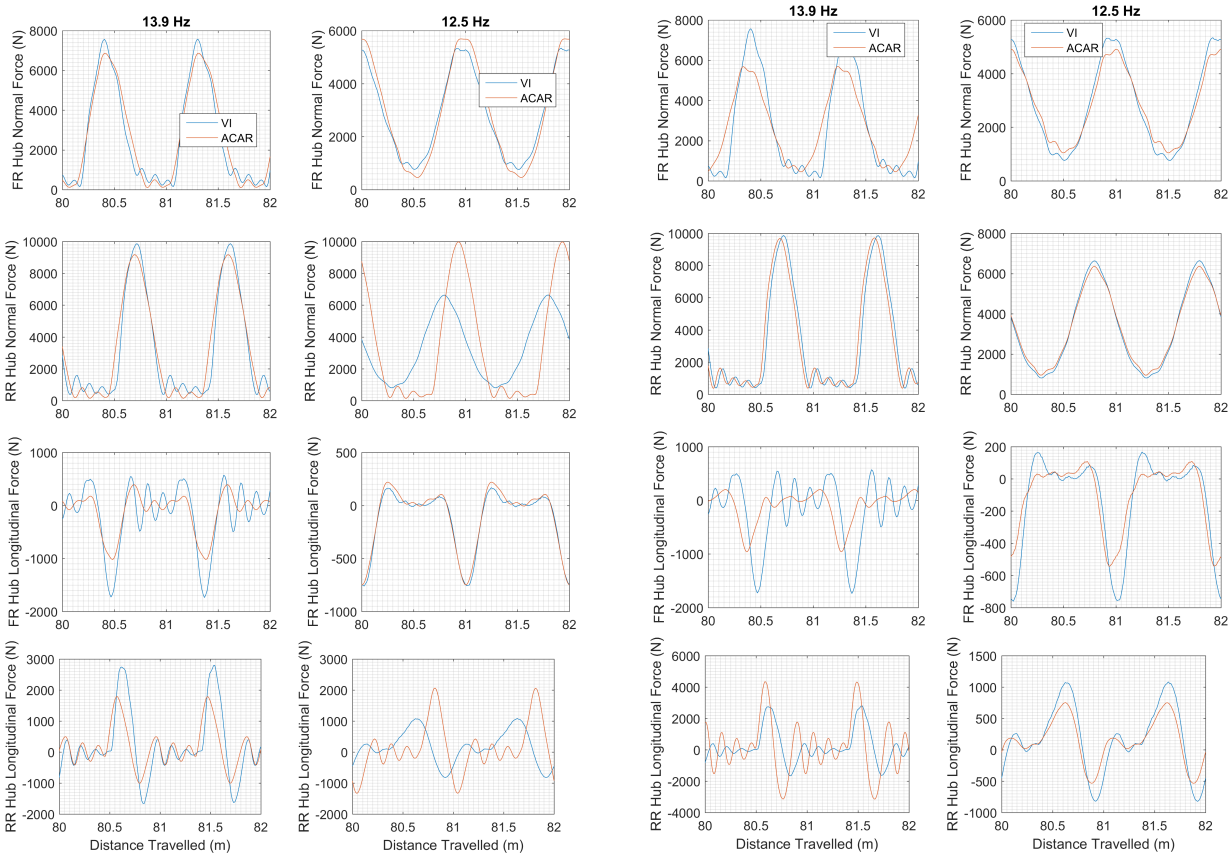
Regarding Figure 4.44a at 12.5 Hz, rear tire normal and longitudinal forces are poorly correlated. However, this has been significantly improved by choosing the correct FTire free mass modification setting as shown by the same subplot in Figure 4.44b.

Despite the improvements made at 12.5 Hz, allowing FTire free mass modification led to growing discrepancies between front tire forces at 13.9 Hz. Hence, it must be acknowledged in the end there is still considerable disagreement between the tire forces when the road input frequency is around 13 Hz. There are other mass and inertia properties in VI-CarRealTime, such as longitudinal dynamic mass and spin inertia, which are not fully explored due to time restraint. Attempts at removing free tire inertia in the same manner as the removal of free tire mass have been made. However, the process is less straightforward. Guessing the correct inertia properties by sweeping through different values is inefficient as it is ineffective. Formally exporting the vehicle model with the appropriate tire model is the best way to determine the correct values, and time should be invested in debugging this process.

Finally, VI-CarRealTime with 25 kg tire mass on all four wheels and ADAMS/Car allowing FTire free mass modification tire forces from the sine road sweep is summarized in Figure 4.45. The x-axis represent the road input frequency and the y-axis is the peak force captured during each road frequency.

With reference to normal forces, for the front wheel, the gap between the data lines is small except for 13-15 Hz road frequencies; for the rear wheel, the comparison is very ideal. Comparing longitudinal forces, for the front wheel, the gap between the data lines is overall small; for the rear wheel, the difference is large when road frequency is higher than 13 Hz.

To summarize, at road frequencies lower than 12 Hz the tire forces between ADAMS/Car and VI-CarRealTime is closely comparable. However, as the input frequencies increase the comparison between the software become less certain. Moreover, as described earlier, a setting change that led to improvement in longitudinal tire forces at one road frequency saw worsened comparison in normal tire forces at another road frequency. Therefore, this trial-and-error approach at estimating tire masses is not efficient and not recommended.



(a) *"No" Setting* (b) *"Yes" Setting*

Figure 4.44: *Allows ADAMS/Tire To Adjust Wheel Mass and Inertia Switch*

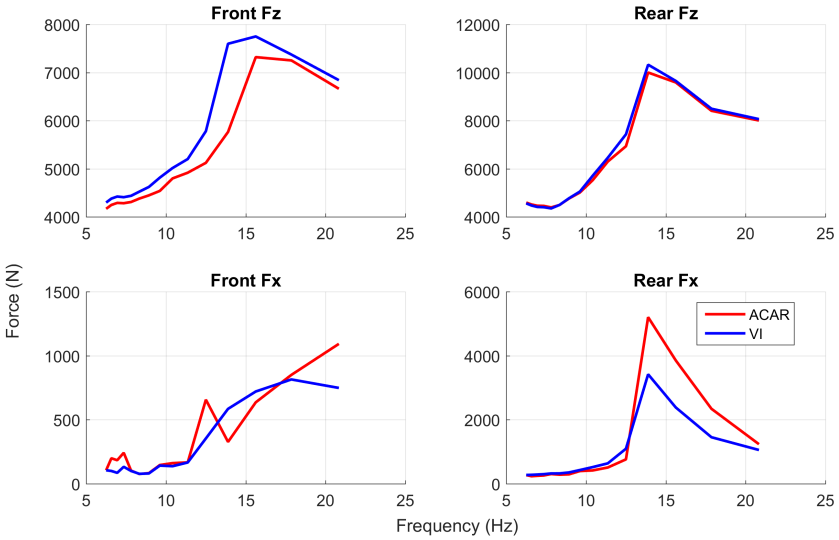


Figure 4.45: *ADAMS/Car vs. VI-CarRealTime Road Input Frequency Test: Rear Tire Normal Force Comparison*

5 CEVT Control Model Results

5.1 CEVT Control Model Issues

At first when simulation switched over to focusing on the CEVT Control Model, large longitudinal tire forces represented by the pairs of giant opposing red arrows were viewed in VI-Animator as shown in Figure 5.1. Clearly the results are highly erroneous - some of which are due to wrong software setup, while others are due to glitches in ADAMS/Car model export. Various setting changes that brought the VI-CarRealTime result closer to that of ADAMS/Car will be described in this section.

5.1.1 ADAMS/Car 2015 Setting

As mentioned in section 4.7.6, the CEVT models are built upon the 2013 version of ADAMS/Car. Thus, it is verified in ADAMS/Car that the free tire mass modification permission has been set to "No".

```
! Allows Adams/Tire to adjust wheel mass & inertia for belt properties
! of FTire and PAC2002
ENVIRONMENT    MSC_ADAMS_TIRE_DIS_M_AND_I   no
```

5.1.2 Ftire Setting

During initial simulations with the CEVT model, large oscillating longitudinal forces were found. As a result, incorrect Ftire settings in VI-CarRealTime were brought to light. It was learned that correct Ftire setting is necessary in order to deal with suspension compliance. The key parameters related to suspension compliance is highlighted in Figure 5.2. The procedure has been discussed in detail in section 4.4.

5.1.3 Powertrain

Differences were observed with the powertrain properties when exported out of ADAMS/Car. It was evident when examining the engine torque map. Several fixes in VI-CarRealTime have been made to improve its resemblance to ADAMS/Car:

1. Correcting the engine torque versus engine rpm map
2. Changing from Rear Wheel Drive to Front Wheel Drive
3. Changing the differential setting: turning on "front differential" and disabling "rear differential"

5.1.4 Suspension Compliance Map

There exists a Demo model with compliance in the VI-CarRealTime example database. Examining the model's compliance settings, one notable difference between Compliant Demo model's suspension compliance map and that of the CEVT model is the force range that is tabulated. The Base Variation versus Braking F_x versus Jounce (normal to page) compliance map is shown in Figure 5.3 as an example. As shown by the figure, the Demo model's compliance are evaluated at forces ranging from -5500 N to 5500 N, while the CEVT model compliance are only evaluated between -1500 N and 1500 N. As a result, spline extrapolation errors could have occurred, which was also indicated by the solver in VI-CarRealTime. Incorrect extrapolation could have affected the tire forces.

The second major difference between the Demo model and the CEVT model suspension compliance maps is the level of details. Regarding Figure 5.4, for every left side jounce value, the demo model has a set of "Toe vs. Fx vs. Jounce" splines (solid line) for different right side wheel travel, and vice versa. While for the CEVT model, only a single spline (dashed line) is described in the suspension compliance irregardless of the opposite wheel jounce.

These two differences may have a profound impact on wheel displacement and orientation as it travels over an obstacle, which leads to differences in longitudinal tire forces. Concerns regarding the correctness of the compliance map are further discussed in section 5.4.3.

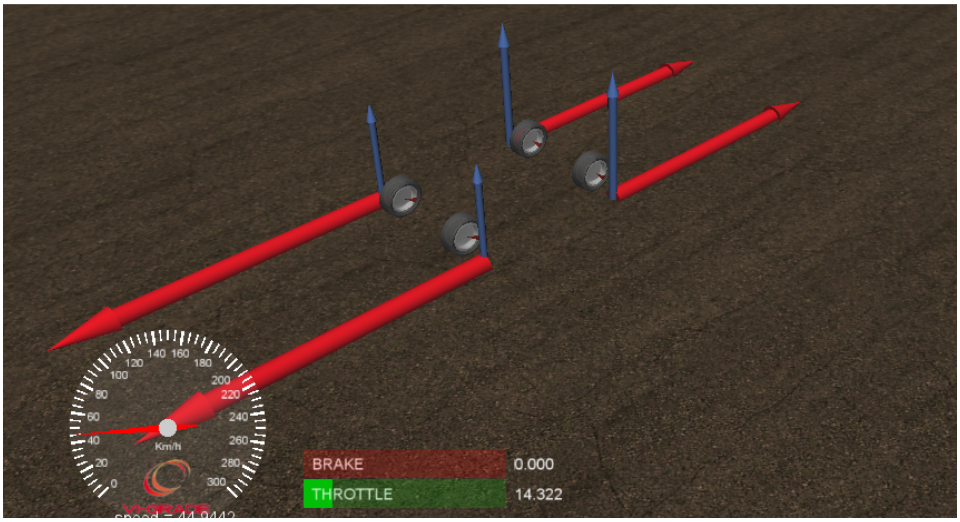


Figure 5.1: *Initial Tire Force Comparison Result*

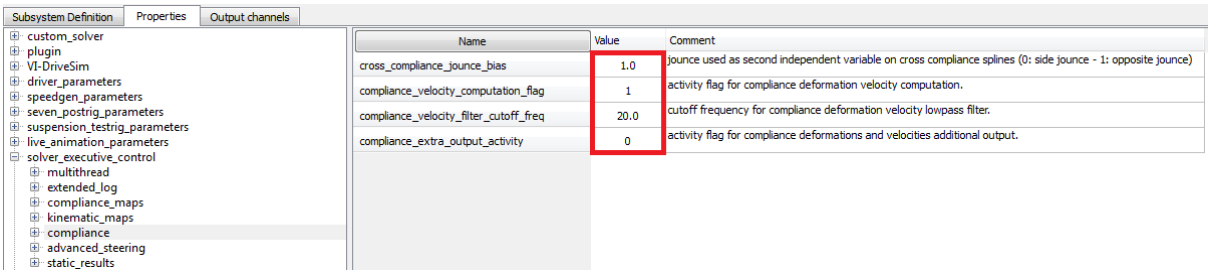


Figure 5.2: *VI: Recommended Ftire Settings*

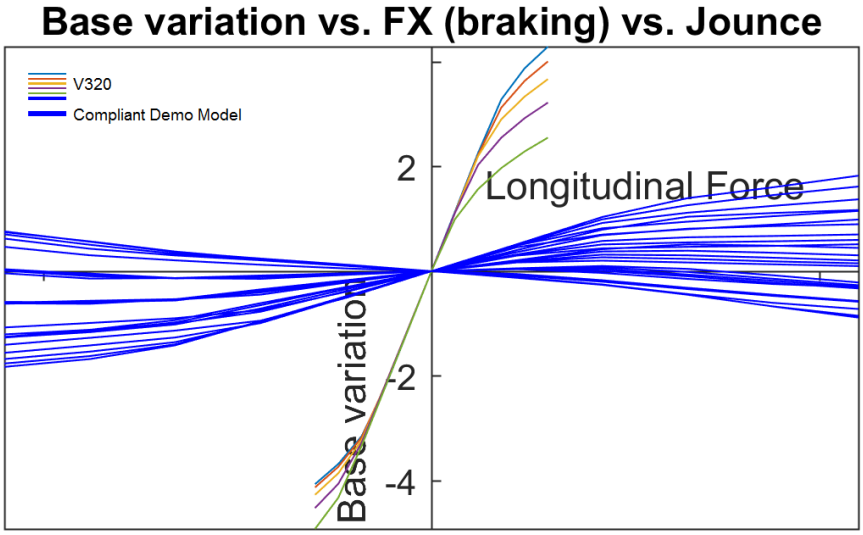


Figure 5.3: *Suspension Compliance Curve Comparison: 2D View*

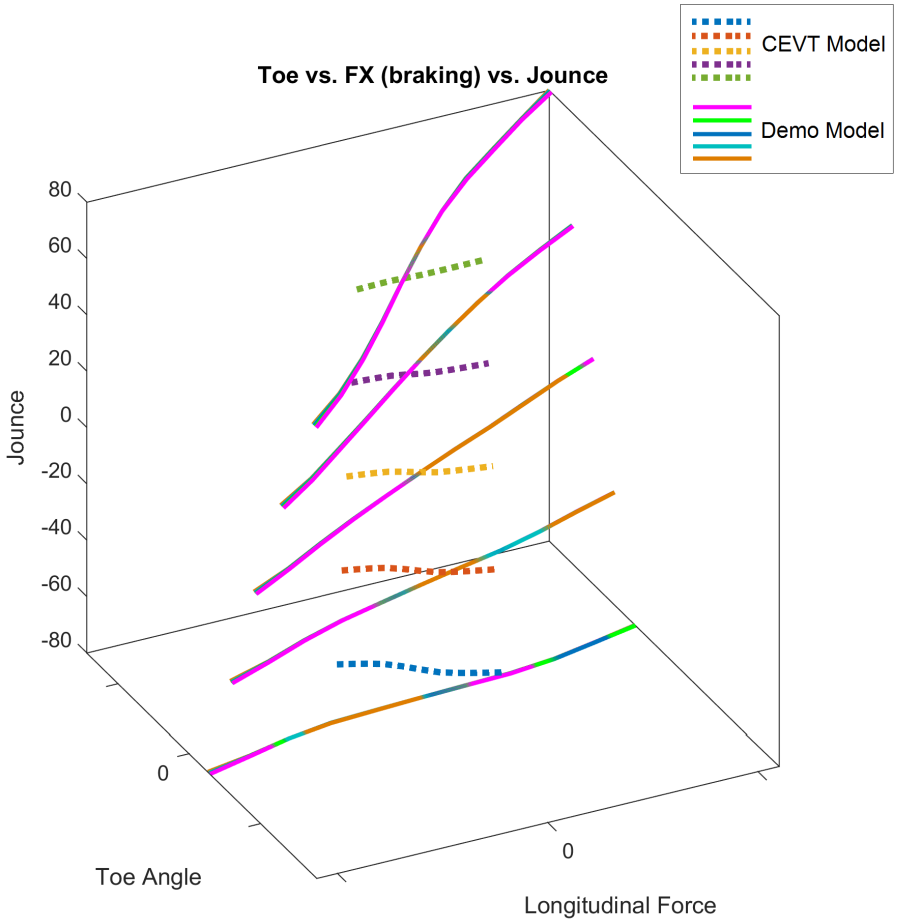


Figure 5.4: *Suspension Compliance Curve Comparison: 3D View*

5.2 2D Flat Road

Following the methodology of increasing complexity, the comparison process started with the Pacejka tire model on a flat road and then moved on to the CEVT Continental-225/40R19 FTire. The event parameters are the same as for the Demo model, which are listed below:

- Road: Flat road (`flat.rdf`)
- Model: CEVT model (with compliance) + CEVT model powertrain
- Driving Event: 3rd gear with no shifting, straight line, 10 seconds at 40 kph (11111.11 mm/s)

5.2.1 Pacejka Tires

The events for the flat road are run for 10 seconds (which corresponds to 111.11 m of distance travelled) in order to have time for the vehicle to settle after initial transient response as observed in Figure 5.6a. However the plot abscissa is restricted to 20m for visualisation purposes.

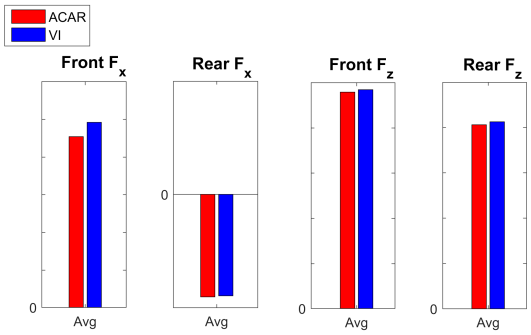
The longitudinal forces in Figure 5.6a show excellent correlation and are almost identical once the driver model has reached steady state. Since the CEVT models are front wheel driven the front longitudinal forces are positive while the rear is negative which is the opposite of what was observed in the results of the Demo model.

The normal forces in Figure 5.6a are different for the left and right wheels which could seem strange at first glance after viewing the series of Demo model results. But this is due to the lateral positioning of the center of gravity which is +2.72 mm. The positive sign implies it is towards the left wheel when viewed as per the VI-CarRealTime co-ordinate system in Figure 2.8. In summary The normal forces are in good agreement trend wise and vary by 50N in the front and the rear which can be considered acceptable for conceptual level evaluations. Please note that the wheel masses in VI-CarRealTime remain unchanged and the unsprung mass values after exporting from ADAMS/Car are assumed to be correct. This is unlike the demo model where iterations were conducted to obtain the correct unsprung mass for which the plots correlated very well.

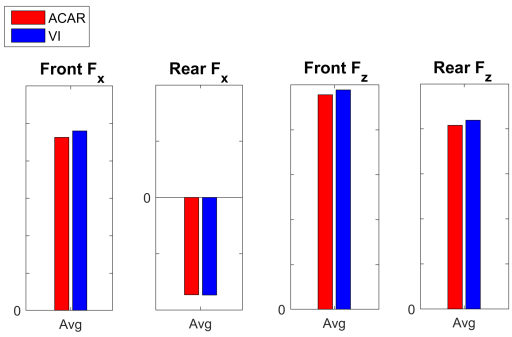
5.2.2 Continental - 225-40R19

The tire model complexity was then increased by using the Continental - 225-40R19 which is an FTire model. The same simulation setup as for the CEVT model with Pacejka tire was run and the results are illustrated below in Figure 5.6b. The forces differ from the Pacejka tire simulations since the tire properties of Pac2002 and the Continental - 225/40R19 are different.

A similar trend as that of the Pacejka tires are observed with small differences between the VI-CarRealTime and the ADAMS/Car forces. The bar graphs are an exaggerated version of differences and inferences should be made only after carefully viewing the magnitudes which unfortunately cannot be displayed. The front F_x minimum force values differ and this can be attributed to the variation of the VI-CarRealTime forces during initialization. To summarize, no major surprises were observed by increasing the complexity to the Continental FTire. The normal and longitudinal forces correlate fairly well as seen in Figure 5.5b and the results can be deemed acceptable for a concept stage evaluation.

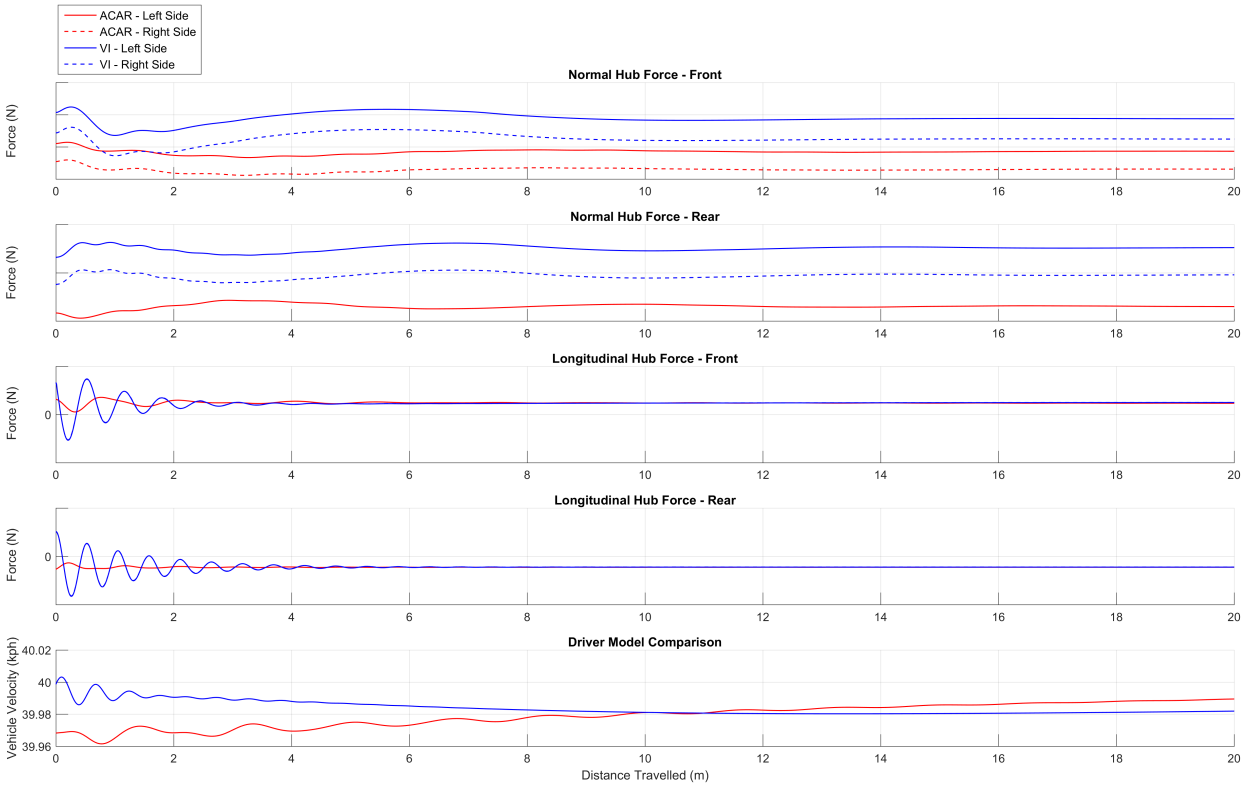


(a) *Pacejka Tire*

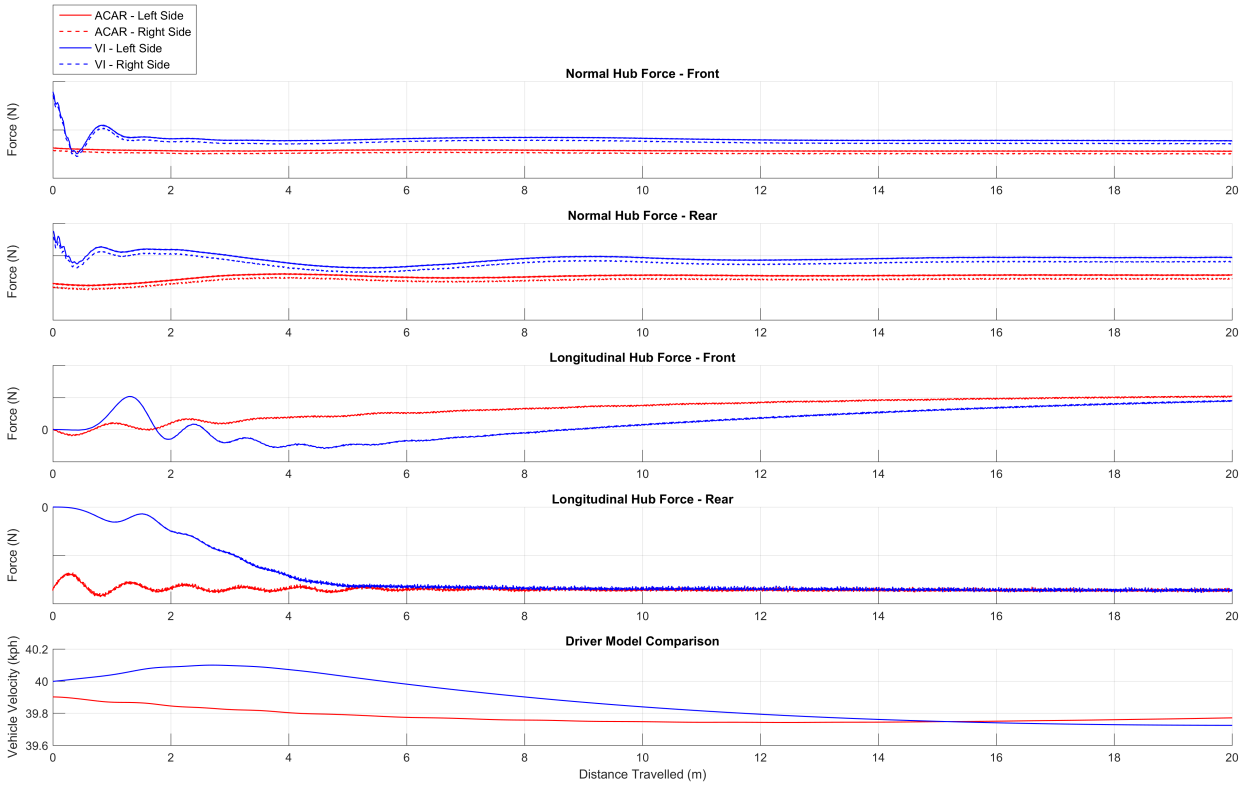


(b) *Continental 225-40R19 Ftire*

Figure 5.5: *CEVT model on Flat Road: Force Comparisons*



(a) *Pacejka Tire*



(b) *Continental 225-40R19 Ftire*

Figure 5.6: *CEVT model on Flat Road: Tire F_x and F_z*

5.3 Cleat Road

- Road: Cleat road (`Cleat10x50mm.crg`)
- Model: CEVT model (with compliance) + CEVT model powertrain
- Driving Event: 3rd gear with no shifting, straight line, 3 seconds at 40 kph (11111.11 mm/s)

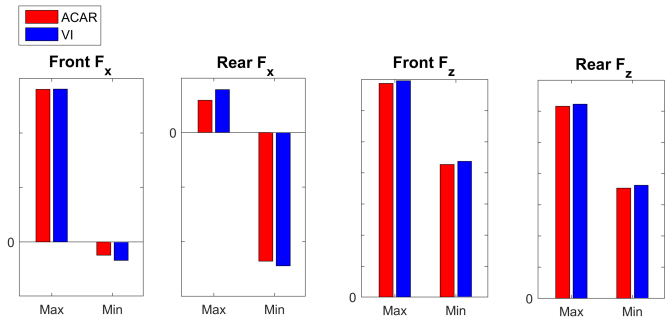
5.3.1 Pacejka Tire

An interesting point to note is that the initialization for VI-CarRealTime is quite different when compared to initialization of VI-CarRealTime for a flat road. However this is due to the different scales used for the plots.

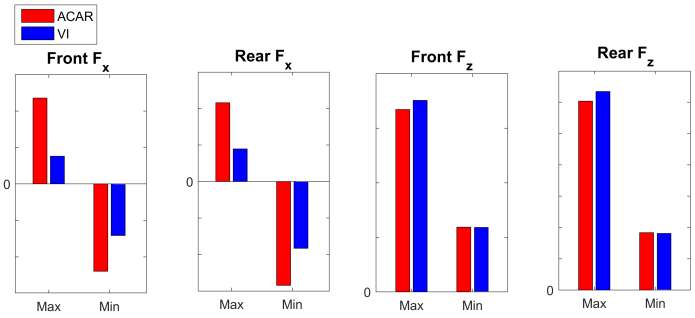
The same exercise as for the flat road is repeated starting with the Pacejka (Pac2002) tires. The cleat is 10 mm in height and 50 mm in width. A negligible difference in velocities (driver model) exists. A good correlation is observed for the normal and longitudinal forces even as the vehicle hits the cleat. As expected the peaks for the rear wheels are at a later point than the front since the front wheels hit the cleat first. A slightly higher normal force peak magnitude is observed for the front as the CEVT model front distribution is more. A slight lag like phenomenon is observed with the ADAMS/Car normal force curve but can be ignored during a conceptual evaluation. Overall the results of the Pacejka tire on a cleat road match extremely well in terms of the maximum and minimum normal forces for both the front and rear wheels with small differences in the maximum and minimum longitudinal forces as seen in Figure 5.7a which are acceptable for a conceptual evaluation.

5.3.2 Continental 225-40R19 Ftire

The same simulation event as that of the CEVT model with Pacejka model is repeated with the Continental FTire. The shape of the peak as the vehicle hits the cleat is better defined with the Continental FTire model than when compared to plots with Pac2002 tire. The normal forces again exhibit an excellent correlation. The average longitudinal forces are agreeable over the whole simulation period with a noticeable difference between the maximum and minimum forces. It remains unclear what the cause of such difference is. Differences in the suspension compliance maps due to lower forces considered during export may have played a contributing factor.

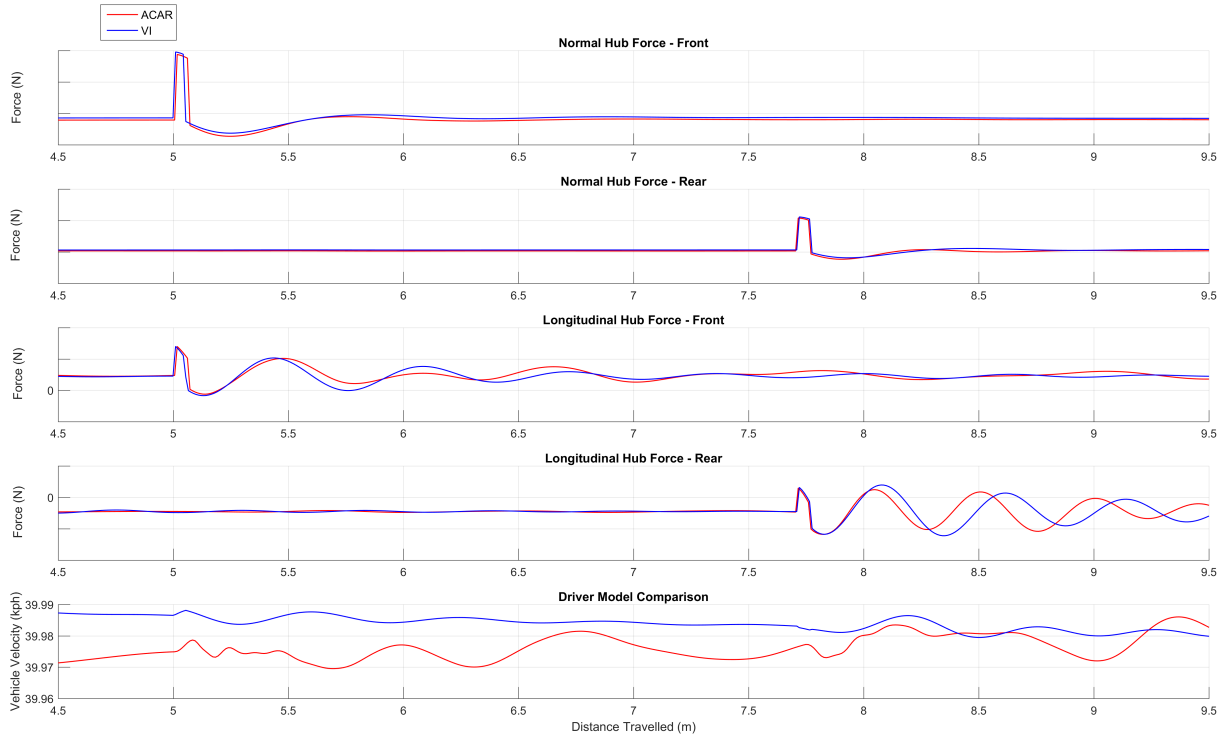


(a) *Pacejka Tire*

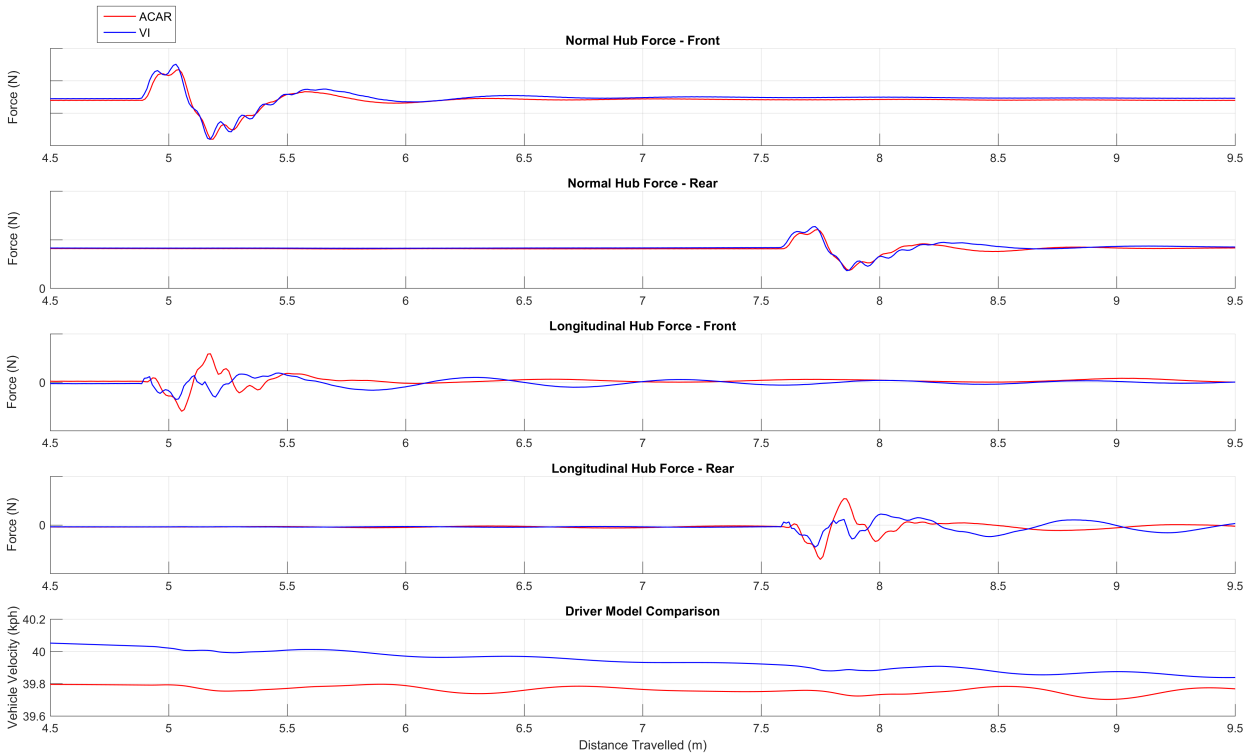


(b) *Continental 225-40R19 Ftire*

Figure 5.7: *CEVT model on Cleat Road: Force Comparisons*



(a) *Pacejka Tire*



(b) *Continental 225-40R19 Ftire*

Figure 5.8: *CEVT model on Cleat Road: Tire F_x and F_z*

5.4 Washboard Road

5.4.1 Continental Ftire - Maintain Velocity

This section deals with the results of the CEVT model on advanced roads namely the in-phase washboard and the Belgian block. In phase washboard is run with event control files which were available at CEVT. An excerpt of the file keeping in line with the event setup formats of the previous roads is shown below:

- Road: Washboard in-phase (`washb_iph_asm_ccw_smooth_rgr.rdf`)
- Model: CEVT model (with compliance)
- Driving Event: 3rd gear with no shifting, straight line, 3 seconds at 45 kph (12500.00 mm/s)

Keeping in mind the initialization and stabilization differences the washboard road which is actually 165 m is extended to 182m with 17m of extra flat road before the washboard begins. Note that for all washboard events only FTire was used and hence any lack of mention of the tire model in the washboard events can be assumed to be with FTire.

The first plot in Figure 5.9 shows the wavelength variation of the washboard road as the distance progresses. As the plot shows, the wavelength increases suggesting that we move from closely spaced bumps to widely spaced bumps. The next two plots show the comparison of the normal force results for the front and rear left wheels. The right wheels exhibit a similar trend but with lower magnitude and is not illustrated in the plots. As can be seen, the front wheels show excellent correlation for the normal forces. Differences are noticed for the 40 to 50m range in the rear wheels. Although this corresponds to the range where the ADAMS/Car driver model fluctuates the most one cannot attribute this as directly contributing to the differences.

Another theory is that there is a resonance that is being captured. A quick calculation of the wheel hop frequency using the relations in the 'natural frequency' section shows $14.8Hz$ for the rear wheels and $13.2Hz$ for the front wheels. This is in proximity to the frequency calculated for the ratio of velocity to wavelength which corresponds to $11.1Hz$ ($(44.5/3.6 * 0.9)$). The new feature in ADAMS/Car for Static Vehicle Analysis which would give the wheel hop and other parameters as output did not work for the CEVT models. The differences thus could also depend on the solvers differ, presence of flexible bodies in ADAMS/Car and how the MBD model differ between the two software. This will require further investigation. However for a concept stage evaluation this agreement between the two software can be claimed good enough.

The longitudinal forces do not show the same level of agreement as the normal forces. The differences in the model velocities is for sure one aspect contributing to the differences but one cannot conclude it as the the only contributor since varying parameters such as compliance will have an effect on the longitudinal forces as will be seen in the later sections. Tuning the longitudinal velocity controller parameters to match the velocities is one way of eliminating the 'what if' scenario regarding velocities, however that exercise was not pursued due to time constraints. Figures 5.10a and 5.10b give a detailed view of the forces between certain ranges and gives a good idea of the correlation between the results from the two software. One can notice good correlation (50 to 55 m in the front and rear) in some ranges but not so in some (35 to 40 m for the front).

5.4.2 Continental Ftire - Coasting

To observe the 'what if' concern regarding the driver model and parameters, the washboard event was run in 'coasting' mode. The models were initialized at the same velocity as the previously defined washboard event but with the throttle control parameter as zero. This means that the vehicle 'shuts off' and the speed drops as shown in driver model comparison of Figure 5.11. Although the velocities are not identical the rate of drop is nearly identical.

The normal forces show the same correlation and magnitude as that of the regular washboard event. The peaks do differ for the rear wheels and this is in the range of 30 to 40 m which is earlier than for the regular washboard event. This is an acceptable trend with respect to the resonance theory since the velocity is lesser and the bumps are closely spaced in the beginning.

The longitudinal forces show a better correlation than the regular washboard if looking at the minimum longitudinal forces. The maximum forces show similar values in terms of magnitude. The longitudinal forces look similar shape-wise if you look at the detailed plots in Figures 5.12a and 5.12b.

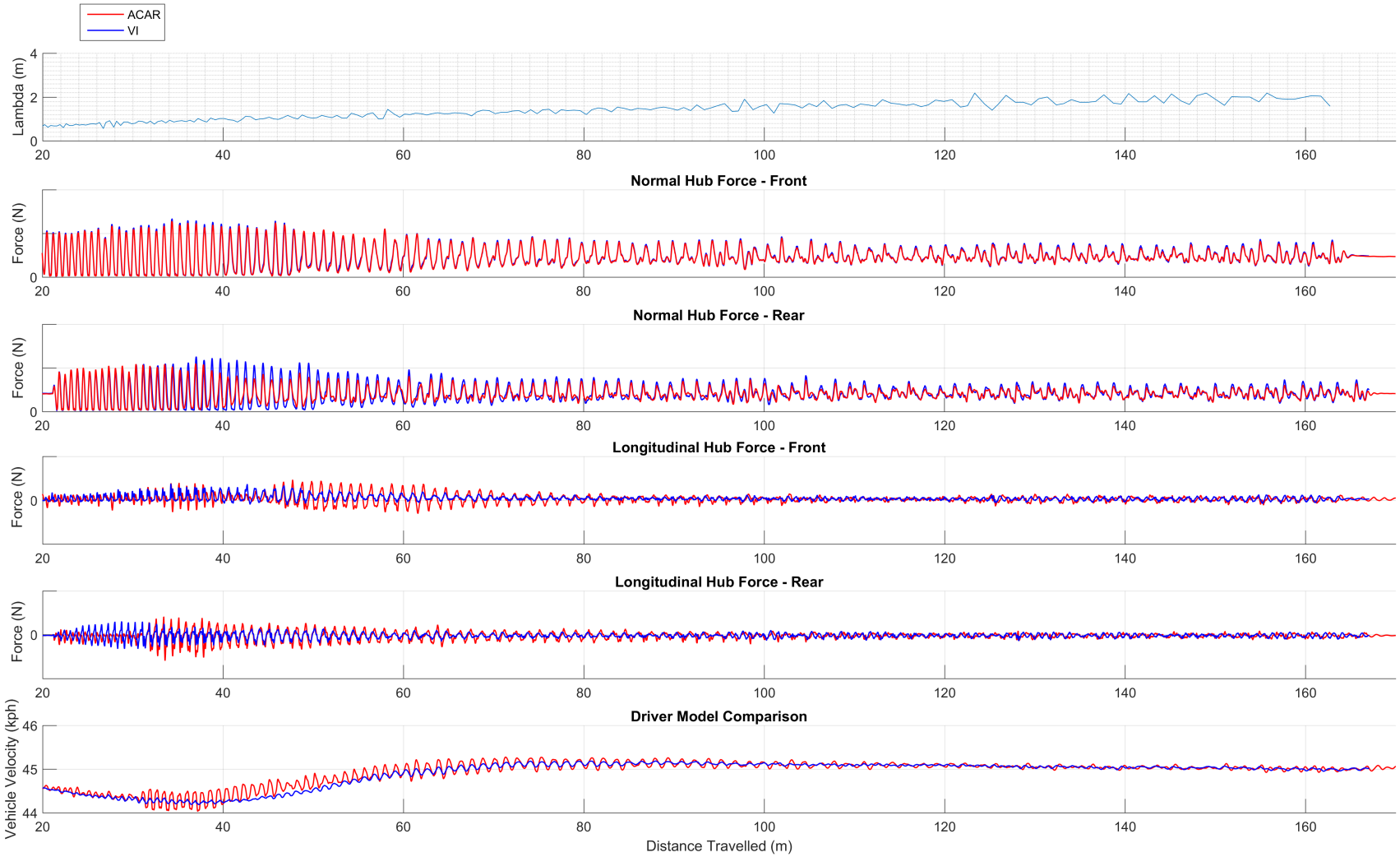
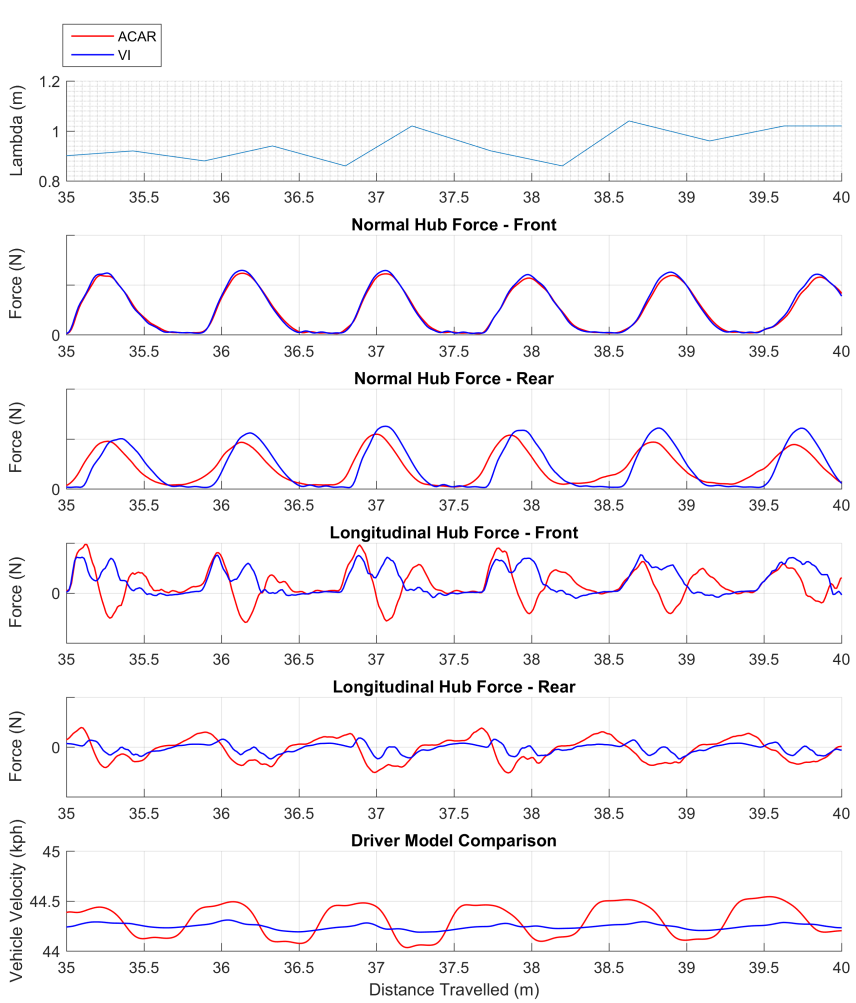
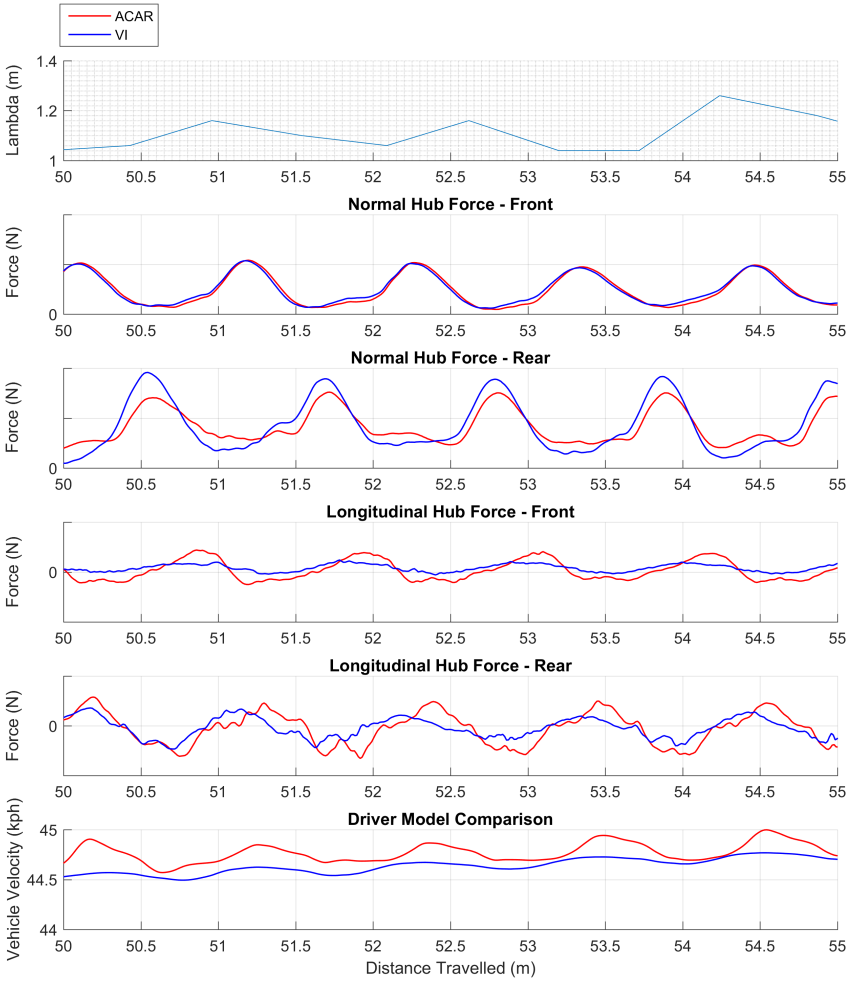


Figure 5.9: *CEVT model with Continental Ftire: Washboard, Maintain Velocity*



(a) *35-40m*



(b) *55-60m*

Figure 5.10: *CEVT model with Continental Ftire on Washboard, Maintain Velocity: Tire F_x and F_z*

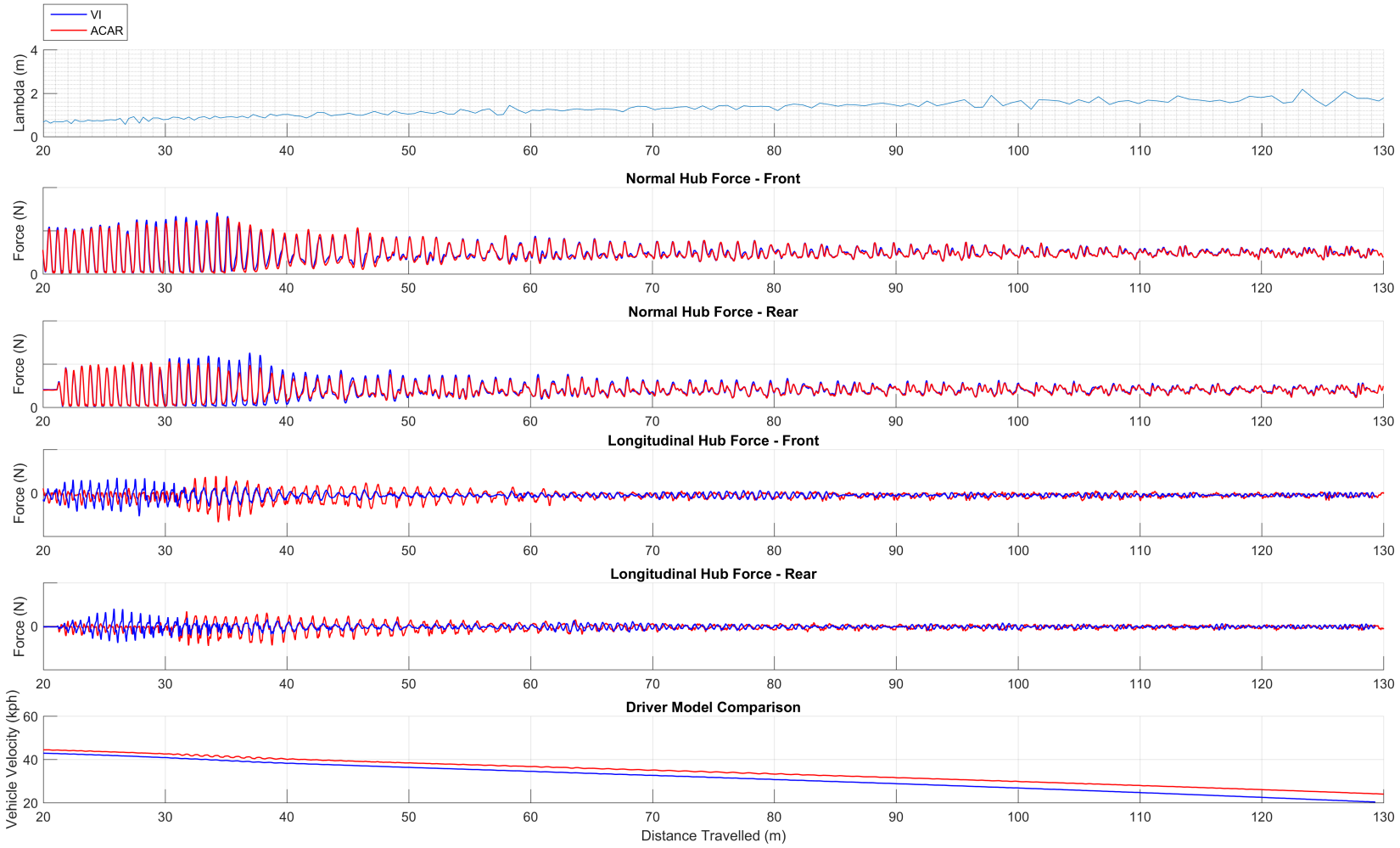
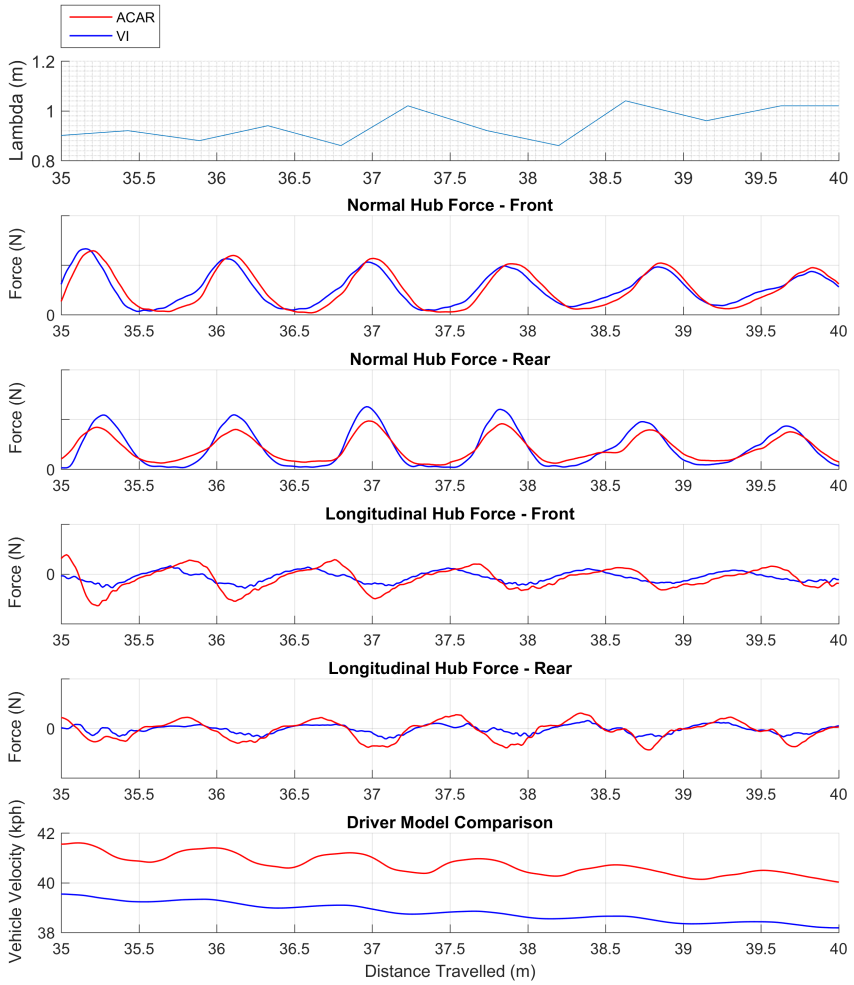
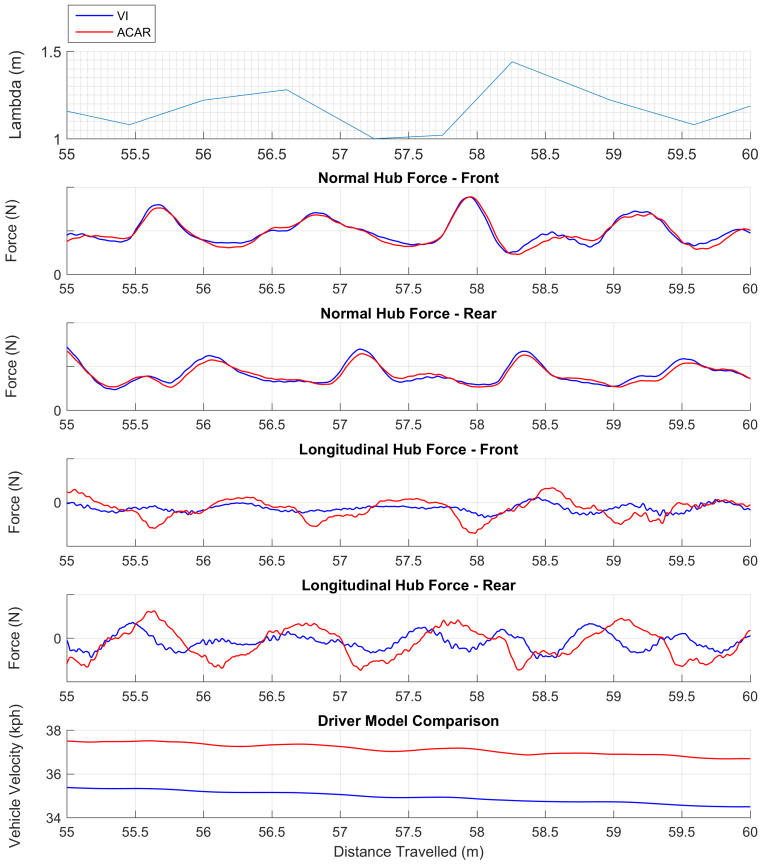


Figure 5.11: *CEVT model with Continental Ftire on Washboard: Coasting*

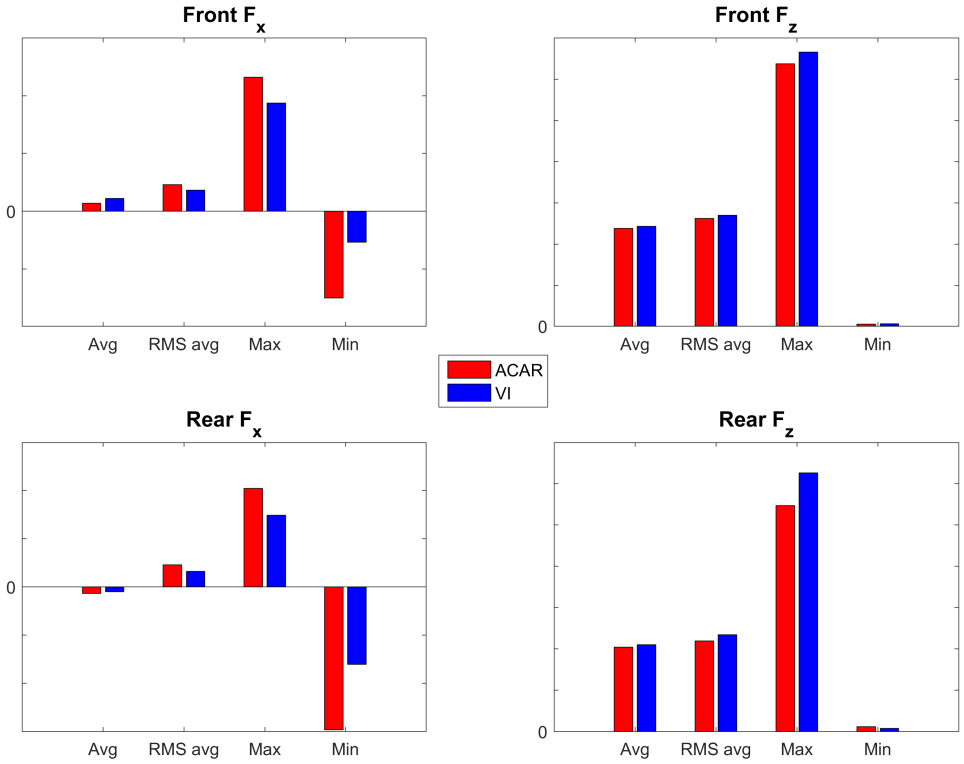


(a) *35-40m*

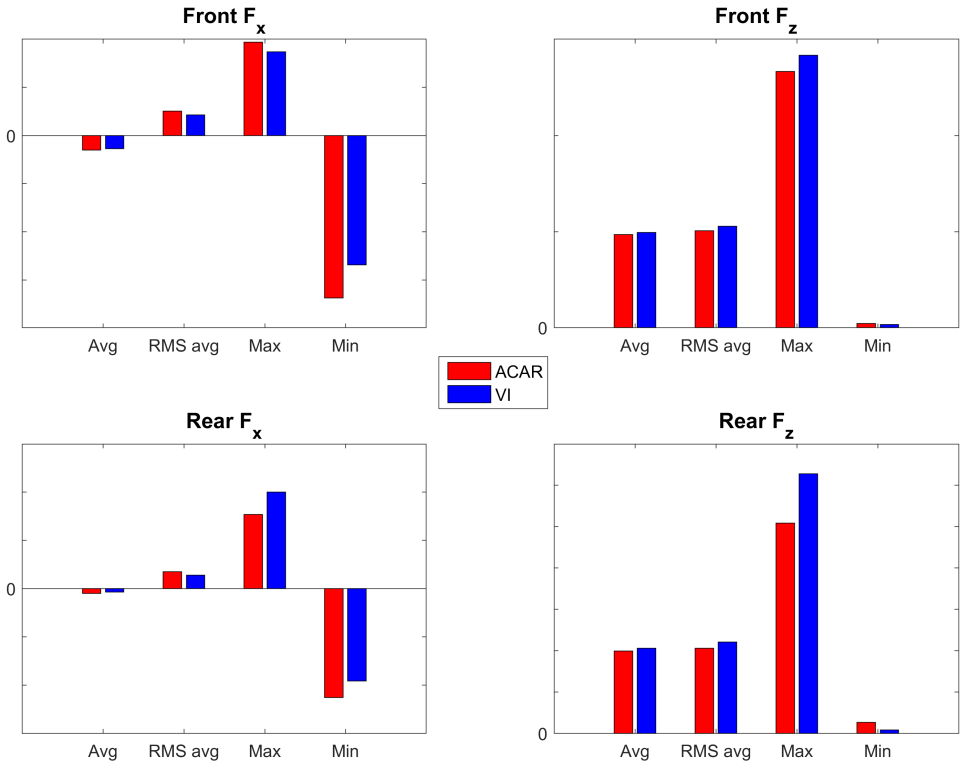


(b) *55-60m*

Figure 5.12: *CEVT model with Continental Ftire on Washboard: Tire F_x and F_z*



(a) *Maintain Velocity*



(b) *Coasting*

Figure 5.13: *CEVT model on Washboard with Continental 225-40R19 Ftire: Force Comparisons*

5.4.3 CEVT model - Suspension Compliance Investigation

An experiment was conducted where the idea was to compare the variation of the VI-CarRealTime results with and without compliance against the ADAMS/Car results. This was because extremely high and unreasonable longitudinal forces were observed when work was first started with the CEVT models. Although this was solved by turning on the 'compliance velocity computation' flag. This experiment whose results are illustrated in Figure 5.14 compares the CEVT model in VI-CarRealTime with compliance (and the compliance flag activated) and without compliance.

One can observe that the normal forces are the same with and without compliance. The story however differs when it comes to the longitudinal forces. Removing compliance enabled a very good match for the front longitudinal forces and the rear longitudinal forces in the 35m to 36 m range. However the same cannot be said for the front longitudinal forces at the 55 to 56.5 m range. This supports the earlier statement that the driving model cannot be considered as the only contributing factor to the longitudinal force differences.

Another important aspect to consider is that the ADAMS/Car model consists of all the bodies with some being flexible. Also the compliance splines (look-up tables) could vary based on the forces considered during export. To evaluate this, the compliance splines in VI-CarRealTime were scaled up by certain factors. Although a scaling factor of 1.5 showed a better match of the longitudinal forces at least in the rear wheels, it resulted in unexpected lateral forces. This suggests a more detailed parametric study would be beneficial and finally enable a better tuned VI-CarRealTime result which is more in line with the ADAMS/Car results. This however would be a time consuming exercise and was not pursued further in detail.

5.4.4 Pirelli Ftire - Maintain Velocity

To observe if the washboard results with the Continental FTire was an isolated phenomenon, the tires were replaced with a Pirelli - 235 45R20 FTire. This yielded in similar results as that of the results with the Continental FTire. The plots are illustrated in Figure 10 in the Appendix section A.3.

Another simulation conducted with the Pirelli FTire was the unsprung mass sweep, where the unsprung mass was increased and decreased by the free tire mass indicated in the FTire file. The motivation behind is to see if similar effects as that of the demo model are observed for the CEVT model as well. Figure 11 in the Appendix section A.3 shows the illustration of the unsprung mass variation. Reducing rear wheel mass, the rear normal forces show a better match with ADAMS/Car. However the front normal forces show better conformance with the unchanged VI-CarRealTime unsprung mass. It is however not so easy to make such a clear distinction for the longitudinal forces as the conformance differs for different ranges in Figure 11.

5.5 Belgian Block

The Belgian block road as mentioned in the roads section is a curved path with rectangular stones.

During our simulations, there were difficulties in making the model follow the curved path correctly. Due to this difficulty, the CEVT model with the Pacejka tires (Pac 2002) was run straight on the curved path. This implies that not all wheels will be in contact with the stones. One can imagine instances where the left wheels are on a flat road while at the same instances the right wheels are in contact with the stones. This simulation was run with the Pacejka tire to see if the discrepancies seen in longitudinal forces with the case of FTires in washboard are repeated. Note that the simulations with Pacejka tires did not run in the washboard event due to high input frequencies.

Figure 5.18 shows excellent conformance in the shape and also the magnitude for the normal forces. The longitudinal forces however show magnitude differences with fairly decent shape conformance. A comparison of the minimum longitudinal forces show similar magnitudes for the rear and a difference of 500N in the front wheels. Figures 5.20a and 5.20b show magnified versions of the forces. An interesting observation is the vehicle in ADAMS/Car offsets by 0.3 m during the whole run as illustrated in Figure 5.21.

5.5.1 Belgian Block - Coast

The simulation in the 'coast' mode was run on the Belgian block road. The system parameters are listed below:

- Road: Stochastic - Belgian Hipped Tiles
- Model: CEVT model with CEVT powertrain

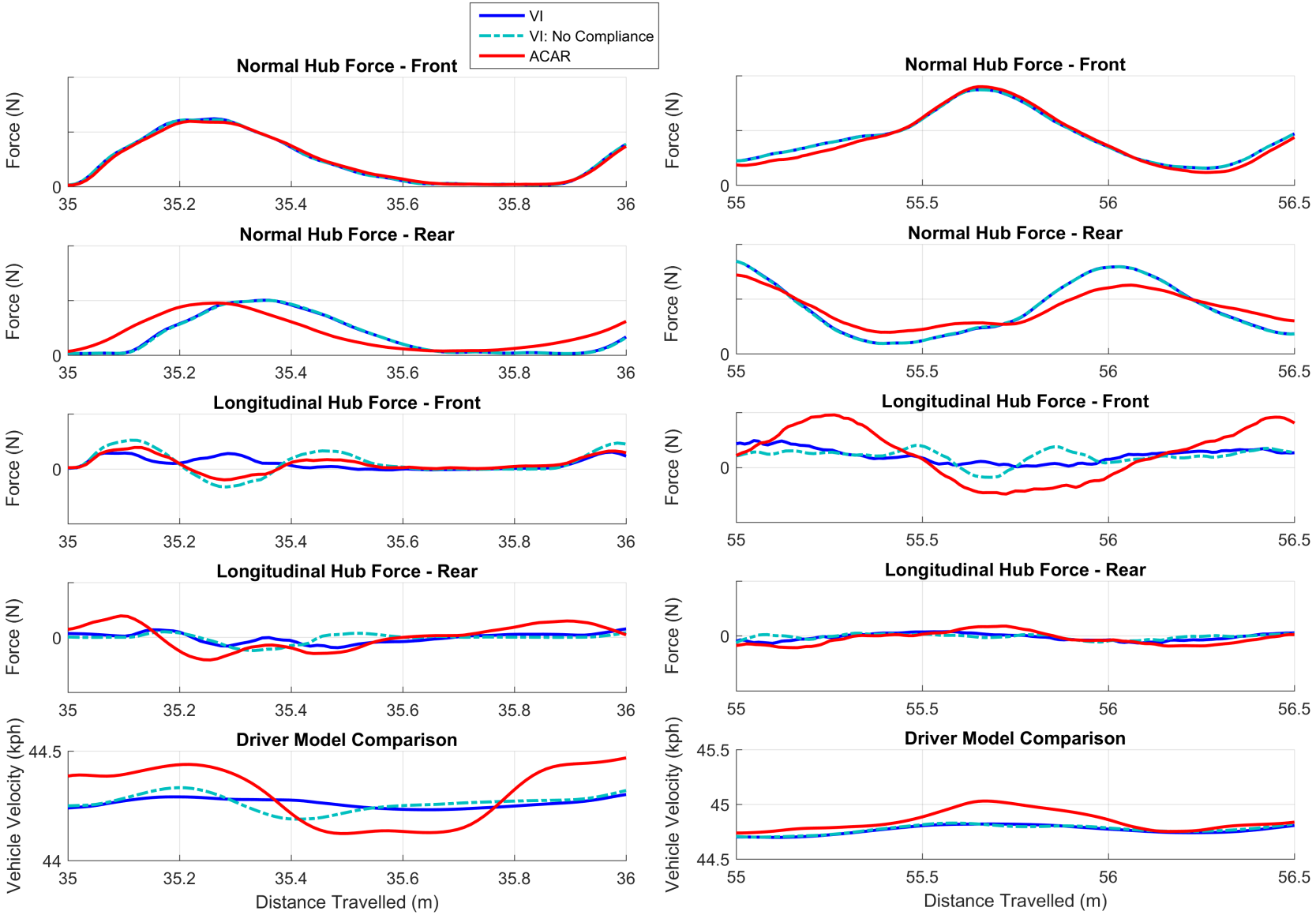


Figure 5.14: *CEVT model with Continental Ftire on Washboard: Washboard with and without Suspension Compliance*

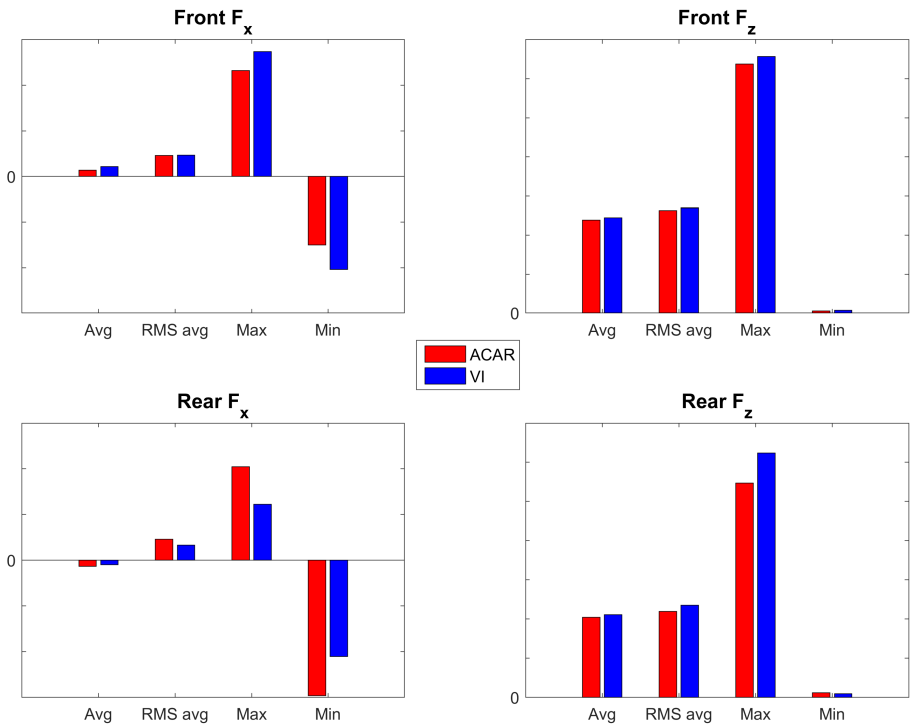


Figure 5.15: *CEVT model with Continental Ftire without Suspension Compliance on Washboard: Force Comparisons*

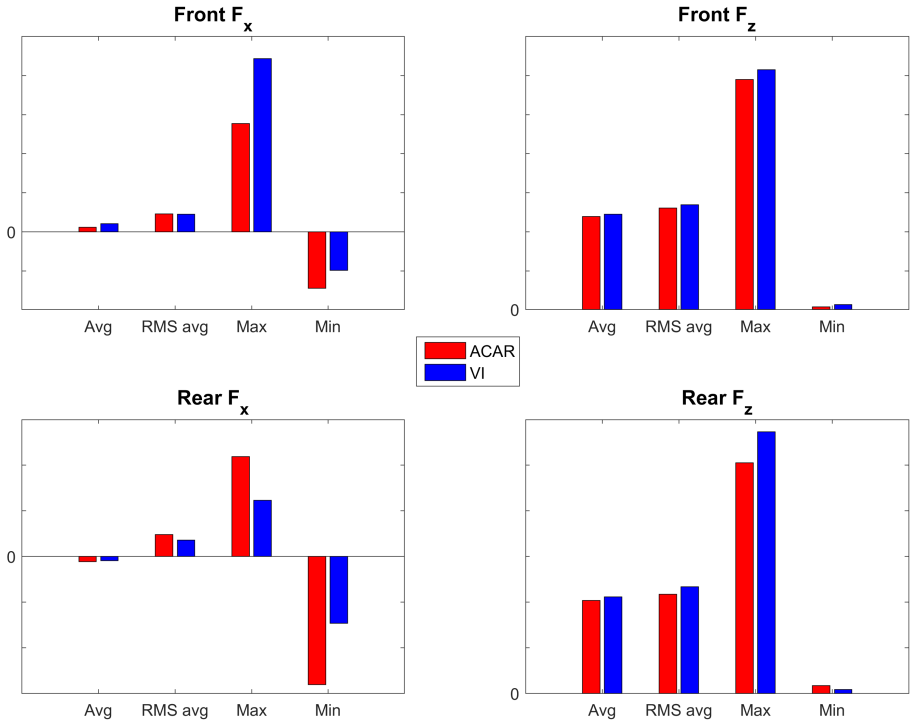


Figure 5.16: *CEVT model with Pirelli Ftire on Washboard: Force Comparisons*

- Tire: Pacejka 2002
- Driving Event: Coast (No throttle, braking, steering, gear shifting) from 40 kph for 5 seconds

The tire forces are plotted in Figure 12 in the Appendix section A.3. As before, the normal tire forces between the software resembled each other well. Compared to the maintain velocity simulation in the previous section, there is some improvement in similarities between the longitudinal tire forces, especially within the first ten meters of distance travelled. Differences in the F_x can be explained by the slightly different driving path beyond the first 10 m. However, this does not explain why the F_z matched very well throughout the path.

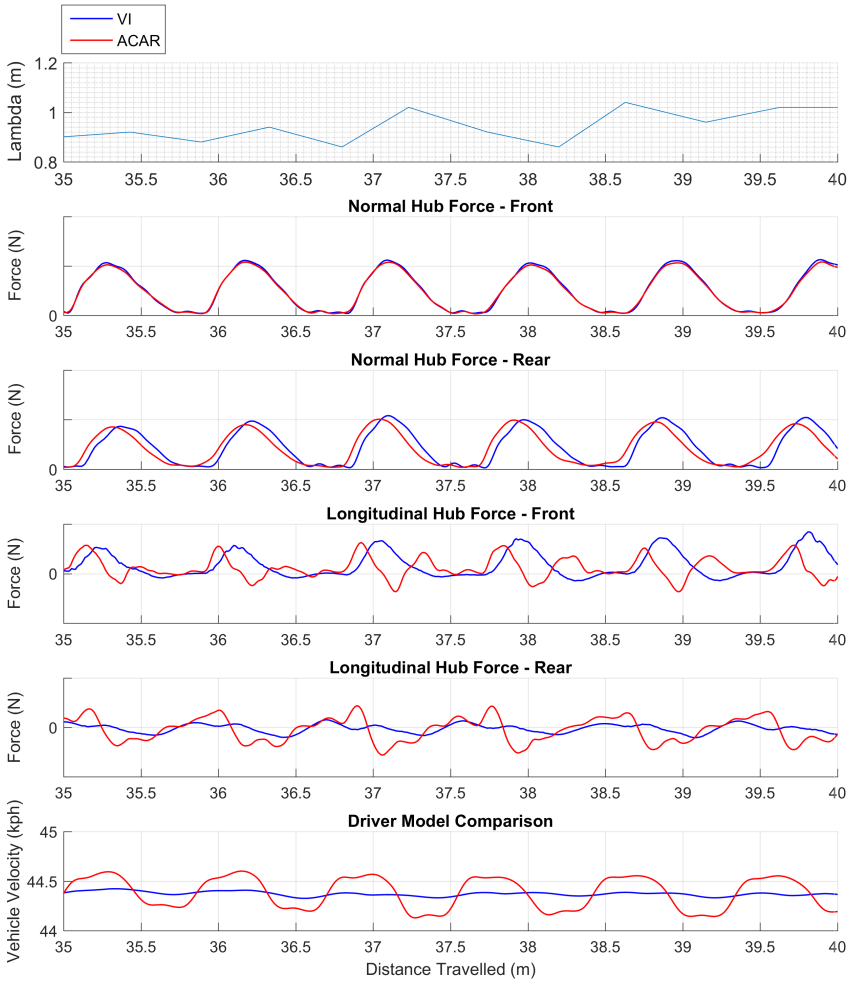
Between the maintain velocity and the coasting events on the Belgian Block road, powering off driver control certainly produced better force comparisons. It is also noted that ADAMS/Car model slowed down significantly after driving 17 m, while VI-CarRealTime maintained its velocity. This may be contributed to several reasons, such as difference in engine inertia and model simplifications made by the VI-CarRealTime.

In addition, suspension compliance splines were modified and simulated with this scenario. Scaling up the compliance modifies the force outcome, but without notable improvements. On the other hands, lateral force is affected adversely and appears unreasonable.

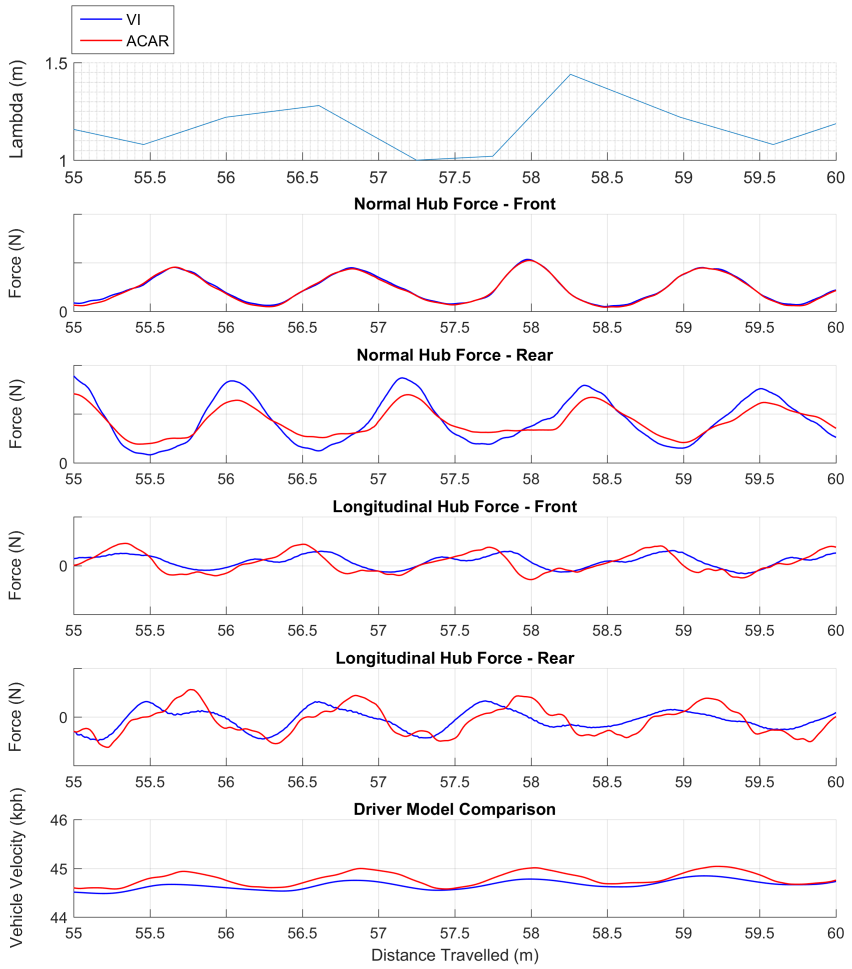
5.5.2 Belgian Block - Compliance Setting

To further understand the influence of suspension compliance, coasting on the Belgian Block is simulated with and without suspension compliance in the CEVT model. The tire force comparison graph is shown in Figure 5.24. The VI-CarRealTime model with 'no compliance' illustrated a better conformance with ADAMS/Car for the front longitudinal forces in the 10 to 10.5 m range. There were contrasting differences in the 17 to 18m range where the model with compliance showed better conformance (not seen in plots). So at this point it is difficult to come to a definite conclusion as to which is the directly affecting parameter to the differences in forces.

Although the 'Compliance Velocity Computation' flag activation was recommended for FTire in the VI-CarRealTime manual, the flag also had an impact on the models with Pacejka tires as well. If the flag is not



(a) *35-40m*



(b) *55-60m*

Figure 5.17: *Continental 225-40R19: Tire F_x and F_z*

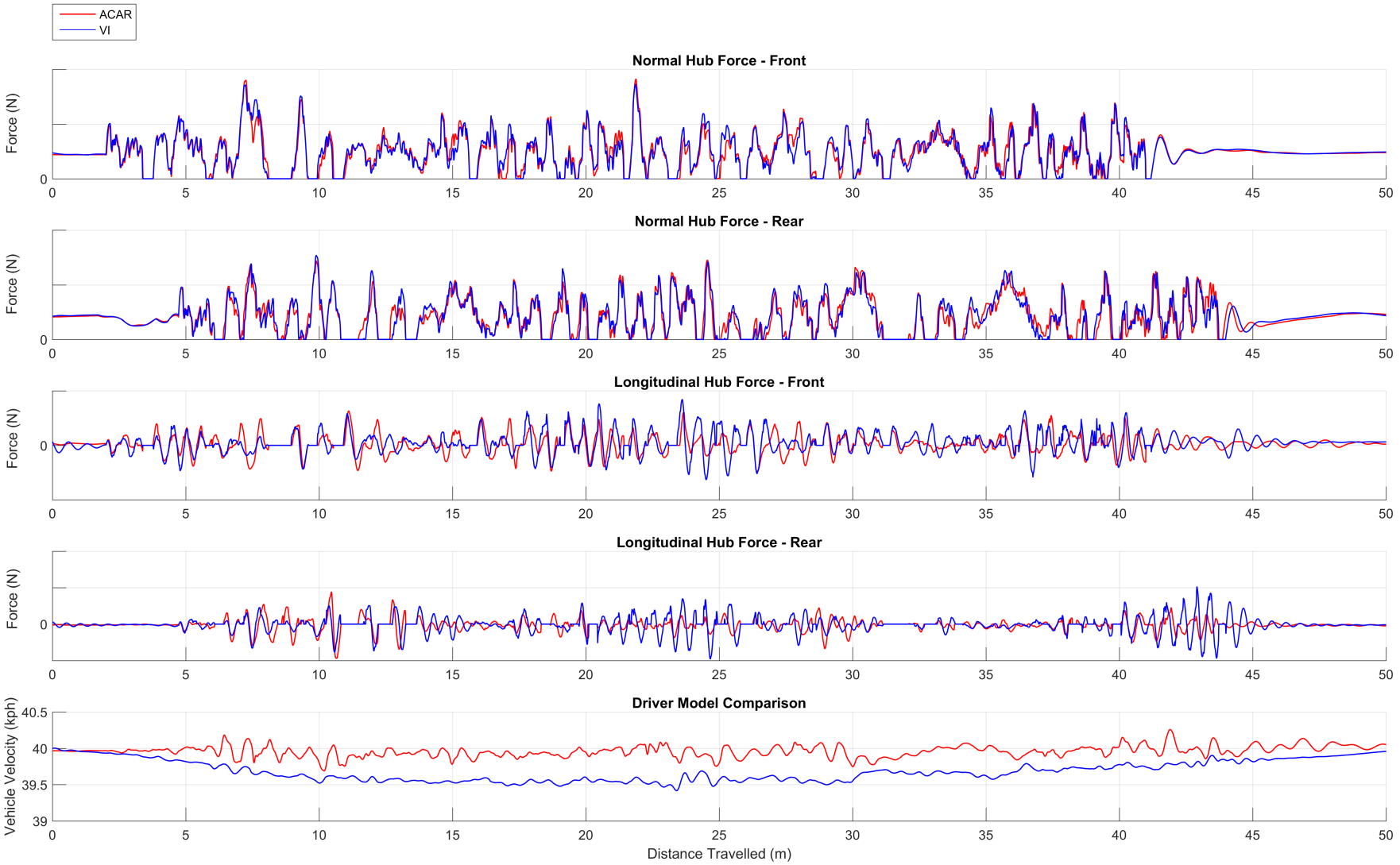


Figure 5.18: *CEVT model with Pacejka Tires: Belgian Block*

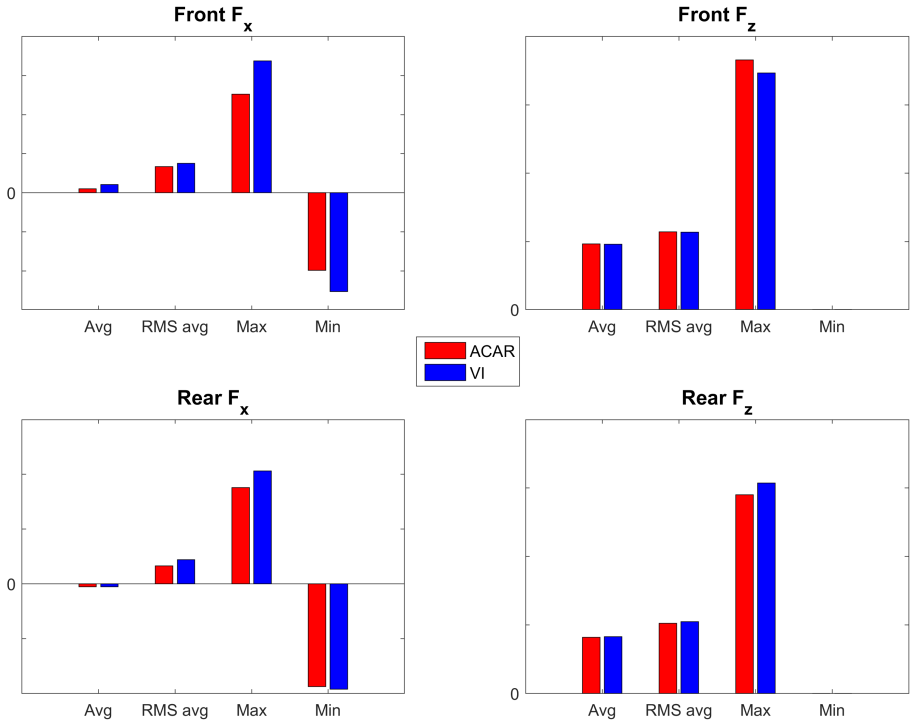
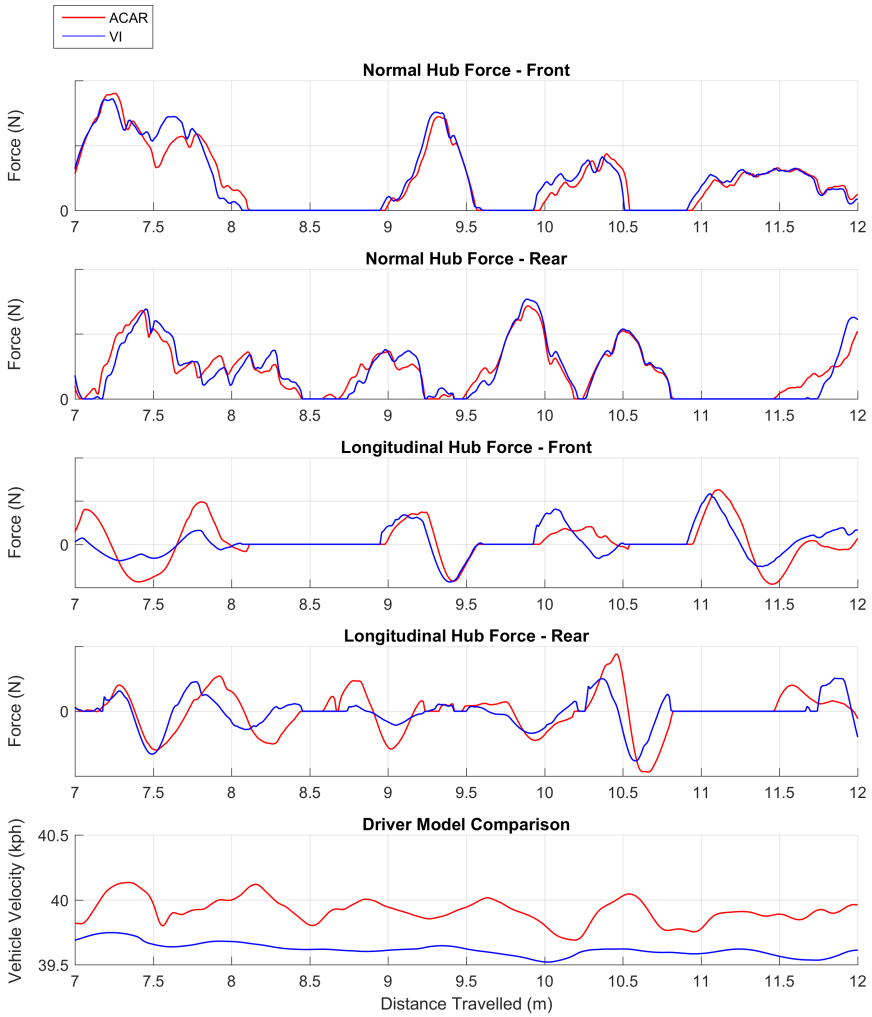
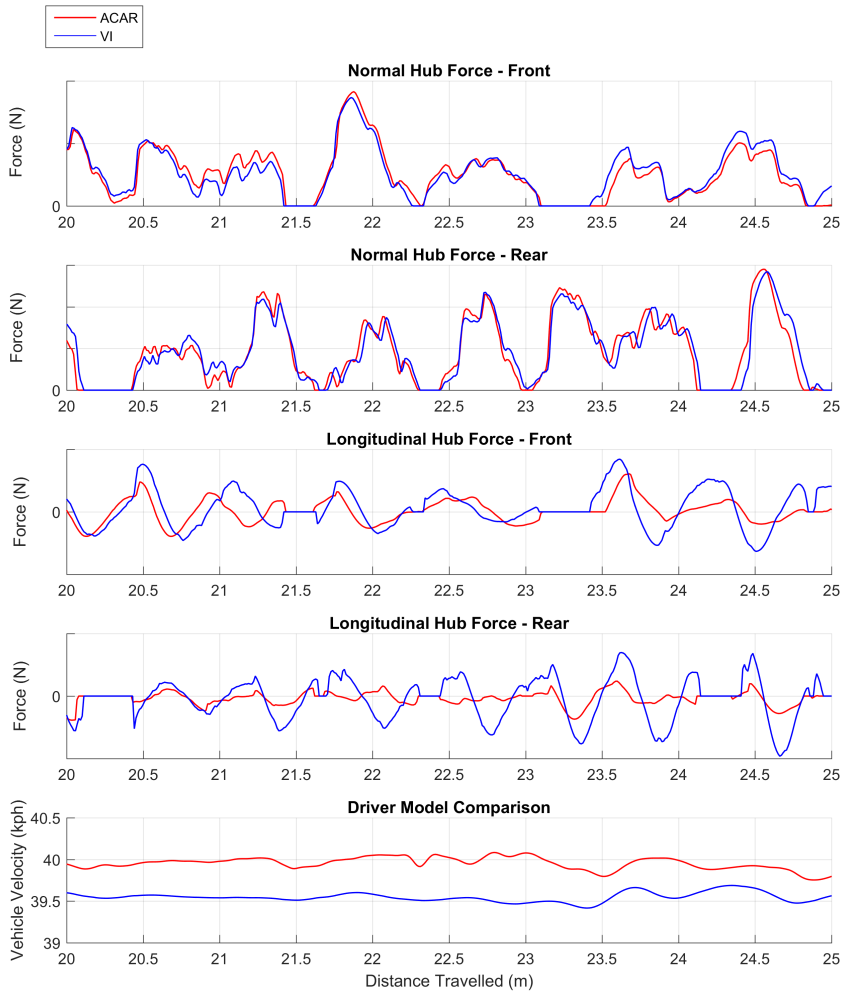


Figure 5.19: *CEVT model with Pacejka Tires on Belgian Block: Maintain Velocity, Force Comparisons*

activated, the vehicle with Pacejka tire behaves as if it has no suspension compliance.



(a) *7-12m*



(b) *20-25m*

Figure 5.20: *Belgian Block Pac 2002: Tire F_x and F_z*

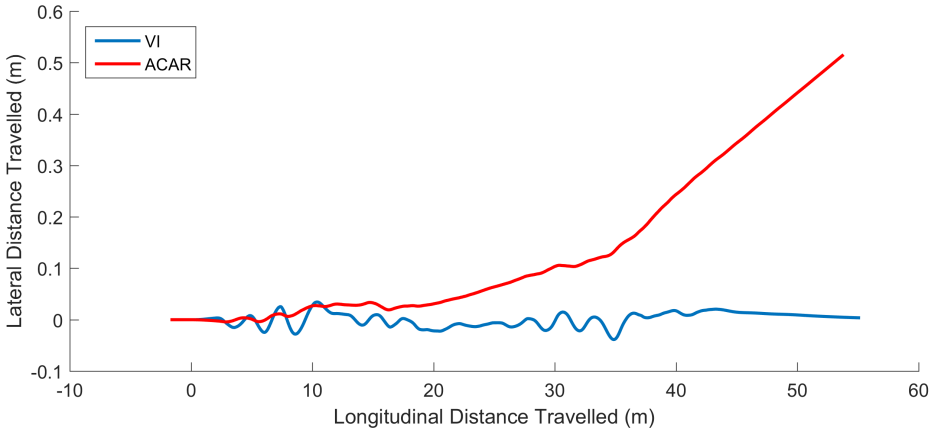


Figure 5.21: *Belgian Block Vehicle Position*

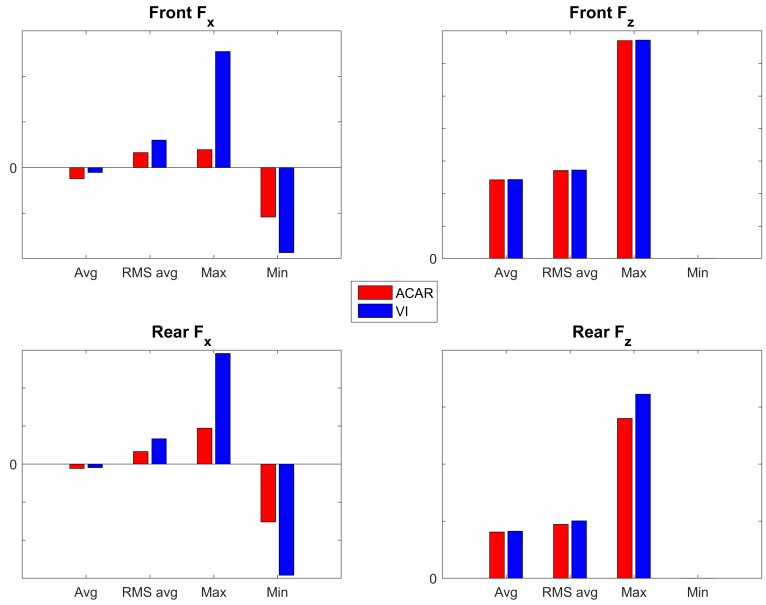


Figure 5.22: *CEVT model with Pacejka Tires on Belgian Block: Coasting, Force Comparisons*

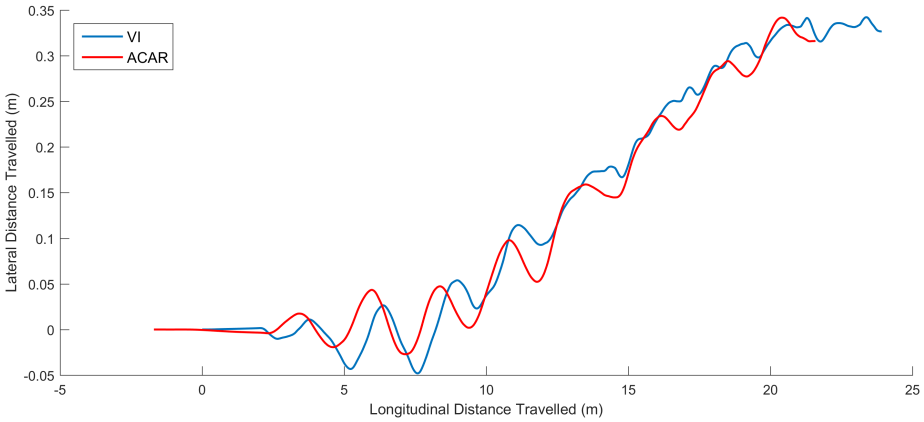


Figure 5.23: *CEVT model with Pacejka Tires on Belgian Block: Vehicle Position*

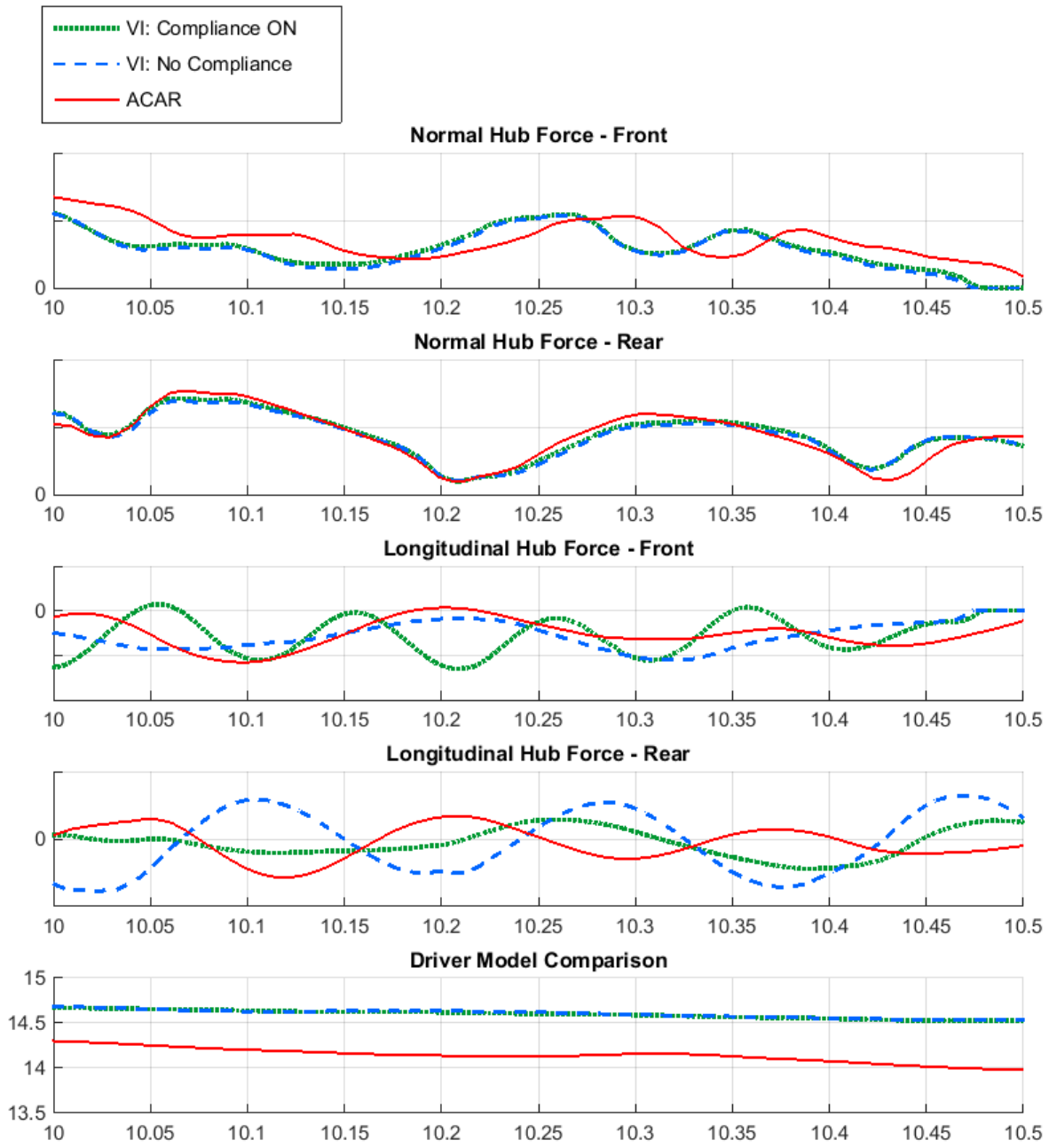


Figure 5.24: *CEVT model with Pacejka Tires: Coasting on Belgian Block with and without Compliance*

5.6 Time Comparison and trade-off

This section provides an overview regarding the simulation time comparisons and trade-offs between ADAMS/Car and VI-CRT. This section also answers the question regarding real time capabilities of VI-CarRealTime. One important aspect to note is that real time capability is not something that is default. One needs to incorporate some setting changes in order to observe real time performance. Although one sees real time performance with Pac2002 tires, simulation time can be accelerated for FTire with the following modifications:

- Activate the 'multi-thread' flag in Solver Executive controls which enables parallel computation
- Modify the FTire Run Time mode from 0 to 3 in the FTire property file (`.tir`)

Note that the Continental FTire was run in run mode '0' due to issues running with run mode 3. Figure 5.25 shows that VI-CarRealTime is capable of real time simulations and in some cases faster than real time. Simulations with FTire took less than one tenth the time taken by ADAMS/Car while with Pac 2002 VI-CarRealTime took less than one hundredth the time taken by ADAMS/Car.

With regard to the trade-off between simulation time saved and the accuracy of load calculation with ADAMS/Car results as the reference, the Figure 5.26 gives a pictorial overview. For the simpler cases, such as the flat and cleat roads with Pacejka tires there is an excellent trade-off between the simulation time saved and load accuracy with close to 99 % time saved to less than 10 % difference to the ADAMS/Car force values. Note that the percentage force difference is the average force difference of the normal and longitudinal forces of ADAMS/Car and VI-CarRealTime. For the more complicated events, the trade-off differs with 90 % time saved to approximately 30 % force difference for the most complicated case.For a concept stage evaluation this trade-off can be deemed acceptable especially given the potential for further improvement of the trade-off.

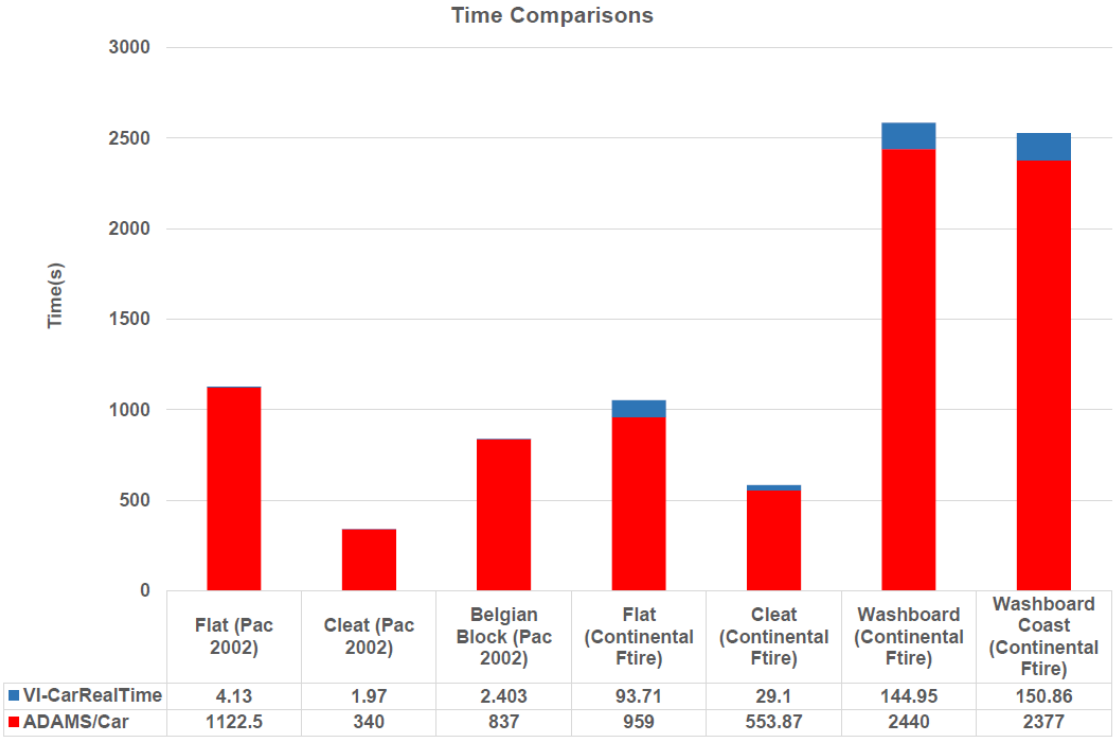


Figure 5.25: *Simulation Time Comparison Between ADAMS/Car and VI-CarRealTime*

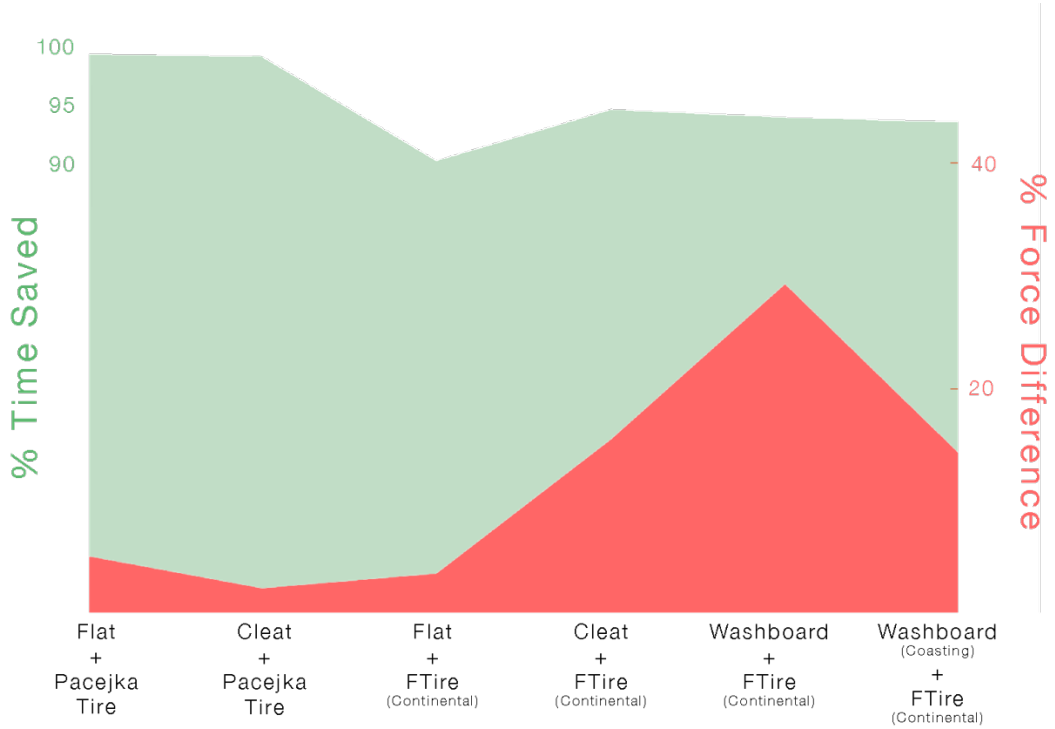


Figure 5.26: *Trade-off between ADAMS/Car and VI-CarRealTime: Simulation Time Saved and Force Difference*

6 Conclusion

- Given the simulation time saved for the accuracy provided for the maneuvers covered in this thesis, VI-CarRealTime makes a more than fair claim to be used as a conceptual level MBD software.
- VI-CarRealTime with its real-time potential is an excellent tool for conceptual level evaluation once the necessary validation and robustness checks of all the parameters are done.
- Literature review on benchmarking of different MBS programs has not been a fruitful exercise [15]. One needs to understand that differences will always exist between results and one must be careful before making conclusions with CAE results even if the results are validated physically (which will depend on another set of parameters).
- VI-CarRealTime exhibits great potential as an MBD tool. Like any other software, it is however not entirely plug and play and needs some level of vehicle dynamics insights, reasoning and experience. This thesis is a good foundation for a thorough evaluation of the software even though not every manoeuvre is covered, especially considering the bypasses that were required to solve problems.
- For the demo model, tire force differences on the washboard track is most like attributed to incorrect Ftire masses. On the other hand, incorrect suspension compliance curves in the CEVT model is reasonably the biggest source of tire force errors.
- Having the correct Ftire solver settings in VI-CarRealTime is essential to produce correct tire force data. Similar, providing ADAMS/Car with the appropriate permission to modify Ftire free mass and inertia is necessary to produce correct results.
- Incorrect tire mass cannot be easily detected through simple tests, such as driving on a cleat road. The model can be exported into VI-CarRealTime with wrong settings, and the best way to establish the model's fidelity is by performing a wide sweep of input frequencies. Comparing tire forces generated by different road frequency inputs is also a practical way to compare the software solvers' ability.
- VI-CarRealTime is a fantastic complementary tool to ADAMS/Car but cannot replace it entirely throughout the CAE process at this point of time.

7 Future Work

- This thesis work assesses VI-CarRealTime's ability to calculate tire forces by comparing its results against those of ADAMS/Car. While average force and peak force are good indicators, fatigue life estimations remain the most direct comparison, which was unfortunately not achieved due to time constraint. Thus, it is strongly recommended to conduct fatigue life estimation and damage number comparison between VI-CarRealTime and ADAMS/Car.
- The demo model is an excellent model for learning. A great deal can be learnt from the demo model with compliance in its subsystems `VI_CRT_Demo_compl.xml`. Comparing the compliant demo model in ADAMS/Car and VI-CarRealTime may offer insights to improve the longitudinal force comparisons.
- Only straight line manoeuvres are performed in this thesis. It would be highly interesting to observe the normal and longitudinal tire forces when notable lateral tire forces are present.
- The simulations are performed at constant velocities. Further experiments could compare tire forces under high acceleration and hard braking conditions.
- Parametric studies and evaluation of the suspension compliance splines will lead to data driven design property values and targets for components.
- Sensitivity analyses of the parameters affecting longitudinal forces can be pursued. This can of course be extended to other vehicle dynamic parameters.
- The smooth interface with Matlab provides opportunities for running VI-CarRealTime events via Matlab. Some of the demo model simulations and sweeps in this thesis were run via Matlab. This opens up the possibility for a tool which uses Matlab as a substitute pre-processor with benefits of running sweeps of parameter changes which would be tedious if being done manually. Care has to be taken to validate such a tool if made and robustness checks are to be done appropriately.
- Optimization studies with the help of MDO software can enable a certain level of automation during conceptual evaluation.

Appendices

A.1 Resreader Matlab Code

```
clear all
close all
clc

tic
time = [];

%%%%%%%%%%%%%%%%%%% INITIATION %%%%%%%%%%%%%%%%%%%
% addpath_vicrt;
% addpath ('C:\Users\jianqiao.liu\DataProcessing')
% addpath ('C:\Users\jianqiao.liu\DataProcessing\Matlab_Functions')


% %%%%%%%%%%%%%%%%%%% SETTINGS %%%%%%%%%%%%%%%%%%%
MainWorkingFolder = 'C:\Users\jianqiao.liu\Analysis\CEVT';
cd (MainWorkingFolder)

%%%%%%%%%%%%%%%%%%% LOAD DATA %%%%%%%%%%%%%%%%%%%
fileName = 'CEVT_225R19_Washboard'; % NO .res HERE!
fileID = fopen([fileName, '.res'],'r');

%%%%%%%%%%%%%%%%%%%%%%%%%%%%%%%%%%%%%%%%%%%%%%%%%%%%%%%%%%%%%%%%%%%%%%%%%%%
temp = textscan(fileID,'%s', 22000,'Delimiter','\n');
LineNum = find(not(cellfun('isempty',strfind(temp{1,1}(:),'<Step type="input">'))))
% search for number of line of text

fclose(fileID);

%%%%%%%%%%%%%%%%%%%%%%%%%%%%%%%%%%%%%%%%%%%%%%%%%%%%%%%%%%%%%%%%%%%%%%%%%%%
fileID = fopen([fileName, '.res'],'r');
temp = textscan(fileID,'%s', LineNum,'Delimiter','\n');

Block = 1;
getName = temp{1,1}; % Get entity and variable names

%%%%%%%%%%%%%%%%%%% GET ENTITY NAMES %%%%%%%%%%%%%%%%%%%

parfor i = 1:length(getName)
    str = getName(i,1);
    expression = '"';
    indQuotation = cell2mat(regexp(str,expression));
    if ~isempty(indQuotation) && length(indQuotation)>2
        getNameEntity{i,1} = genvarname(regexprep(str{1,1}(indQuotation(3)+1:indQuotation(4)-1),'\W','_'));
    elseif ~isempty(indQuotation) && length(indQuotation)<3
        getNameEntity{i,1} = genvarname(regexprep(str{1,1}(indQuotation(1)+1:indQuotation(2)-1),'\W','_'));
    end
end

iEntity = find(not(cellfun('isempty',strfind(temp{1,1}(:),'Entity name'))));
% Find all rows containing entity names
parfor i = 1:length(iEntity)
    nameEntity{i,1} = char(getNameEntity(iEntity(i)));
end
```

```
%%%%%%%%%%%%%%%%%% GET COMPONENT NAMES %%%%%%%%%%%%%%%%%%

parfor i = 1:length(getName)
    str = getName(i,1);
    expression = '"';
    indQuotation = cell2mat(regexp(str,expression));
    if ~isempty(indQuotation)
        getName{i,1} = genvarname(regexprep(str{1,1}(indQuotation(1)+1:indQuotation(2)-1),'\W','_'));
    end
end

iComponent = find(not(cellfun('isempty',strfind(temp{1,1}(:),'Component name='))));
% Find all rows containing entity names
iComponentEnd = [iComponent(find(diff(iComponent)>1)); iComponent(end,1)]; % New Entity

parfor i = 1:length(iComponentEnd)
    nameComponent{i,:} = getName(iEntity(i)+1:iComponentEnd(i),1)';
end

%%%%%%%%%%%%%%%%% IMPORT DATA %%%%%%%%%%%%%%%%%%
tic

while (~feof(fileID))  % For each block:

    InputText = textscan(fileID,'%f', 'delimiter',' ');

    if ~isempty(InputText{1,1})
        Data(:,Block) = InputText{1,1};
        % OPEN AND SEE FIND THE EMPTY ROWS! Data{Block,1} = InputText{1,1};
    else
        Block = Block-1;
    end

    eob = textscan(fileID,'%s',2,'delimiter','\n');  % Read and discard end-of-block marker

    Block = Block+1; % Increment block index
end

fclose(fileID);
toc

%%%%%%%%%%%%%%%%% COPY DATA INTO STRUCT %%%%%%%%%%%%%%%%%%
IndRow = 1;

for i = 1:length(nameEntity)
    for j = 1:length(nameComponent{i})

        ACAR.(char(nameEntity{i})).(char(nameComponent{i}(1,j))) = Data(IndRow,:);

        IndRow = IndRow+1;

    end
end

save (fileName,'ACAR')
time = [time, 'fill in data took ', num2str(toc), 's. END']

% sendolmail('gimmyliu@gmail.com',[fileName, 'conversion to .mat complete'], time)
```

```
% quit
```

A.2 Tire Properties

A.2.1 Pacejka Tire

```
pac2002_235_60R16.tir
$----------------------------------------------------------------------DIMENSION
[DIMENSION]
UNLOADED_RADIUS          = 0.344               $Free tyre radius
WIDTH                    = 0.235               $Nominal section width of the tyre
ASPECT_RATIO             = 0.6                 $Nominal aspect ratio
RIM_RADIUS               = 0.19                $Nominal rim radius
RIM_WIDTH                = 0.16                $Rim width
```

A.2.2 Demo FTire

```
ftire_205_55R16.tir
$----------------------------------------------------------------------DIMENSION
[DIMENSION]
$these data are not used by FTire, but only by the calling solver
 unloaded_radius =                316.389               $ mm
 width =                          205                   $ mm
 aspect_ratio =                   0.55                  $ -
 rim_radius =                     203.2                 $ mm
 rim_width =                      165.1                 $ mm

 $-----------------------------------------------------------------MASS_CORRECTION
[MASS_CORRECTION]
$these data are not used by FTire, but only by the calling solver
 free_tire_mass =                 7.51307               $ kg
 free_tire_jxx_jzz =              3.49426e5             $ kgmm^2
 free_tire_jyy =                  6.98851e5             $ kgmm^2

 $-------------------------------------------------------------------------DATA
[FTIRE_DATA]
$.....................................................basic data and geometry
 tire_section_width =             205                   $ mm
 tire_aspect_ratio =              55                    $ %
 rim_diameter =                   406.4                 $ mm
 load_index =                     90                    $ -
 speed_symbol =                   'S'
 rim_width =                      165.1                 $ mm
 rolling_circumference =          1916.3                $ mm
 tire_mass =                      9.37                  $ kg
 belt_width =                     160                   $ mm
 tread_width =                    160                   $ mm
 interior_volume =                3.0e7                 $ mm^3
 belt_lat_curvature_radius =      1000                  $ mm$
```

A.2.3 CEVT FTire: Pirelli

```
235_45R20.tir
$----------------------------------------------------------------------DIMENSION
```

```
[DIMENSION]
$these data are not used by FTire, but only by the calling solver
 unloaded_radius =                359.4491              $ mm
 width =                          235                   $ mm
 aspect_ratio =                   0.45                  $ -
 rim_radius =                     254                   $ mm
 rim_width =                      203.2                 $ mm

 $-----------------------------------------------------------------MASS_CORRECTION
[MASS_CORRECTION]
$these data are not used by FTire, but only by the calling solver
 free_tire_mass =                 8.58                  $ kg
 free_tire_jxx_jzz =              5.17e5                $ kgmm^2
 free_tire_jyy =                  1.034e6               $ kgmm^2

 $-----------------------------------------------------------------------DATA
[FTIRE_DATA]
$.....................................................basic data and geometry
 manufacturer =                   'Pirelli'
 type =                           'Pzero'
 tire_section_width =             235                   $ mm
 tire_aspect_ratio =              45                    $ %
 rim_diameter =                   508                   $ mm
 load_index =                     100                   $ -
 speed_symbol =                   'W'
 rim_width =                      203.2                 $ mm
 rolling_circumference =          2192.512              $ mm
 tire_mass =                      13.2                  $ kg
 belt_width =                     186                   $ mm
 tread_width =                    185                   $ mm
 belt_lat_curvature_radius =      1435.24               $ mm
```

A.2.4 CEVT FTire: Continental

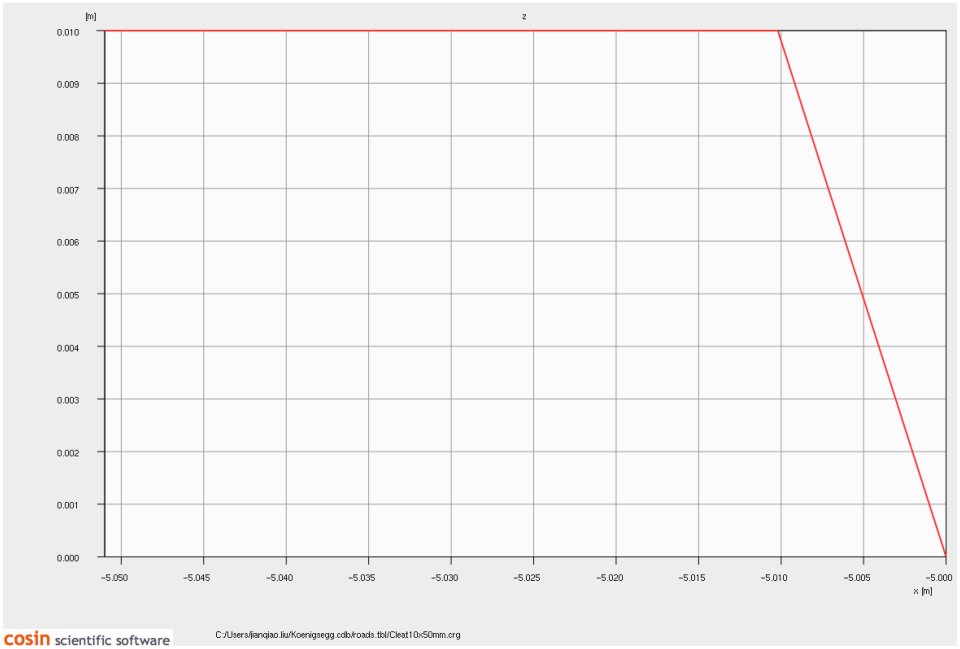
```
225_40R19.tir
$-----------------------------------------------------------------------DIMENSION
[DIMENSION]
$these data are not used by FTire, but only by the calling solver
 unloaded_radius =                333.9317              $ mm
 width =                          225                   $ mm
 aspect_ratio =                   0.4                   $ -
 rim_radius =                     241.3                 $ mm
 rim_width =                      203.2                 $ mm

 $-----------------------------------------------------------------MASS_CORRECTION
[MASS_CORRECTION]
$these data are not used by FTire, but only by the calling solver
 free_tire_mass =                 9.780968              $ kg
 free_tire_jxx_jzz =              5.131671e5            $ kgmm^2
 free_tire_jyy =                  1.026334e6            $ kgmm^2

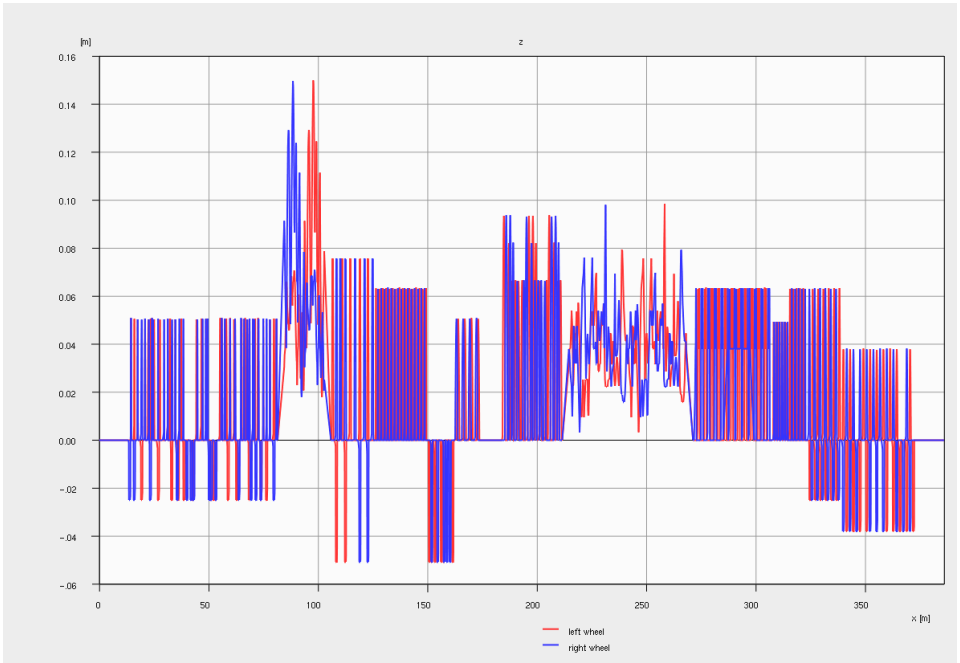
 $-----------------------------------------------------------------------DATA
[FTIRE_DATA]
$.....................................................basic data and geometry
 manufacturer =                   'Continental'
 type =                           'ContiSportContact 5'
```

```
tire_section_width =            225                 $ mm
tire_aspect_ratio =             40                  $ %
rim_diameter =                  482.6               $ mm
load_index =                    93                  $ -
speed_symbol =                  'V'
rim_width =                     203.2               $ mm
rolling_circumference =         2035.323            $ mm
tire_mass =                     10                  $ kg
belt_width =                    205.7143            $ mm
tread_width =                   206.6327            $ mm
belt_lat_curvature_radius =     1588.776            $ mm
```

A.3 Supporting Figures



(a) *Cleat Road X-Z Profile*



(b) *Silver Creek X-Z Profile*

Figure 1: *Road Profiles*

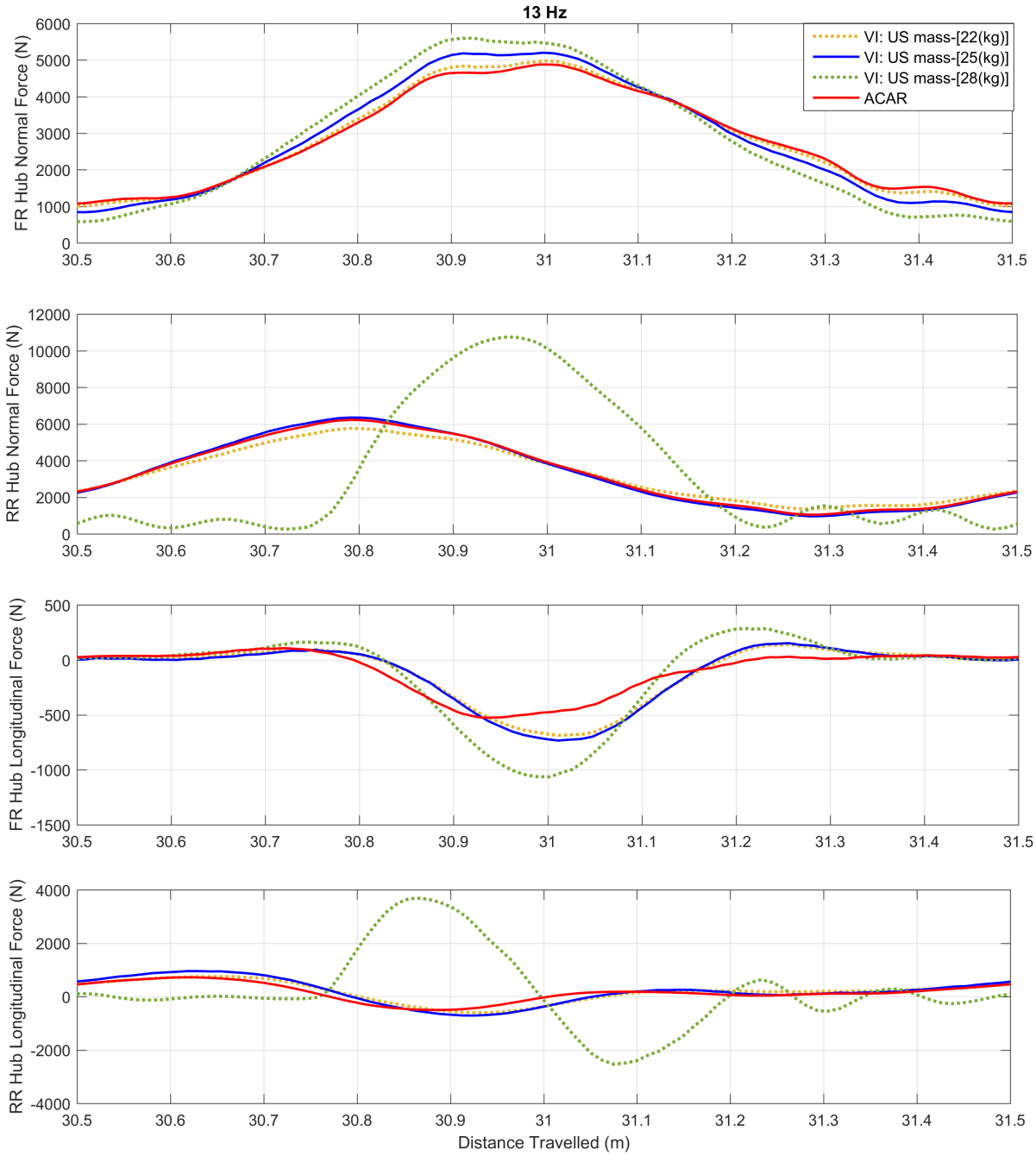


Figure 2: *Unsprung Mass Sweep with Pirelli Tires*

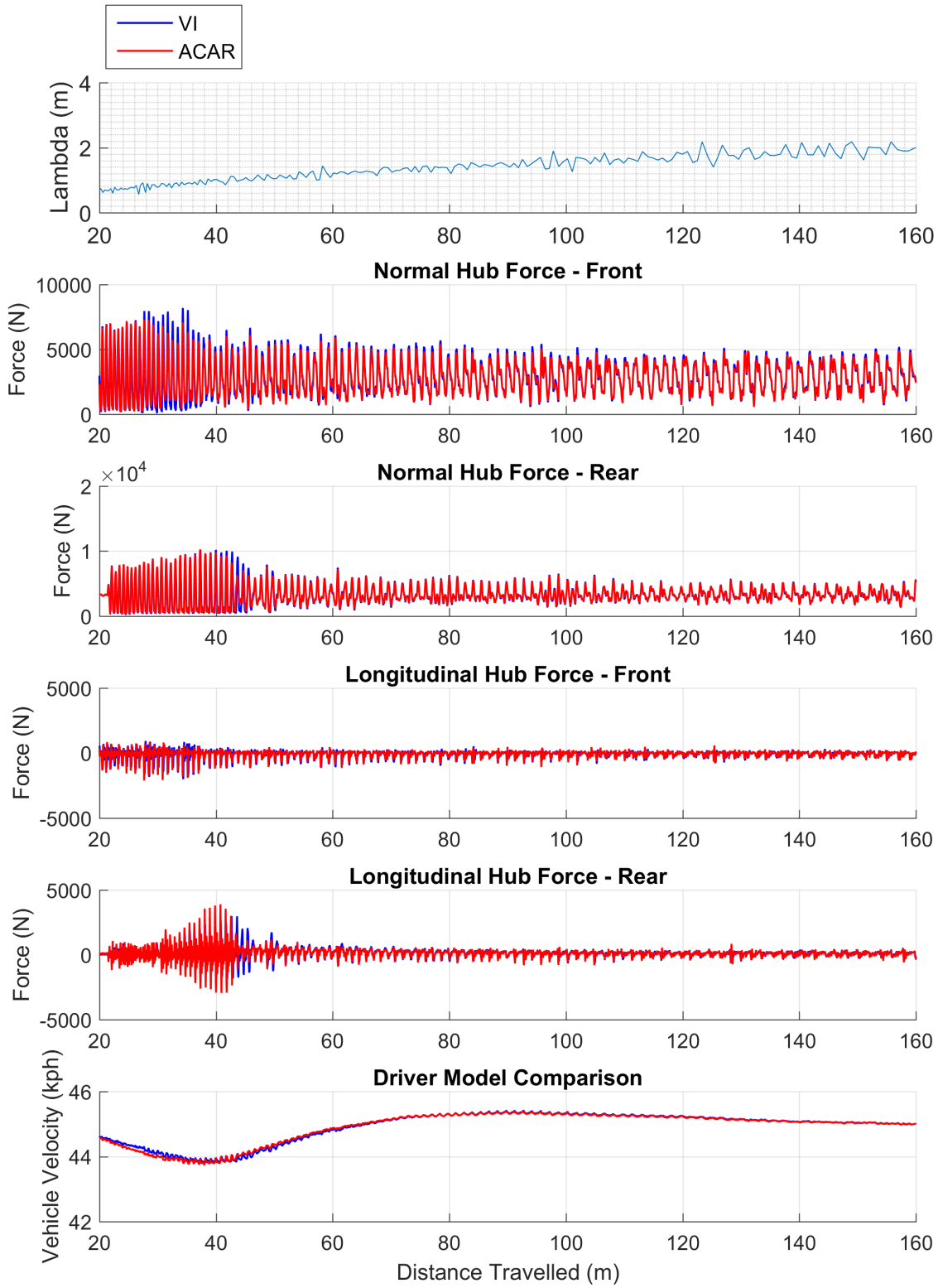


Figure 3: *Washboard Overview*

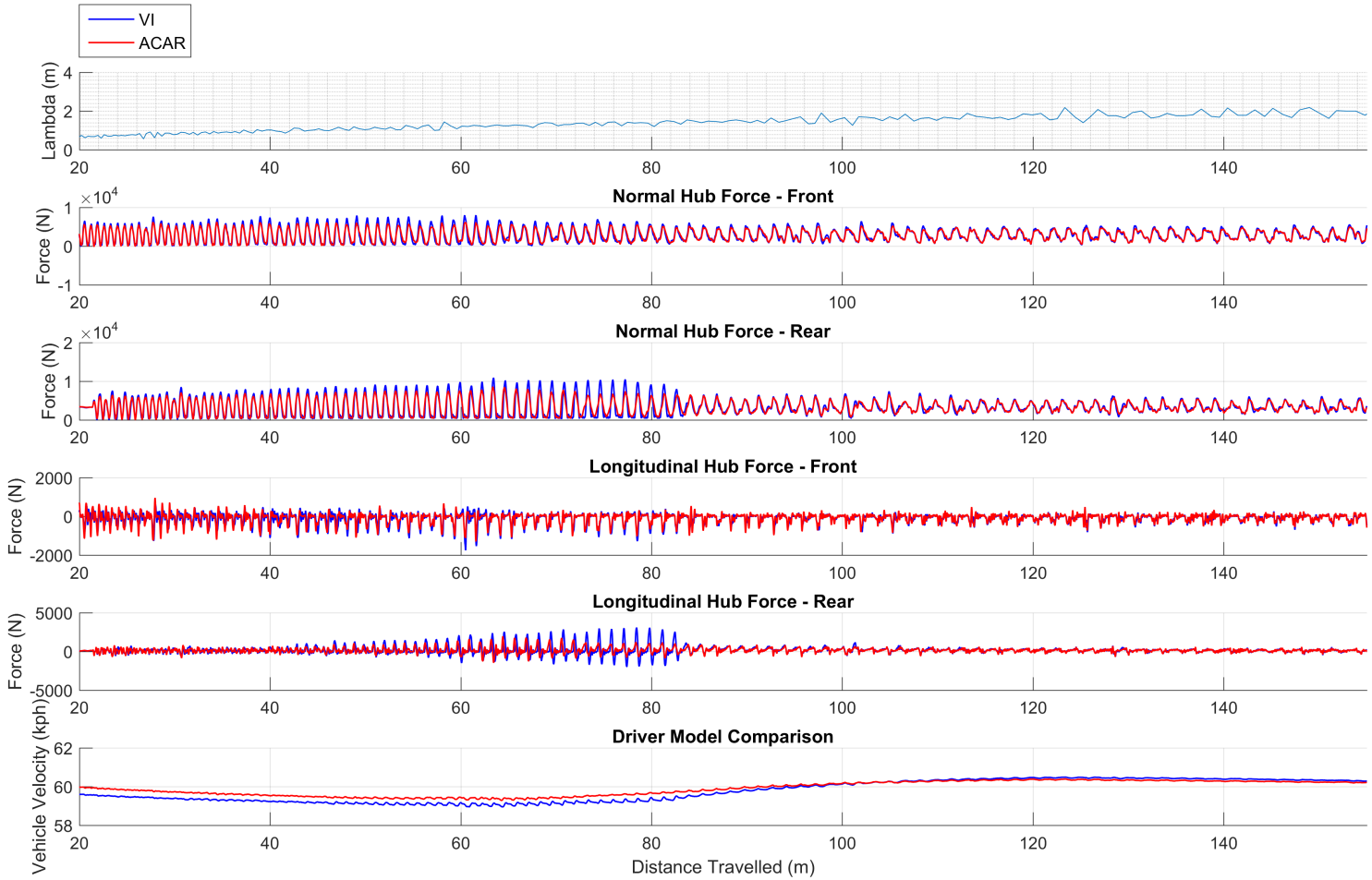


Figure 4: *ADAMS/Car vs. VI-CarRealTime at 60 kph: Tire Force Comparisons*

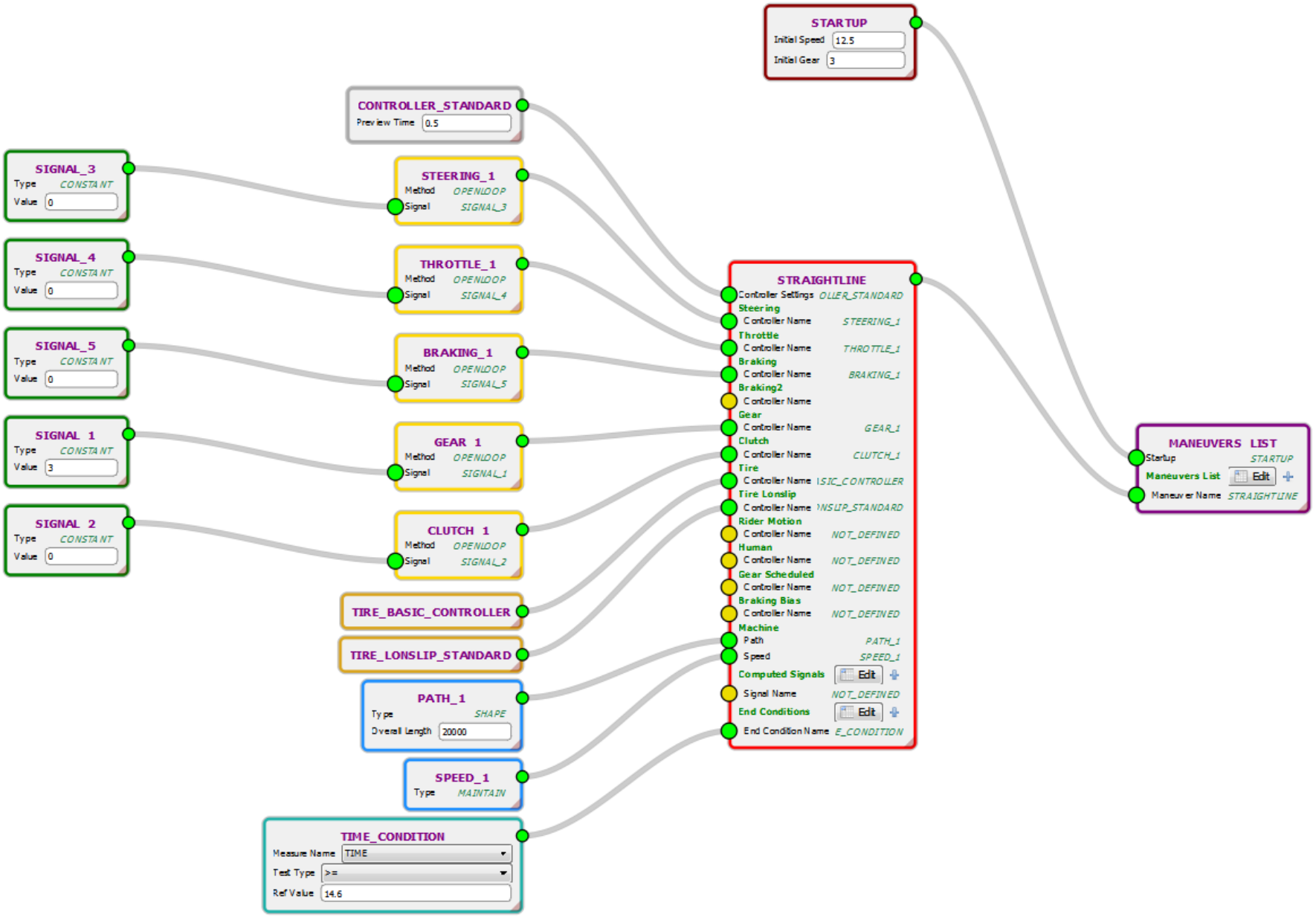


Figure 5: *Coasting: VI Driving Machine File*

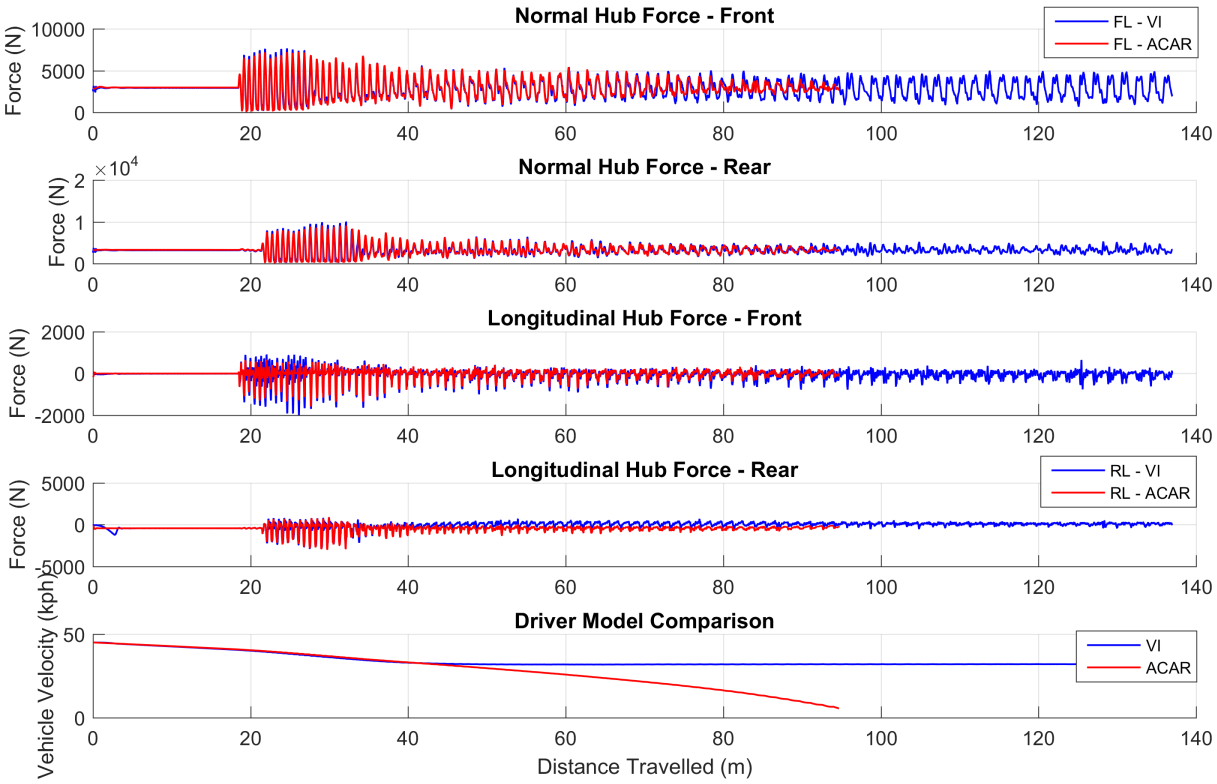
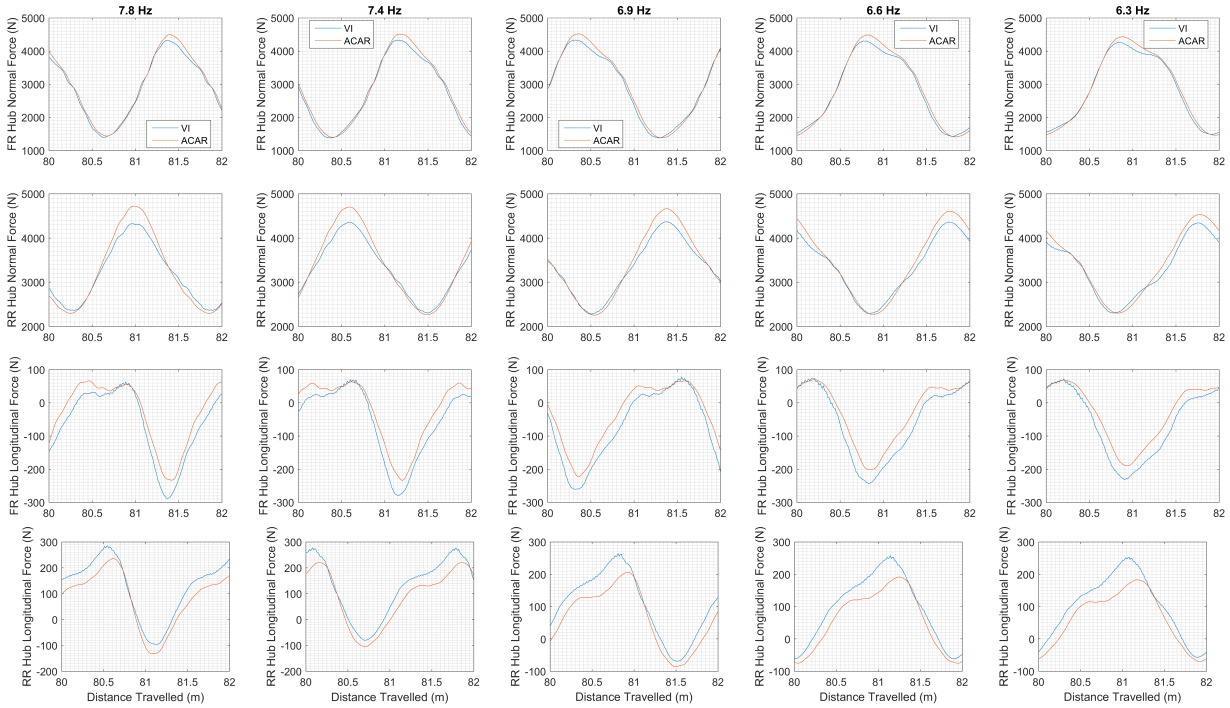
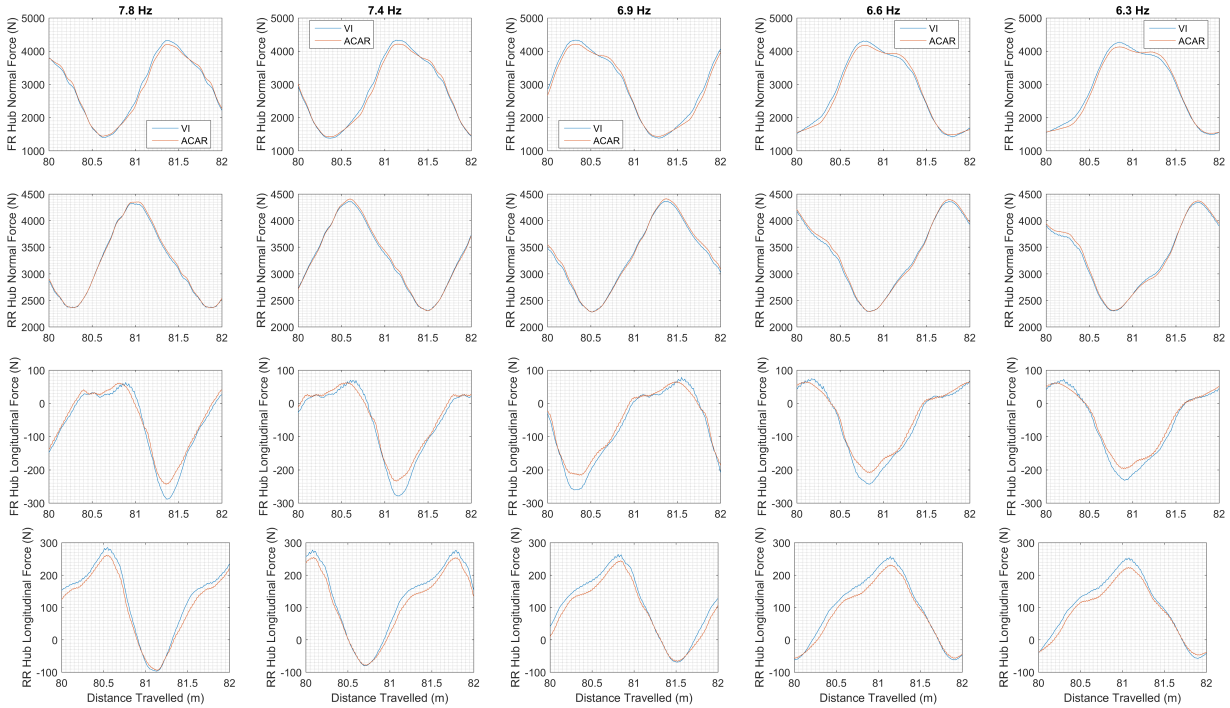


Figure 6: *Demo Model with Pirelli Ftire: Coasting on Washboard Overview*

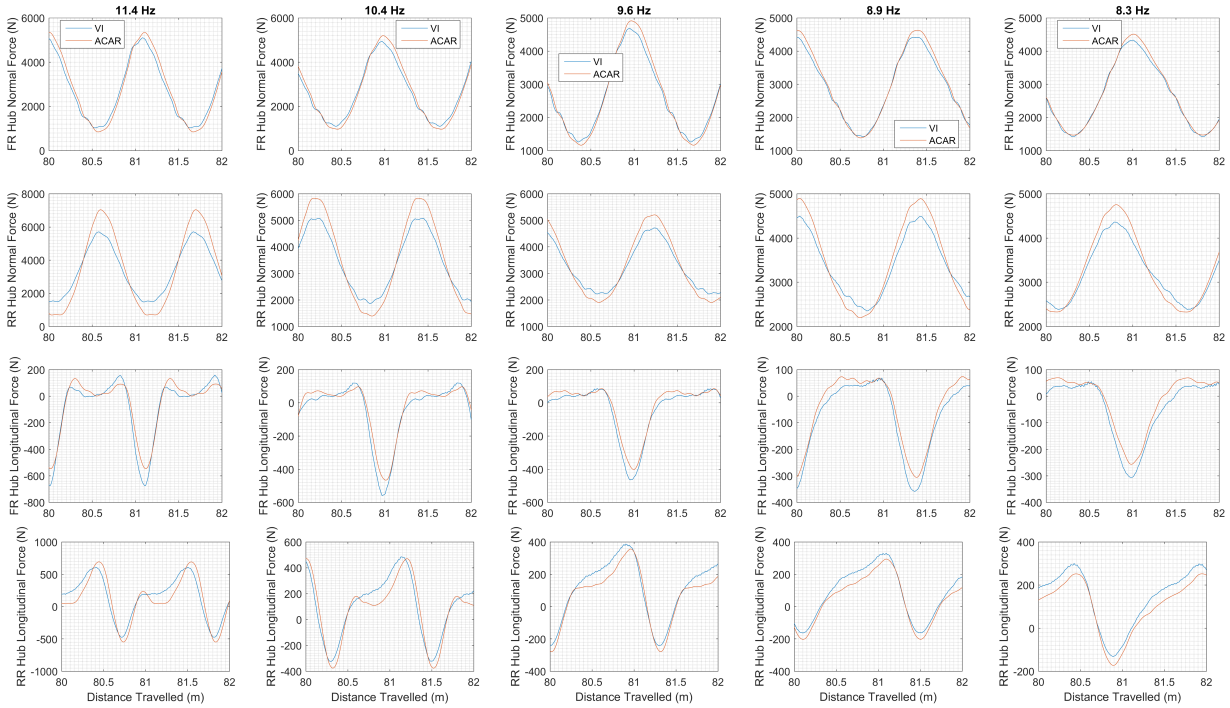


(a) *No Tire Mass and Inertia Modification*

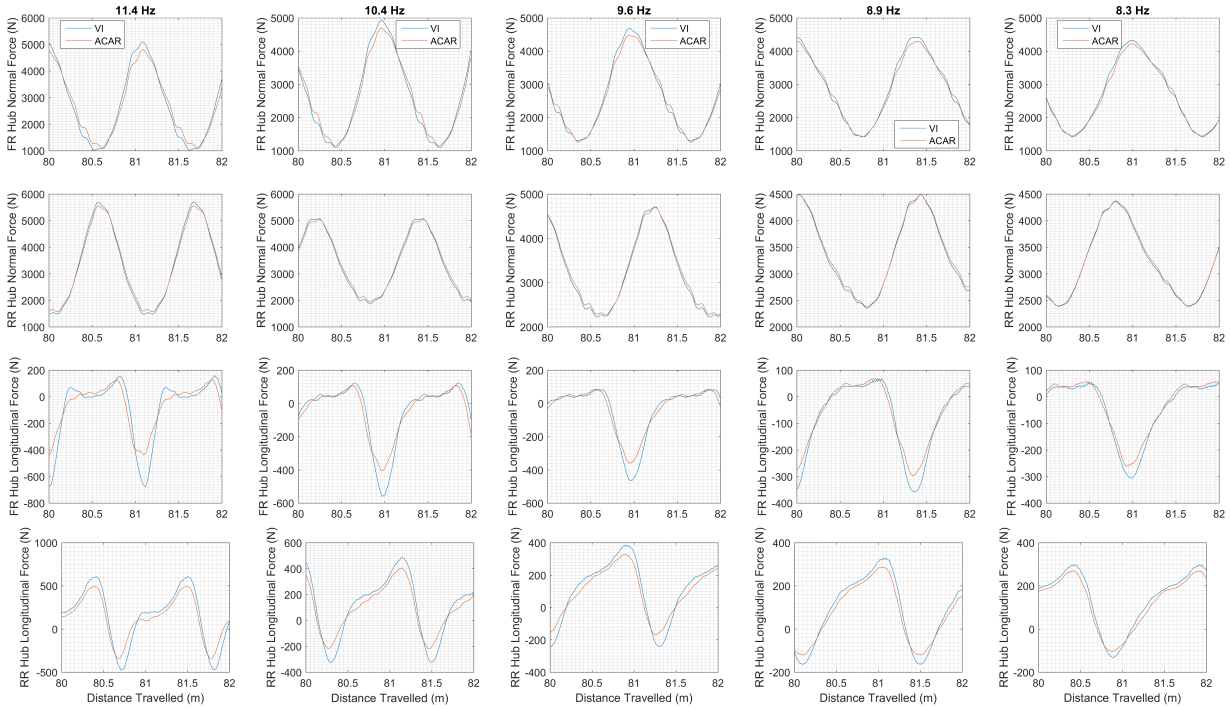


(b) *Allow Tire Mass and Inertia Modification*

Figure 7: *Sine Road Input Frequency: 6-8 Hz*

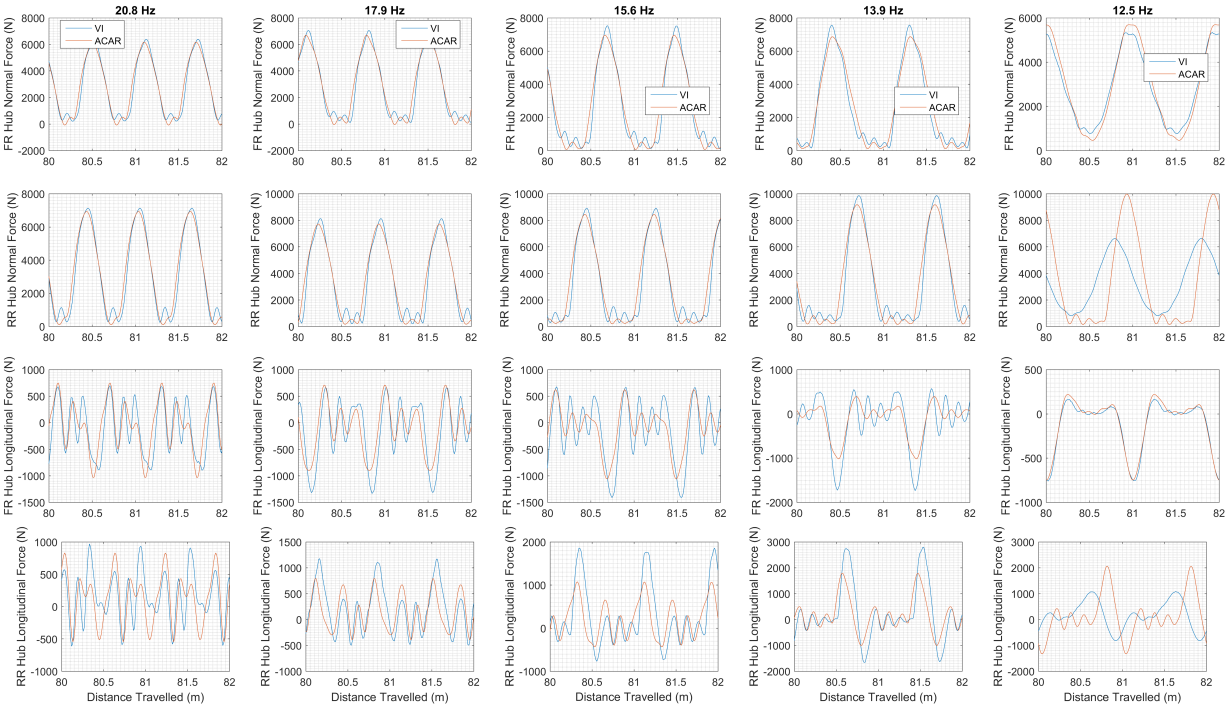


(a) *No Tire Mass and Inertia Modification*

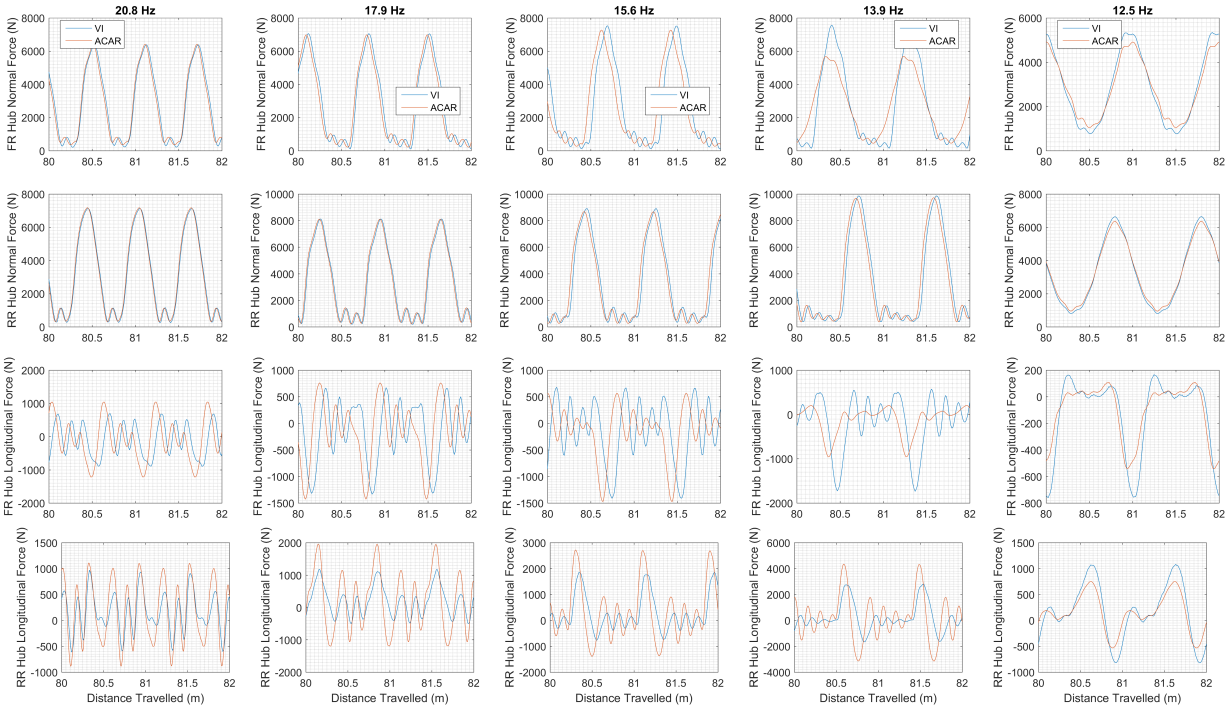


(b) *Allow Tire Mass and Inertia Modification*

Figure 8: *Sine Road Input Frequency: 8-11 Hz*



(a) *No Tire Mass and Inertia Modification*



(b) *Allow Tire Mass and Inertia Modification*

Figure 9: *Sine Road Input Frequency: 12-21 Hz*

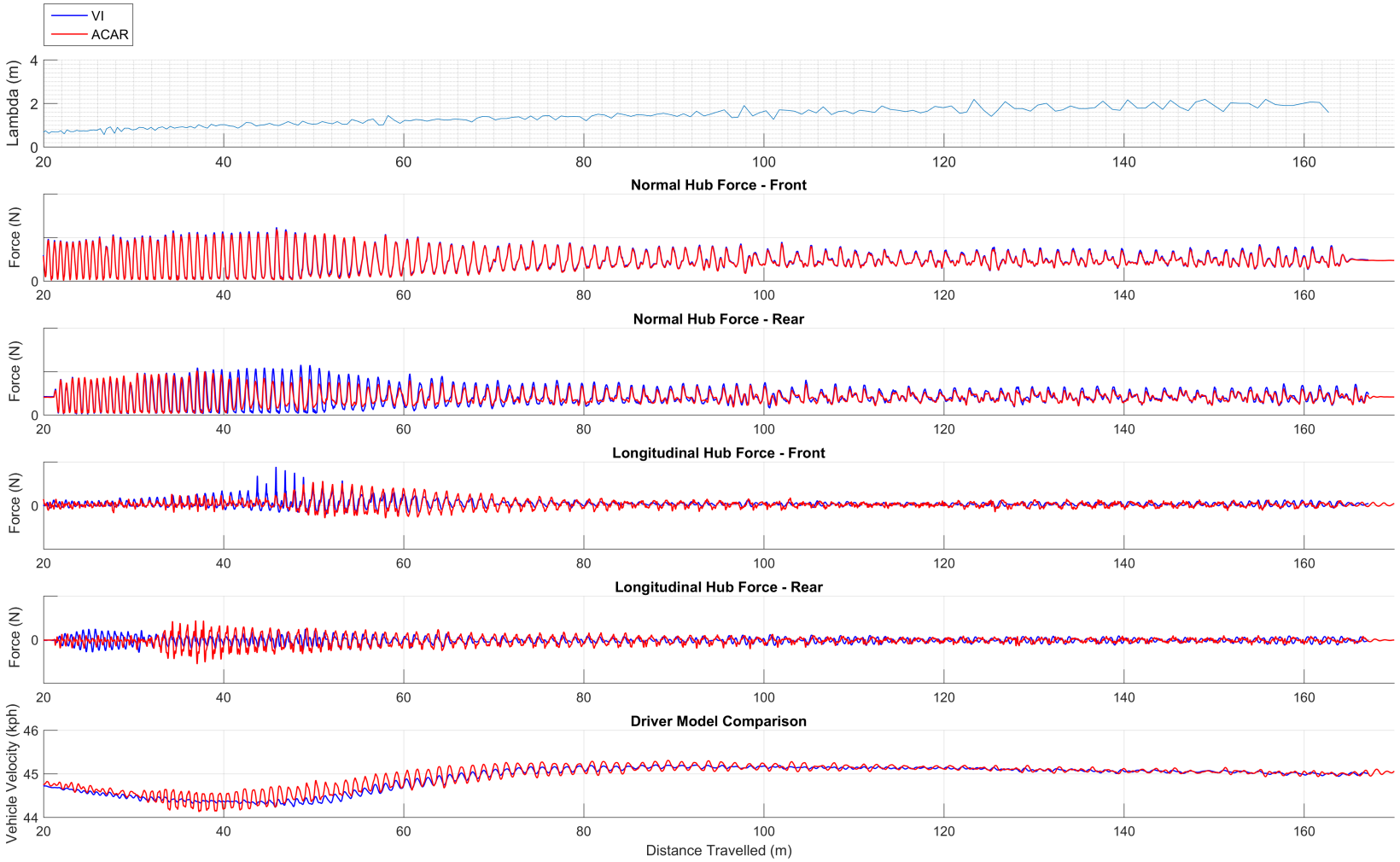


Figure 10: *V320 with Pirelli Ftire on Washboard: Washboard*

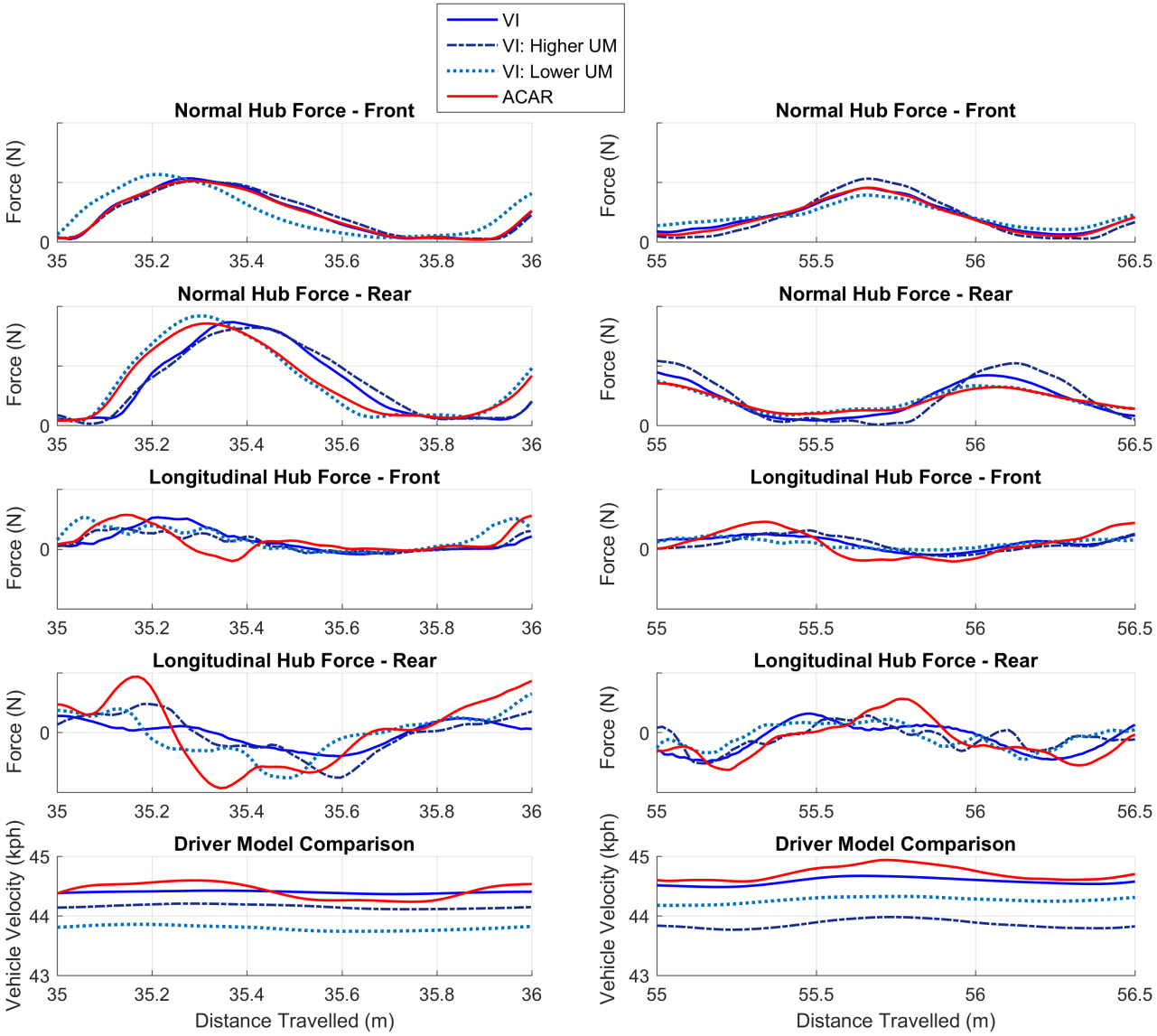


Figure 11: *V320 + Pirelli: Washboard with different Unsprung Masses*

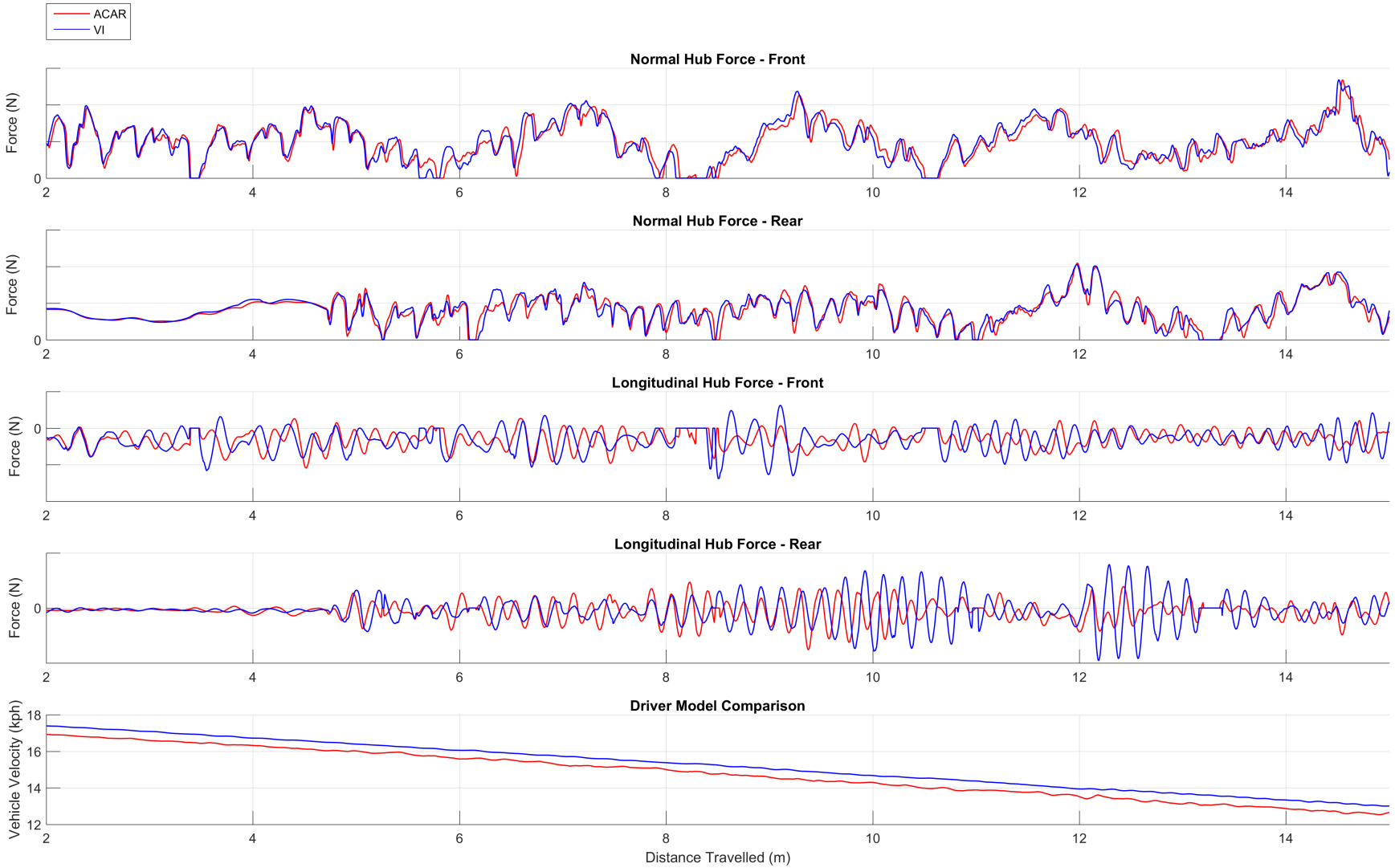


Figure 12: *V320 with Pacejka Tires on Belgian Block: Coasting*

A.4 Tire Force Results

A.4.1 Demo Model Result Tables

Longitudinal Forces		FL	FR	RL	RR
Average	*ACAR*	-31	-31	56	56
	VI	-36	-36	67	67
	Difference	5	5	-11	-11
	% Difference	-16.4%	-16.8%	19.0%	19.3%
RMS Average	*ACAR*	31	31	56	56
	VI	36	36	68	68
	Difference	-5	-5	-11	-11
	% Difference	16.5%	16.9%	19.8%	20.0%
Max	*ACAR*	-30	-30	59	59
	VI	-33	-33	80	80
	Difference	3	2	-22	-22
	% Difference	-8.5%	-7.5%	37.1%	37.1%
Min	*ACAR*	-31	-31	55	56
	VI	-39	-39	43	43
	Difference	8	8	12	12
	% Difference	-24.1%	-25.3%	22.4%	22.1%
Normal Forces		**FL**	**FR**	**RL**	**RR**
Average	*ACAR*	2993	2993	3478	3478
	VI	2950	2951	3387	3388
	Difference	43	42	91	91
	% Difference	1.4%	1.4%	2.6%	2.6%
RMS Average	*ACAR*	2993	2993	3478	3478
	VI	2950	2951	3387	3388
	Difference	43	42	91	91
	% Difference	1.4%	1.4%	2.6%	2.6%
Max	*ACAR*	2994	2994	3480	3480
	VI	2958	2958	3395	3396
	Difference	36	36	85	84
	% Difference	1.2%	1.2%	2.4%	2.4%
Min	*ACAR*	2992	2992	3476	3476
	VI	2943	2946	3372	3375
	Difference	49	46	104	101
	% Difference	1.6%	1.5%	3.0%	2.9%

Table 2: Demo Model with Demo Ftire: Flat Road

Longitudinal Forces		FL	FR	RL	RR
Average	*ACAR*	-31	-31	57	57
	VI	-31	-31	61	61
	Difference	0	0	-4	-4
	% Difference	-0.3%	-0.3%	7.7%	7.7%
RMS Average	*ACAR*	31	31	57	57
	VI	31	31	61	61
	Difference	-0	-0	-5	-5
	% Difference	0.3%	0.3%	8.2%	8.2%
Max	*ACAR*	-31	-31	57	57
	VI	-31	-31	70	70
	Difference	-0	-0	-13	-13
	% Difference	-0.5%	-0.5%	23.8%	23.8%
Min	*ACAR*	-31	-31	57	57
	VI	-31	-31	41	41
	Difference	0	0	15	15
	% Difference	-0.6%	-0.6%	27.2%	27.2%
Normal Forces		**FL**	**FR**	**RL**	**RR**
Average	*ACAR*	2919	2919	3405	3405
	VI	2922	2922	3402	3402
	Difference	-2	-2	3	3
	% Difference	0.1%	0.1%	0.1%	0.1%
RMS Average	*ACAR*	2919	2919	3405	3405
	VI	2922	2922	3402	3402
	Difference	-2	-2	3	3
	% Difference	0.1%	0.1%	0.1%	0.1%
Max	*ACAR*	2919	2920	3405	3406
	VI	2924	2924	3403	3403
	Difference	-4	-4	2	2
	% Difference	0.2%	0.1%	0.1%	0.1%
Min	*ACAR*	2919	2919	3404	3404
	VI	2920	2920	3399	3399
	Difference	-2	-1	5	5
	% Difference	0.1%	0.0%	0.1%	0.2%

Table 1: Demo Model with Pacejka Tire: Flat Road

Table 3: Demo Model: Cleat Road

Table 4: Pacejka Tire

Longitudinal Forces		**FL**	**FR**	**RL**	**RR**
Average	*ACAR*	-31	-31	57	57
	VI	-30	-30	57	57
	Difference	-1	-1	-1	-1
	% Difference	-1.7%	-1.7%	0.9%	0.9%
RMS Average	*ACAR*	31	31	57	57
	VI	30	30	59	59
	Difference	0	0	-2	-2
	% Difference	1.6%	1.6%	3.3%	3.3%
Max	*ACAR*	30	26	134	134
	VI	35	35	105	105
	Difference	-6	-9	28	28
	% Difference	19.3%	34.1%	21.3%	21.3%
Min	*ACAR*	-82	-80	21	21
	VI	-80	-80	-26	-26
	Difference	-1	0	46	47
	% Difference	-1.7%	-0.3%	226.5%	226.4%
Normal Forces		**FL**	**FR**	**RL**	**RR**
Average	*ACAR*	2919	2919	3405	3405
	VI	2870	2870	3300	3300
	Difference	49	49	104	104
	% Difference	1.7%	1.7%	3.1%	3.1%
RMS Average	*ACAR*	2920	2920	3405	3405
	VI	2870	2870	3301	3301
	Difference	49	49	104	104
	% Difference	1.7%	1.7%	3.1%	3.1%
Max	*ACAR*	4982	4986	5474	5473
	VI	4975	4975	5382	5381
	Difference	8	11	92	92
	% Difference	0.2%	0.2%	1.7%	1.7%
Min	*ACAR*	2585	2596	2985	2984
	VI	2558	2558	2903	2903
	Difference	27	38	82	81
	% Difference	1.0%	1.5%	2.7%	2.7%

Table 5: ACAR Demo Ftire

Longitudinal Forces		**FL**	**FR**	**RL**	**RR**
Average	*ACAR*	-35	-35	61	61
	VI	-36	-36	58	58
	Difference	1	1	3	3
	% Difference	-1.9%	-2.2%	5.2%	4.9%
RMS Average	*ACAR*	76	76	87	87
	VI	77	77	87	86
	Difference	-1	-2	-0	0
	% Difference	1.9%	2.1%	0.3%	0.3%
Max	*ACAR*	651	652	755	756
	VI	821	807	744	738
	Difference	-171	-155	11	18
	% Difference	26.2%	23.7%	1.4%	2.4%
Min	*ACAR*	-1210	-1213	-877	-880
	VI	-1269	-1271	-1047	-1044
	Difference	59	58	171	163
	% Difference	-4.9%	-4.8%	-19.5%	-18.6%
Normal Forces		**FL**	**FR**	**RL**	**RR**
Average	*ACAR*	2992	2992	3479	3479
	VI	2951	2952	3386	3386
	Difference	41	40	93	93
	% Difference	1.4%	1.4%	2.7%	2.7%
RMS Average	*ACAR*	2995	2995	3482	3482
	VI	2956	2956	3390	3390
	Difference	39	39	91	92
	% Difference	1.3%	1.3%	2.6%	2.6%
Max	*ACAR*	4642	4643	4949	4950
	VI	4828	4830	5047	5030
	Difference	-186	-186	-98	-81
	% Difference	4.0%	4.0%	2.0%	1.6%
Min	*ACAR*	1823	1825	2275	2280
	VI	1161	1185	1356	1401
	Difference	663	640	919	879
	% Difference	36.3%	35.1%	40.4%	38.6%

Table 6: Demo Model: Cleat Road

Table 7: CEVT Pirelli Ftire

Longitudinal Forces		**FL**	**FR**	**RL**	**RR**
Average	*ACAR*	-28	-28	53	53
	VI	-36	-36	65	65
	Difference	8	8	-12	-12
	% Difference	-30.1%	-30.7%	21.7%	21.9%
RMS Average	*ACAR*	45	45	62	62
	VI	51	51	73	73
	Difference	-5	-6	-12	-12
	% Difference	11.9%	12.2%	19.0%	18.8%
Max	*ACAR*	737	744	588	585
	VI	821	807	744	738
	Difference	-84	-63	-157	-153
	% Difference	11.4%	8.4%	26.6%	26.2%
Min	*ACAR*	-1347	-1340	-1065	-1067
	VI	-1269	-1271	-1047	-1044
	Difference	-77	-69	-17	-23
	% Difference	-5.8%	-5.2%	-1.6%	-2.2%
Normal Forces		**FL**	**FR**	**RL**	**RR**
Average	*ACAR*	3003	3003	3489	3489
	VI	2951	2951	3387	3387
	Difference	52	52	102	102
	% Difference	1.7%	1.7%	2.9%	2.9%
RMS Average	*ACAR*	3004	3004	3491	3491
	VI	2952	2952	3388	3389
	Difference	52	52	102	102
	% Difference	1.7%	1.7%	2.9%	2.9%
Max	*ACAR*	4970	4972	5234	5239
	VI	4828	4830	5047	5030
	Difference	142	143	187	209
	% Difference	2.9%	2.9%	3.6%	4.0%
Min	*ACAR*	1168	1168	1618	1616
	VI	1161	1185	1356	1401
	Difference	7	-18	262	215
	% Difference	0.6%	1.5%	16.2%	13.3%

Table 8: CEVT Pirelli Ftire: Front Tire 30 kg, Rear Tire 35 kg

Longitudinal Forces		**FL**	**FR**	**RL**	**RR**
Average	*ACAR*	-28	-28	53	53
	VI	-35	-35	55	55
	Difference	7	7	-1	-2
	% Difference	-25.4%	-25.9%	2.7%	2.9%
RMS Average	*ACAR*	45	45	62	62
	VI	77	77	87	86
	Difference	-31	-31	-25	-25
	% Difference	68.7%	68.9%	41.0%	39.8%
Max	*ACAR*	737	744	588	585
	VI	911	896	790	790
	Difference	-174	-152	-203	-205
	% Difference	23.6%	20.4%	34.5%	35.0%
Min	*ACAR*	-1347	-1340	-1065	-1067
	VI	-1282	-1281	-1076	-1062
	Difference	-65	-58	12	-5
	% Difference	-4.8%	-4.4%	-1.1%	-0.5%
Normal Forces		**FL**	**FR**	**RL**	**RR**
Average	*ACAR*	3003	3003	3489	3489
	VI	3005	3005	3487	3488
	Difference	-2	-2	2	2
	% Difference	0.1%	0.1%	0.1%	0.1%
RMS Average	*ACAR*	3004	3004	3491	3491
	VI	3009	3009	3492	3492
	Difference	-5	-5	-1	-1
	% Difference	0.2%	0.2%	0.0%	0.0%
Max	*ACAR*	4970	4972	5234	5239
	VI	4935	4937	5281	5263
	Difference	34	36	-47	-24
	% Difference	0.7%	0.7%	0.9%	0.5%
Min	*ACAR*	1168	1168	1618	1616
	VI	1219	1241	1501	1543
	Difference	-51	-74	117	73
	% Difference	4.4%	6.3%	7.2%	4.5%

Table 9: Demo Model: Washboard

Table 10: Demo FTire

Longitudinal Forces		**FL**	**FR**	**RL**	**RR**
Average	*ACAR*	-71	-71	110	110
	VI	-45	-45	150	150
	Difference	-25	-25	-40	-40
	% Difference	-35.7%	-35.7%	36.5%	36.3%
RMS Average	*ACAR*	236	236	283	284
	VI	211	211	307	307
	Difference	25	25	-24	-24
	% Difference	10.5%	10.5%	8.5%	8.3%
Max	*ACAR*	891	892	1668	1671
	VI	970	971	2012	2014
	Difference	-79	-79	-344	-343
	% Difference	8.8%	8.9%	20.6%	20.5%
Min	*ACAR*	-1598	-1598	-1535	-1541
	VI	-1550	-1549	-965	-966
	Difference	-48	-49	-570	-574
	% Difference	-3.0%	-3.1%	-37.1%	-37.3%
Normal Forces		**FL**	**FR**	**RL**	**RR**
Average	*ACAR*	2916	2916	3422	3422
	VI	2942	2941	3393	3393
	Difference	-25	-26	29	29
	% Difference	0.9%	0.9%	0.9%	0.8%
RMS Average	*ACAR*	3136	3136	3629	3628
	VI	3200	3201	3642	3641
	Difference	-64	-65	-12	-13
	% Difference	2.0%	2.1%	0.3%	0.4%
Max	*ACAR*	6151	6152	8205	8210
	VI	7227	7227	8900	8905
	Difference	-1076	-1075	-695	-696
	% Difference	17.5%	17.5%	8.5%	8.5%
Min	*ACAR*	181	181	326	328
	VI	13	13	288	289
	Difference	168	168	38	39
	% Difference	92.9%	93.0%	11.6%	12.0%

Table 11: CEVT Pirelli Ftire

Longitudinal Forces		**FL**	**FR**	**RL**	**RR**
Average	*ACAR*	-71	-71	110	110
	VI	-48	-48	151	151
	Difference	-23	-23	-41	-41
	% Difference	-32.8%	-32.8%	37.2%	37.1%
RMS Average	*ACAR*	266	266	426	427
	VI	218	219	379	380
	Difference	48	47	47	47
	% Difference	17.9%	17.8%	11.0%	11.0%
Max	*ACAR*	917	917	3887	3906
	VI	985	980	3232	3247
	Difference	-68	-63	655	659
	% Difference	7.5%	6.9%	16.9%	16.9%
Min	*ACAR*	-2107	-2108	-2942	-2965
	VI	-1630	-1639	-1624	-1634
	Difference	-477	-470	-1319	-1331
	% Difference	-22.6%	-22.3%	-44.8%	-44.9%
Normal Forces		**FL**	**FR**	**RL**	**RR**
Average	*ACAR*	2829	2829	3340	3341
	VI	2948	2949	3406	3407
	Difference	-119	-120	-66	-66
	% Difference	4.2%	4.2%	2.0%	2.0%
RMS Average	*ACAR*	3084	3084	3627	3626
	VI	3240	3240	3705	3705
	Difference	-156	-156	-78	-79
	% Difference	5.0%	5.1%	2.2%	2.2%
Max	*ACAR*	7281	7286	10250	10252
	VI	8350	8352	10261	10263
	Difference	-1069	-1067	-11	-11
	% Difference	14.7%	14.6%	0.1%	0.1%
Min	*ACAR*	179	179	263	262
	VI	162	163	287	279
	Difference	17	15	-25	-17
	% Difference	9.4%	8.6%	9.5%	6.6%

References

[1] *ASTM E1049-85(2011)e1 Standard Practices for Cycle Counting in Fatigue Analysis*. http://dx.doi.org/10.1520/E1049-85R11E01. ASTM International. West Conshohocken, PA, Oct. 2011.

[2] G. Erdogan. Tire Modeling: Lateral and Longitudinal Tire Forces. *Lecture notes - University of Minnesota* (Apr. 2009).

[3] *Essentials of Vehicle Dynamics*. Butterworth-Heinemann, 2015, p. 386. ISBN: 978-0-08-100036-6.

[4] M. Giaraffa. *Tech Tip: Springs '—&' Dampers, Part One: The Phantom Knowledge*. http://www.optimumg.com/docs/Springs&Dampers_Tech_Tip_1.pdf. (Visited on 06/06/2016).

[5] M. Gipser. *ADAMS/FTire - A Tire Model for Ride '—&' Durability Simulations*.

[6] M. Gipser. The FTire Tire Model Family. *Esslingen University of Applied Sciences, Automotive Engineering Department* (2003).

[7] G. Glinka. *The Rainflow Cycle Counting Procedure*. Apr. 2014.

[8] B. Jacobson. *Vehicle Dynamics, Compendium for Course MMF062*. Department of Applied Mechanics, Chalmers University of Technology, 2014.

[9] M. M. Kanafi. *One dimensional surface roughness power spectrum*. http://www.mathworks.com/matlabcentral/fileexchange/54315. MATLAB Central File Exchange, May 2016. (Visited on 01/05/2016).

[10] P. McNally. Adams Goes Real Time, Design Integration between Suppliers and OEMs. *Simulating Reality (MSC Software Magazine)* (2011). http://www.mscsoftware.com/submitted-content/Documents/7_about_us/2011_SRM_Winter2011_9_web.pdf, 22–23.

[11] C. Ortmann. ADAMS/Car Modelle mit Hilfe von VI-CarRealTime nutzbar machen für Fahrsimulatoren sowie HIL- und SIL-Anwendungen. *ADAMS User Meeting May 2011* (May 2011). http://pages.mscsoftware.com/rs/mscsoftware/images/adamsusermeeting2011-vigrade-vicarrealtime.pdf.

[12] H. B. Pacejka. *Tire and vehicle dynamics*. Oxford Butterworth-Heinemann, 2006. ISBN: 0-7680-1702-5.

[13] M. Schmid. *Tire Modeling for Multibody Dynamics Applications*. Tech. rep. http://sbel.wisc.edu/documents/TR-2011-02.pdf. 2011.

[14] G. Syal. *CAE - PROCESS AND NETWORK. A methodology for continuous product validation process based on network of various digital simulation methods*. KIT Scientific Publishing, 2013. ISBN: 978-3-7315-0090-2.

[15] *The multibody systems approach to Vehicle Dynamics*. Butterworth-Heinemann, 2015. ISBN: 978-0-08-099425-3.

[16] *VI-CarRealTime Documentation*. VI-Grade, 2015.

[17] D. Widmann and J. Liu. *Vibration Dynamic Analysis and Parameter Identification Assignment 2*. Chalmers University of Technology, Nov. 2015.